

2009

## Quantifying the Overwash Component of Barrier Island Morphodynamics: Onslow Beach, NC

Amy C. Foxgrover

*College of William and Mary - Virginia Institute of Marine Science*

Follow this and additional works at: <https://scholarworks.wm.edu/etd>



Part of the [Geomorphology Commons](#), and the [Physical and Environmental Geography Commons](#)

---

### Recommended Citation

Foxgrover, Amy C., "Quantifying the Overwash Component of Barrier Island Morphodynamics: Onslow Beach, NC" (2009). *Dissertations, Theses, and Masters Projects*. Paper 1539617888.

<https://dx.doi.org/doi:10.25773/v5-7tf6-vh68>

This Thesis is brought to you for free and open access by the Theses, Dissertations, & Master Projects at W&M ScholarWorks. It has been accepted for inclusion in Dissertations, Theses, and Masters Projects by an authorized administrator of W&M ScholarWorks. For more information, please contact [scholarworks@wm.edu](mailto:scholarworks@wm.edu).

Quantifying the Overwash Component of Barrier Island Morphodynamics:  
Onslow Beach, NC

---

A Thesis  
Presented to

The Faculty of the School of Marine Science  
The College of William and Mary

In Partial Fulfillment  
of the Requirements for the Degree of  
Master of Science

---


Amy C. Foxgrover  
2009

# Approval Sheet

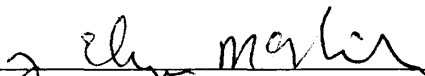
This Thesis is submitted in partial fulfillment of


the requirements for the degree of

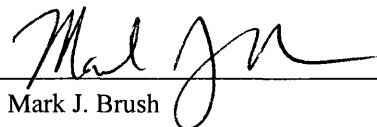
Master of Science


  
\_\_\_\_\_  
Amy C. Foxgrover

Approved by the Committee, October 1, 2009

  
\_\_\_\_\_  
Dr. Jesse E. McNinch  
Co-advisor

  
\_\_\_\_\_  
Dr. Carl T. Friedrichs  
Co-advisor

  
\_\_\_\_\_  
Dr. Mark J. Brush

  
\_\_\_\_\_  
Dr. Antonio B. Rodriguez  
University of North Carolina, Institute of Marine Science  
Morehead City, NC

## TABLE OF CONTENTS

<b>ACKNOWLEDGEMENTS .....</b>	<b>V</b>
<b>LIST OF TABLES .....</b>	<b>VI</b>
<b>LIST OF FIGURES .....</b>	<b>VII</b>
<b>LIST OF APPENDICES .....</b>	<b>XI</b>
<b>ABSTRACT .....</b>	<b>2</b>
<b>CHAPTER 1 - INTRODUCTION.....</b>	<b>3</b>
1.1 MOTIVATION .....	4
1.2 DCERP PROJECT .....	4
1.3 STUDY AREA .....	5
1.4 BARRIER ISLAND FORMATION AND GEOMORPHOLOGY.....	8
1.5 OVERWASH PROCESSES AND MORPHOLOGIES.....	9
1.6 OBJECTIVES, HYPOTHESES, AND OUTLINE .....	11
1.7 CHAPTER 1 FIGURES .....	12
<b>CHAPTER 2 - WASHOVER VOLUME AND SEDIMENTARY CHARACTERISTICS.....</b>	<b>20</b>
2.1 INTRODUCTION .....	21
2.2 BACKGROUND .....	22
2.2.1 Hurricanes Bertha and Fran.....	22
2.2.2 Geologically-Defined Sand Prism .....	22
2.2.3 Previous Overwash Studies .....	23
2.2.4 Sedimentary Characteristics of Washover Deposits .....	24
2.2.5 Ground-Penetrating Radar in Geologic Studies .....	26
2.3 METHODS AND MATERIALS.....	27
2.3.1 Sediment Samples .....	28
2.3.2 Ground-Penetrating Radar .....	31
2.3.3 Spatial Correlation with Shoreline Change .....	35
2.3.4 Uncertainties and Errors .....	35
2.4 RESULTS .....	38
2.4.1 Sedimentary Characteristics of Washover Deposits .....	38
2.4.2 Relevant-Sand Prism and Washover Volumes .....	39
2.5 CHAPTER 2 TABLES.....	42
2.6 CHAPTER 2 FIGURES .....	48
<b>CHAPTER 3 - SPATIAL AND TEMPORAL TRENDS IN SHORELINE MIGRATION AND OVERWASH OCCURRENCE: 1938-2008.....</b>	<b>72</b>
3.1 INTRODUCTION .....	73
3.1.1 Motivation .....	73
3.1.2 Study Area Background .....	74
3.2 METHODS .....	75
3.3 RESULTS .....	80
3.4 CHAPTER 3 TABLES .....	83
3.5 CHAPTER 3 FIGURES .....	87



<b>CHAPTER 4 - DISCUSSION, FUTURE WORK, AND CONCLUSIONS .....</b>	<b>107</b>
4.1 DISCUSSION .....	108
4.2 FUTURE WORK .....	111
4.3 MAJOR CONCLUSIONS .....	113
4.4 CHAPTER 4 FIGURES .....	114
<b>8 APPENDICES .....</b>	<b>116</b>
<b>9 VITA .....</b>	<b>146</b>
<b>10 REFERENCES .....</b>	<b>147</b>

## ACKNOWLEDGEMENTS

I would like to thank my co-advisors Jesse McNinch and Carl Friedrichs for their guidance throughout my time at VIMS and committee members Mark Brush (VIMS) and Antonio Rodriguez (UNC IMS) for their input on this study. Extended thanks go out to Antonio for allowing us to drag his GPR unit around the beach in the off-chance that we would actually see something of interest...I think we were all a bit shocked when it revealed such amazing data. Antonio's assistance and enthusiasm was critical in the collection and processing of GPR data. Thanks to all the ladies in the Pelican Lab: Kate Brodie, Lindsey Kraatz, and Heidi Wadman and to the Pelicans that came before me, Jennifer Miselis and Dave Perkey. A special thanks to Heidi Wadman for taking time out of her insanely busy schedule to join me on the numerous expeditions to MCBCL for data collection and to Emily Timmons and Steve Fegley (UNC IMS) for their assistance in the field. Dave Doyle, Adam Bode (NOAA), and Emily Himmelstoss (USGS) helped me track down historic surveys of Onslow Beach and assisted with georeferencing. Sharon Day (USACE, Wilmington District) provided historical aerial photos of the study area. Laura Moore (UVA) supplied valuable advice on the use of GPR in coastal environments. Susan Cohen granted us access to MCBCL, put us in touch with all the need-to-know people, and kept us in line during DCERP meetings. Lastly, a heartfelt thanks to my family for all of their support, especially over the final months of my research while I was a hermit and absolutely no fun whatsoever and to Creedence, the love of my life, I know it sounds cliché, but I truly could not have done this without you.

This research was conducted under the Defense Coastal/Estuarine Research Program (DCERP), funded by the Strategic Environmental Research and Development Program (SERDP). Views, opinions, and/or findings contained in this report are those of the author(s) and should not be construed as an official U.S. Department of Defense position or decision unless so designated by other official documentation. For more information on DCERP visit <http://dcerp.rti.org>.

## LIST OF TABLES

<b>CHAPTER 2 TABLES</b> .....	42
<b>TABLE 2-1.</b> ERROR ESTIMATES FOR SURFACE AREA AND VOLUME CALCULATIONS.....	43
<b>TABLE 2-2.</b> ELEVATION OF SAND/SILT CONTACT AS DETERMINED FROM BOTH GPR AND SEDIMENT CORES. THE DIFFERENCE BETWEEN THE TWO PROVIDES AN ASSESSMENT OF VERTICAL ERROR (TABLE 2-1).....	44
<b>TABLE 2-3.</b> SUMMARY OF SEDIMENTARY CHARACTERISTICS CALCULATED FROM RSA DATA AND SORTED BY DEPOSITIONAL ENVIRONMENT. VALUES REPORTED IN PSI WITH THE STANDARD DEVIATION IN BRACKETS. N IS THE NUMBER OF SAMPLES. ....	45
<b>TABLE 2-4.</b> SURFACE AREA AND RELEVANT-SAND PRISM VOLUME ESTIMATES BY SETTING .....	46
<b>TABLE 2-5.</b> CUMULATIVE WASHOVER THICKNESS AND DEPTH TO SAND/SILT CONTACT WITHIN EACH SEDIMENT CORE, SORTED BASED UPON COLLECTION SITE (FIGURE 2-4). ....	47
<b>CHAPTER 3 TABLES</b> .....	83
<b>TABLE 3-1.</b> TABLE OF IMAGERY USED IN ANALYSES. ....	84
<b>TABLE 3-2.</b> ESTIMATE OF SOURCES CONTRIBUTING TO POSITIONAL ERRORS OF THE SHORELINE AND VEGETATION LINE. TOTALS COMPUTED BY SUMMING IN QUADRATURE.....	85
<b>TABLE 3-3.</b> SAMPLE OF DATA GENERATED FROM DSAS. ....	86

# LIST OF FIGURES

<b>CHAPTER 1 FIGURES</b> .....	12
<b>FIGURE 1-1.</b> LOCATION MAP OF STUDY AREA. ....	13
<b>FIGURE 1-2.</b> AN 1872 US COAST AND GEODETIC SURVEY TOPOGRAPHIC SHEET SHOWING ONSLOW BEACH PRIOR TO CONSTRUCTION OF THE AIWW (1932) OR USE AS A MILITARY BASE (1941). THE OVERLYING SHORELINES PUBLISHED BY THE US GEOLOGICAL SURVEY (MILLER ET AL., 2005) DEPICT CHANGES IN SHORELINE POSITION FROM 1872 TO 1997. 14	
<b>FIGURE 1-3.</b> MODIFIED FROM DAVIS (1994), CLASSIFICATION OF COASTS BASED UPON MORPHOLOGY RESULTING FROM THE RELATIVE INFLUENCE OF MEAN WAVE HEIGHT VS. MEAN TIDAL RANGE. THE RED STAR INDICATES THE LOCATION OF ONSLOW BEACH WITHIN WAVE-DOMINATED/MIXED ENERGY SETTING (AFTER HAYES, 1979). ....	15
<b>FIGURE 1-4.</b> WASHOVER HISTORY MAP FROM CLEARY AND HOSIER (1979) INDICATING THE FREQUENCY OF OVERWASH EPISODES FROM CAPE LOOKOUT TO THE SOUTH CAROLINA BORDER BASED UPON PHOTOGRAMMETRIC ANALYSES OF THREE TIME PERIODS: 1) PRE-1938, 2) 1954-55, AND 3) 1962. AREAS THAT EXPERIENCED AT LEAST THREE EPISODES OF OVERWASH DURING THIS TIME SPAN WERE CLASSIFIED AS SEVERE, TWO EPISODES AS MODERATE, AND ONE AS OCCASIONAL. THE RED ARROW INDICATES THE LOCATION OF OUR STUDY, COINCIDING WITH A TRANSITION FROM SEVERE OVERWASH OCCURRENCE TO THE SOUTHWEST AND MINIMAL OVERWASH TO THE NORTHEAST. ....	16
<b>FIGURE 1-5.</b> FULL FEATURE LIDAR DATA COLLECTED IN 2005 BY THE US ARMY CORPS OF ENGINEERS’ SHOALS SYSTEM AND COLORED BY ELEVATION. THE PROFILES DEPICT THE VARIATION IN TOPOGRAPHIC RELIEF BETWEEN THE NORTHERN AND SOUTHERN ENDS OF ONSLOW BEACH. LIDAR DATA OBTAINED FROM NOAA’S COASTAL SERVICES CENTER WEBSITE (WWW.CSC.NOAA.GOV/DIGITALCOAST). ....	17
<b>FIGURE 1-6.</b> FROM DAVIS (1994) AND BASED ON HAYES (1979) DIAGRAMS OF PREDOMINANT FEATURES OF WAVE-DOMINATED, MIXED ENERGY, AND DRUMSTICK BARRIER ISLANDS .....	18
<b>FIGURE 1-7.</b> FROM DONNELLY ET AL. (2004A), DIAGRAM OF COMMON MORPHOLOGIC DEPOSITS RESULTING FROM OVERWASH. ....	19
<b>CHAPTER 2 FIGURES</b> .....	48
<b>FIGURE 2-1.</b> A TIME SERIES OF AERIAL IMAGERY DOCUMENTING THE DEVELOPMENT OF THE LARGE SHEETWASH LOCATED ~1 KM NORTH OF THE NEW RIVER INLET. THE MARCH 1996 IMAGERY WAS COLLECTED PRIOR TO HURRICANES BERTHA (AUGUST 12TH) AND FRAN (SEPTEMBER 5TH). THE SEPTEMBER 15TH, 1996 PHOTO WAS COLLECTED 10 DAYS AFTER FRAN AND DEPICTS THE LARGE AMOUNTS OF SEDIMENT THAT WERE DELIVERED VIA INUNDATION OVERWASH. THE MAY 2008 IMAGE SHOWS WHAT THIS SITE LOOKS LIKE TODAY. THE TRANSPARENT BLUE LINES ARE SHOWN FOR REFERENCE AND INDICATE THE LOCATION OF CHANNELS SEEN IN THE 1996 IMAGERY. THE LARGE PLANAR SHEETWASH CONTAINS ONLY SPARSE VEGETATION AND FROM THE GROUND, THERE IS NO INDICATION THAT THIS SITE WAS PREVIOUSLY COVERED WITH CHANNELS. ....	49
<b>FIGURE 2-2.</b> LEFT: DIAGRAM MODIFIED FROM McCUBBIN (1982) DEPICTING HOW RISES IN SEA LEVEL AND THE RESULTANT SHORELINE TRANSGRESSION (BARRIER ISLAND RETROGRADATION) CAN RESULT IN THE EXPOSURE OF MASH LAGOONAL DEPOSITS IN THE SURF ZONE. RIGHT: PHOTOGRAPH TAKEN ON ONSLOW BEACH AT LOW TIDE (LOOKING NE TOWARDS RISELEY PIER) WITH PEAT DEPOSITS EXPOSED ON THE BEACH .....	50
<b>FIGURE 2-3.</b> DIAGRAMMATIC CROSS-SECTIONS FROM SCHWARTZ (1975) AND McCUBBIN (1982) SHOWING THE TWO TYPES OF STRATIGRAPHY ASSOCIATED WITH OVERWASH EVENTS. A) STRATIGRAPHY WHEN THE WASHOVER FAN OR LOBE REACHES STANDING WATER, CHARACTERIZED BY PLANAR HORIZONTAL STRATIFICATION OVER THE SUBAERIAL PORTION AND MEDIUM-SCALE FORESET STRATIFICATION WHERE WASHOVER SPILLS INTO WATER. B) PLANAR HORIZONTAL STRATIFICATION ASSOCIATED WITH WASHOVER SEDIMENTS DEPOSITED ON LAND. ....	51
<b>FIGURE 2-4.</b> MAP DEPICTING LOCATION OF GPR TRANSECTS AND SEDIMENT CORES COLLECTED WITHIN THE STUDY AREA. SITES 1-4 INDICATE OVERWASH FOCUS SITES. ....	52

<b>FIGURE 2-5.</b> PHOTOGRAPHS OF GPR COLLECTION. ....	53
<b>FIGURE 2-6.</b> A) 3D PERSPECTIVE FENCE PLOT OF GPR COLLECTED AT SITE 4. THE GREEN DOTTED LINE INDICATES THE SURFACE REFLECTOR AND THE ORANGE LINE CORRESPONDS TO THE SAND/SILT CONTACT OR BASE OF THE RELEVANT-SAND PRISM. THE RED BOX HIGHLIGHTS THE AREA SHOWN IN THE BOTTOM TWO PANELS. B) 200 MHZ GPR PROFILE FROM DIP TRANSECT RUNNING UP THE CENTER OF THE OVERWASH FAN. DEPTH CONVERSION ASSUMES A CONSTANT VELOCITY OF 0.1 M/NS. (C) LINE-DRAWING INTERPRETATION OF GPR PROFILE ABOVE. THE SOLID LINE INDICATES THE SURFACE, THE DASHED LINE THE SAND/SILT CONTACT, AND THE SMALLER ARCED FEATURES ARE HYPERBOLIC REFLECTIONS THAT ARE AN ARTIFACT OF BURIED DEBRIS. THE OVERLAIN SEDIMENT VIBRACORES WERE USED TO AID IN INTERPRETATION OF THE GPR RECORD. ....	54
<b>FIGURE 2-7.</b> A) 3D PERSPECTIVE FENCE PLOT OF GPR COLLECTED AT SITE 3. THE GREEN DOTTED LINE INDICATES THE SURFACE REFLECTOR AND THE ORANGE LINE CORRESPONDS TO THE SAND/SILT CONTACT OR BASE OF THE RELEVANT-SAND PRISM. THE RED BOX HIGHLIGHTS THE AREA SHOWN IN THE BOTTOM TWO PANELS. B) 200 MHZ GPR PROFILE FROM DIP TRANSECT RUNNING UP THE OVERWASH FAN. DEPTH CONVERSION ASSUMES A CONSTANT VELOCITY OF 0.1 M/NS. (C) LINE-DRAWING INTERPRETATION OF GPR PROFILE ABOVE. THE SOLID LINE INDICATES THE SURFACE, THE DASHED LINE THE SAND/SILT CONTACT, AND THE SMALLER ARCED FEATURES ARE HYPERBOLIC REFLECTIONS THAT ARE AN ARTIFACT OF BURIED DEBRIS. THE OVERLAIN SEDIMENT VIBRACORES WERE USED TO AID IN INTERPRETATION OF THE GPR RECORD. ..	55
<b>FIGURE 2-8.</b> A) FROM McCUBBIN (1982), CROSS SECTION PROFILE DEPICTING FACIES ASSOCIATED WITH CHANNEL OR INLET MIGRATION. B) 3D PERSPECTIVE VIEW OF A GPR PROFILE FROM THE SOUTHERN END OF ONSLOW BEACH EXHIBITING A SIMILAR STRATIGRAPHY TO THAT SHOWN ABOVE. GREEN DOTS HIGHLIGHT THE SURFACE REFLECTION AND ORANGE DOTS THE UNDERLYING CHANNEL MORPHOLOGY. THE BLUE-SHADED AREA REPRESENTS A CHANNEL THAT WAS VISIBLE IN EARLIER AERIAL PHOTOGRAPHS BUT FILLED WITH SEDIMENT WHEN HURRICANES BERTHA AND FRAN HIT IN 1996. THE PERSPECTIVE VIEW IS LOOKING NORTHWEST AND THE DISTANCE ALONG THE BOTTOM OF THE IMAGE IS APPROXIMATELY 160 M. ....	56
<b>FIGURE 2-9.</b> 3D PERSPECTIVE VIEW OF GPR TRANSECTS COLLECTED IN THE LARGE SHEETWASH AT SITE 1. THE SURFACE REFLECTION IS TRACED IN GREEN AND THE ORANGE TRACE HIGHLIGHTS THE MORPHOLOGY USED IN DEFINING THE BASE OF THE RELEVANT-SAND PRISM. ....	57
<b>FIGURE 2-10.</b> DATA USED IN INTERPOLATING ELEVATION OF THE SAND/SILT CONTACT. CORE MEASUREMENTS INCLUDE DEPTHS FROM SEDIMENT CORES AS WELL AS GPS MEASUREMENTS OF PEAT EXPOSED ON THE BEACH. GPR MEASUREMENTS ARE DIGITIZED REFLECTION TRACES COLORED BY ELEVATION. THE CONTOURS WITHIN THE SOUTHERN SHEETWASH SITE REPRESENT THE EDGE OF BURIED CHANNELS REVEALED THROUGH GPR AND VISIBLE IN MARCH 1996 PHOTOS. CONTOURS WERE ADDED IN THE AIWW AND OFFSHORE TO EXTRAPOLATE DEPTHS TO THE EDGE OF THE ISLAND, ALL CONTOUR ELEVATIONS ARE BASED UPON THE CLOSEST FIELD MEASUREMENTS. ....	58
<b>FIGURE 2-11.</b> A) INTERPOLATED ELEVATION SURFACE OF THE SAND/SILT CONTACT OR BASE OF THE RELEVANT-SAND PRISM. POINT DATA USED AS THE BASIS FOR INTERPOLATION ARE DISPLAYED FOR REFERENCE. THE STRIPED REGION HIGHLIGHTS AREAS POORLY CONSTRAINED BY FIELD MEASUREMENTS, ELEVATION IN REGIONS DISTANT FROM DIRECT FIELD MEASUREMENTS (NAMELY THE LANDWARD SIDE OF THE ISLAND) SHOULD BE TAKEN ONLY AS A ROUGH APPROXIMATION. B) 2007 NGA BARE EARTH LIDAR DATA. ....	59
<b>FIGURE 2-12.</b> THICKNESS OF THE RELEVANT-SAND PRISM DETERMINED BY SUBTRACTING THE SURFACE REPRESENTING THE SAND/SILT CONTACT (FIGURE 2-11A) FROM 2007 NGA LIDAR DATA (FIGURE 2-11B). THE STRIPED REGION HIGHLIGHTS AREAS WHERE THE DEPTH OF THE SAND/SILT CONTACT IS POORLY CONSTRAINED BY FIELD MEASUREMENTS. ....	60
<b>FIGURE 2-13.</b> A) DIAGRAMMATIC CROSS-SECTION OF WASHOVER STRATIGRAPHY FROM SCHWARTZ (1975) AND McCUBBIN (1982). STRATIFICATION TYPICAL OF WASHOVER DEPOSITS EXTENDING INTO A REGION OF STANDING WATER. B) A GPR PROFILE FROM THE SOUTHERN END OF ONSLOW BEACH (PERSPECTIVE VIEW LOOKING SOUTHWEST TOWARDS NEW RIVER INLET) SHOWING STRATIGRAPHY SIMILAR TO THAT DISPLAYED ABOVE. THE GREEN LINE INDICATES THE SURFACE REFLECTION AND THE ORANGE THE BASE OF A WASHOVER DEPOSIT. THE DISTANCE ALONG THE BOTTOM OF THE IMAGE IS APPROXIMATELY 150 M. ....	61

**FIGURE 2-14.** A) DIAGRAMMATIC CROSS-SECTION OF WASHOVER STRATIGRAPHY FROM SCHWARTZ (1975) AND MCCUBBIN (1982). STRATIFICATION TYPICAL OF WASHOVER DEPOSITS EXTENDING ALONG SUBAERIAL SURFACES. B) A GPR PROFILE FROM ONSLOW BEACH (PERSPECTIVE VIEW LOOKING SOUTHWEST ALONG THE BEACH ACCESS ROAD) SHOWING PLANAR SUB-HORIZONTAL STRATIGRAPHY INDICATIVE OF WASHOVER DEPOSITS. THE GREEN LINE INDICATES THE SURFACE REFLECTOR. THE DISTANCE ALONG THE BOTTOM OF THE IMAGE IS APPROXIMATELY 200 M. ....62

**FIGURE 2-15.** SAMPLE HYDRAULIC SIZE DISTRIBUTION PLOTS GENERATED FROM RSA DATA OF FOUR DIFFERENT DEPTH INTERVALS WITHIN ONSVC04. ....63

**FIGURE 2-16.** SCATTERPLOT OF MEAN GRAIN SIZE VERSUS SORTING (STANDARD DEVIATION). DUNE SAMPLES WERE COLLECTED FROM THE SURFACE OF ACTIVE DUNE SITES. THE REMAINING SAMPLES WERE TAKEN FROM SEDIMENT VIBRACORES AND DIVIDED INTO OVERWASH AND NON-OVERWASH POPULATIONS BASED UPON GRAIN-SIZE CHARACTERISTICS AND VISUAL INSPECTION OF THE CORES. ....64

**FIGURE 2-17.** SCATTERPLOT OF SKEWNESS VERSUS KURTOSIS. DUNE SAMPLES WERE COLLECTED FROM THE SURFACE OF ACTIVE DUNE SITES. THE REMAINING SAMPLES WERE TAKEN FROM SEDIMENT VIBRACORES AND DIVIDED INTO OVERWASH AND NON-OVERWASH POPULATIONS BASED UPON GRAIN-SIZE CHARACTERISTICS AND VISUAL INSPECTION OF THE CORES. ....65

**FIGURE 2-18.** LOCATION OF CROSS-ISLAND TRANSECTS (50-M SPACING) USED IN ASSESSING ALONGSHORE VARIATIONS IN SEDIMENT VOLUME. ....66

**FIGURE 2-19.** PARTITIONING OF CROSS-ISLAND TRANSECTS INTO OVERWASH AND BEACH ENVIRONMENTS. ....67

**FIGURE 2-20.** SCATTERPLOT OF LONG-TERM (1872-1997) SHORELINE CHANGE RATES (MORTON & MILLER, 2005) VERSUS WASHOVER VOLUME PER TRANSECT. ....68

**FIGURE 2-21.** ALONGSHORE VARIATION IN TOTAL VOLUME AND VOLUME PER UNIT SURFACE AREA OF THE RELEVANT-SAND PRISM. ....69

**FIGURE 2-22.** VARIATION IN ALONGSHORE RELEVANT-SAND PRISM VOLUMES COMPARED TO ALONGSHORE LONG-TERM (1872-1997; LINEAR REGRESSION) AND SHORT-TERM (1973-1997; END-POINT) SHORELINE CHANGE RATES (MORTON & MILLER, 2005). ....70

**FIGURE 2-23.** SCATTERPLOT OF LONG-TERM (1872-1997) LINEAR REGRESSION SHORELINE CHANGE RATES (MORTON & MILLER, 2005) VERSUS AREA-NORMALIZED VOLUMES OF THE CROSS-ISLAND RELEVANT-SAND PRISM AND THE PORTION OF THAT PRISM WITHIN THE BEACH OR OVERWASH SETTINGS. ....71

**CHAPTER 3 FIGURES** .....87

**FIGURE 3-1.** A TIME SERIES OF AERIAL IMAGERY DOCUMENTING THE DEVELOPMENT OF THE LARGE SHEETWASH LOCATED ~1 KM NORTH OF THE NEW RIVER INLET. THE MARCH 1996 IMAGERY WAS COLLECTED PRIOR TO HURRICANES BERTHA (AUGUST 12<sup>TH</sup>) AND FRAN (SEPTEMBER 5<sup>TH</sup>). THE SEPTEMBER 15<sup>TH</sup>, 1996 PHOTO WAS COLLECTED 10 DAYS AFTER FRAN AND DEPICTS THE LARGE AMOUNTS OF SEDIMENT THAT WERE DELIVERED VIA INUNDATION OVERWASH. THE MAY 2008 IMAGE SHOWS WHAT THIS SITE LOOKS LIKE TODAY. THE TRANSPARENT BLUE LINES ARE SHOWN FOR REFERENCE AND INDICATE THE LOCATION OF CHANNELS SEEN IN THE MARCH 1996 IMAGERY. THE LARGE PLANAR SHEETWASH CONTAINS ONLY SPARSE VEGETATION AND FROM THE GROUND, THERE IS NO INDICATION THAT THIS SITE WAS PREVIOUSLY COVERED WITH CHANNELS. ....88

**FIGURE 3-2.** AN 1872 US COAST AND GEODETIC SURVEY TOPOGRAPHIC SHEET SHOWING ONSLOW BEACH PRIOR TO CONSTRUCTION OF THE AIWW (1932) OR USE AS A MILITARY BASE (1941). THE OVERLYING SHORELINES PUBLISHED BY THE US GEOLOGICAL SURVEY (MILLER ET AL., 2005) DEPICT CHANGES IN SHORELINE POSITION FROM 1872 TO 1997. 89

**FIGURE 3-3.** FULL FEATURE LIDAR DATA COLLECTED IN 2005 BY THE US ARMY CORPS OF ENGINEERS’ SHOALS SYSTEM AND COLORED BY ELEVATION. THE PROFILES DEPICT THE VARIATION IN TOPOGRAPHIC RELIEF BETWEEN THE NORTHERN AND SOUTHERN ENDS OF ONSLOW BEACH. LIDAR DATA OBTAINED FROM NOAA’S COASTAL SERVICES CENTER WEBSITE (WWW.CSC.NOAA.GOV/DIGITALCOAST). ....90

<b>FIGURE 3-4.</b> LOCATION MAP DIVIDING ONSLOW BEACH UP INTO 4 ZONES BASED UPON PREDOMINANT BEACH ACTIVITIES. ....	91
<b>FIGURE 3-5.</b> COMPARISON BETWEEN OVERWASH EXTENT AS MAPPED FROM RTK DGPS GROUND SURVEYS AND DELINEATION OF VEGETATION LINE BASED UPON AERIAL IMAGERY. ....	92
<b>FIGURE 3-6.</b> TIMELINE OF AERIAL IMAGERY, PUBLISHED SHORELINE DATA (MILLER ET AL., 2005), AND STORMS BETWEEN 1938 AND 2008 THAT HAD SIGNIFICANT IMPACT UPON THE STUDY AREA (CLEARY ET AL., 2000; REIMER 2004; NOAA CSC WEBSITE). DASHED LINES INDICATE WHEN THE AIWW WAS CONSTRUCTED AND WHEN THE PROPERTY WAS PURCHASED BY THE US MILITARY. ....	93
<b>FIGURE 3-7.</b> 1938 IMAGERY OVERLAIN BY DIGITIZED SHORELINE AND VEGETATION LINES. DASHED LINES INDICATE DECREASED CONFIDENCE IN POSITIONING DUE TO POOR CONTRAST OR MISSING IMAGERY. ....	94
<b>FIGURE 3-8.</b> 1956 IMAGERY OVERLAIN BY DIGITIZED SHORELINE AND VEGETATION LINES. DASHED LINES INDICATE DECREASED CONFIDENCE IN POSITIONING DUE TO POOR IMAGERY CONTRAST. ....	95
<b>FIGURE 3-9.</b> 1979 IMAGERY OVERLAIN BY DIGITIZED SHORELINE AND VEGETATION LINES. DASHED LINES INDICATE DECREASED CONFIDENCE IN POSITIONING DUE TO POOR IMAGERY CONTRAST. ....	96
<b>FIGURE 3-10.</b> 1989 IMAGERY OVERLAIN BY DIGITIZED SHORELINE AND VEGETATION LINES. ....	97
<b>FIGURE 3-11.</b> 1998 IMAGERY OVERLAIN BY DIGITIZED SHORELINE AND VEGETATION LINES. ....	98
<b>FIGURE 3-12.</b> 2008 IMAGERY OVERLAIN BY DIGITIZED SHORELINE AND VEGETATION LINES. ....	99
<b>FIGURE 3-13.</b> COMPILATION OF ALL SHORELINES AND VEGETATION LINES OVERLYING THE AREA OF THE ISLAND IN 2008 FOR REFERENCE. ....	100
<b>FIGURE 3-14.</b> LOCATION OF TRANSECTS USED IN CALCULATING RATES OF CHANGE USING DSAS. TRANSECTS ARE SHADED BASED UPON SHORELINE CHANGE RATES DERIVED FROM A LINEAR REGRESSION OF ALL SIX TIME PERIODS FROM 1938 TO 2008. ....	101
<b>FIGURE 3-15.</b> COMPARISON BETWEEN EPR (END-POINT RATE) AND LRR (LINEAR REGRESSION RATE) CALCULATIONS OF SHORELINE CHANGE FOR THE LISTED TIME PERIODS. 1872-1997 RATES PROVIDED BY MORTON AND MILLER (2005). 1938-2008 RATES CALCULATED FROM DIGITIZED WET/DRY LINES USED IN THIS STUDY. 1872-1938 RATES DERIVED FROM THE 1872 T-SHEET SHORELINE (MILLER ET AL., 2005) AND OUR 1938 WET/DRY LINE. ....	102
<b>FIGURE 3-16.</b> SCATTERPLOT COMPARING NET MOVEMENT IN THE SHORELINE AND VEGETATION LINE BETWEEN 1938 AND 2008. ....	103
<b>FIGURE 3-17.</b> SCATTERPLOT OF SHORELINE CHANGE RATE VERSUS VEGETATION LINE CHANGE DERIVED FROM LINEAR REGRESSION OF ALL SIX TIME PERIODS. ....	104
<b>FIGURE 3-18.</b> ALONGSHORE VARIATIONS IN THE DISTANCE BETWEEN THE SHORELINE (HWL) AND THE VEGETATION LINE. THE ROMAN NUMERALS INDICATE THE ZONES OF PRIMARY BEACH ACTIVITY DEPICTED IN FIGURE 3-4. ....	105
<b>FIGURE 3-19.</b> VARIATIONS IN THE DISTANCE BETWEEN THE SHORELINE (HWL) AND THE VEGETATION LINE OVER TIME FOR THE ENTIRE ISLAND (TRANSECTS 1-200) AND THE REGION SOUTH OF RISELEY PIER (TRANSECTS 104-200). ASTERISKS INDICATE YEARS WITH SIGNIFICANT STORM EVENTS (FIGURE 3-6). ....	106
<b>CHAPTER 4 FIGURES</b> .....	114
<b>FIG 4-1.</b> DIFFERENCE IN ELEVATION BETWEEN 1997 ATM II FULL FEATURE LIDAR (COLLECTED APPROXIMATELY 1 YEAR AFTER HURRICANE FRAN HIT) AND 2007 NGA BARE EARTH LIDAR. REGIONS OF EROSION IN EXCESS OF 3 M ARE AN ARTIFACT OF VEGETATION THAT WAS NOT REMOVED FROM THE 1997 LIDAR AND ARE NOT REPRESENTATIVE OF ACTUAL SURFACE ELEVATION CHANGE. VEGETATION IN THE SHEETWASH SITE (ENCIRCLED REGION DENOTED BY RED ARROW) REMAINS VERY SPARSE AND THE AVERAGE ACCRETION OF ~40 CM THAT OCCURRED BETWEEN 1997 AND 2007 IS LIKELY THE RESULT OF AEOLIAN TRANSPORT AND MINOR OVERWASH EVENTS. ....	115

## **LIST OF APPENDICES**

<b>APPENDIX I – PHOTOGRAPHS OF SEDIMENT VIBRACORES .....</b>	<b>117</b>
<b>APPENDIX II – SEDIMENT GRAIN SIZE DATA AND METHOD OF MOMENT STATISTICS GENERATED FROM RSA OUTPUT, GRAY SHADING INDICATES SAMPLES DETERMINED TO BE SEDIMENTOLOGICALLY DISTINCT WASHOVER SEDIMENTS.....</b>	<b>130</b>
<b>APPENDIX III – WATER CONTENT SAMPLES FROM JACKHAMMER CORES .....</b>	<b>137</b>
<b>APPENDIX IV – RELEVANT-SAND PRISM AND WASHOVER VOLUMES LISTED BY TRANSECT .....</b>	<b>141</b>



Quantifying the Overwash Component of Barrier Island Morphodynamics:  
Onslow Beach, NC

## ABSTRACT

A quantification of the role that barrier island overwash plays in the evolution of Onslow Beach, a barrier island located on Marine Corps Base Camp Lejeune, North Carolina, is presented. Ground-penetrating radar (GPR) and sediment vibracores provide an estimate of the relevant-sand prism above a silty/peat contact underlying the island. The average thickness from the surface, as determined from lidar, to this geologically-defined base, is less than 1 m and equates a total volume of approximately  $1.8 \pm 1.1 \times 10^6 \text{ m}^3$  over the 4.8 km stretch of Onslow Beach from 1 km north of the New River Inlet to Riseley Pier ( $\sim 2 \text{ km}^2$ ). Approximately 39% of the relevant-sand prism ( $680 \pm 215 \times 10^3 \text{ m}^3$ ) is contained within the area of the island currently exhibiting signs of overwash events (i.e., the active overwash complex). Based upon the average cumulative thickness of distinct washover facies within 12 sediment cores (52 cm) and the surface area of the active overwash region, it is estimated that the volume sedimentologically distinct washover deposits equals  $199 \pm 88 \times 10^3 \text{ m}^3$  (approximately 29% of the active overwash complex or 11% of the entire relevant-sand prism).

A time series of aerial imagery from 1938 to 2008 details the spatial and temporal trends in migration of both the wet/dry line (a shoreline proxy) and the vegetation line (indicating the landward extent of overwash). Long-term shoreline erosion rates in excess of 3 m/yr occurred over the southern portion of Onslow Beach while the northern portion experienced up to 1.7 m/yr of accretion within the same 80-year time span. Between 1938 and 2008, the vegetation line moved an average of 85 m landward over the length of the entire island and over 450 m in overwash sites at the southern end of the island where shoreline erosion rates are highest. A comparison with long-term shoreline change rates suggests that a simple linear relationship between spatial and temporal variability in shoreline behavior and volume of the relevant-sand prism does not exist.

Trends based upon the past 80 years suggest that a positive correlation exists between storm frequency and overwash extent. Furthermore, the region experiencing the highest rates of shoreline erosion and the highest occurrence of overwash does not coincide with the area regularly subject to military training activities. These data suggest that natural forcings (sea level, wind and wave energy, geology, etc.) exert first-order control on the evolution of this barrier island. The ability to quantify and evaluate the relative importance of such forces is paramount to understanding how, and over what timescales, the nearshore environment responds to changes in external forcings (e.g., sea-level rise, storms, etc.) and, in turn, is fundamental to the development of reliable forecasts of shoreline trends and storm susceptibility models.

**CHAPTER 1**  
**INTRODUCTION**

## **1.1 Motivation**

Barrier islands are dynamic coastal features that migrate in response to changes in natural forcings (e.g., sea-level rise, storms, etc.) and anthropogenic activities through a combination of mechanisms including aeolian transport, inlet dynamics, and oceanic overwash. These processes are, in turn, influenced by factors such as underlying geology, wind and sea energy, and anthropogenic activities. Despite concerted efforts, scientists continue to struggle when it comes to explaining, much less forecasting, the highly variable, alongshore-response of shorelines over seasonal, decadal, and longer timescales. Under the pressure of rising sea level and increased societal impacts of coastal storms (Scavia et al., 2002), it becomes critical that we determine the primary mechanisms driving alongshore variability in shoreline response in order to: 1) improve forecasts of localized shoreline change; and 2) aid in the development of policies that minimize hazards and promotes the management of coastal resources for long-term sustainability. As an initial step towards that goal, this research provides a quantification of one of these mechanisms, barrier island overwash, through a combination of geospatial, geophysical, and sedimentological analyses of Onslow Beach, NC.

## **1.2 DCERP Project**

This study is part of a larger collaborative research project at Marine Corps Base Camp Lejeune (MCBCL) just outside of Jacksonville, NC. The Defense Coastal/Estuarine Research Program (DCERP) is a multi-year, multi-disciplinary project funded by the Strategic Environmental Research and Development Program (SERDP). The program's primary goal is to “enhance and sustain the military mission by developing an understanding of coastal and estuarine ecosystem composition, structure, and function within the context of a military training environment” (<https://dcerp.rti.org>). DCERP consists of five separate research modules: aquatic/estuarine, coastal wetlands, terrestrial, atmospheric, and coastal barrier -- of which this research falls under the latter. One aim of the project that is directly addressed in this thesis is the

need to better quantify short-term barrier evolution related to storms and land-use practices. Although outside of the immediate scope of this thesis, one of the longer-term goals of this research is to improve upon large-scale coastal vulnerability models, such as those developed by Sallenger et al. (2000) and Stockdon et al. (2007), for this specific site. The higher resolution data and tighter constraints on boundary conditions generated through this research can be used as input for future model development.

### **1.3 Study Area**

Extensive geologic studies show that the barrier islands lining the coast of North Carolina arrived at their present-day location via landward translation with rising sea level and lateral movement through inlet migration, in accordance with the mechanisms proposed by De Beaumont (1845) and Gilbert (1885) (Inman & Dolan, 1989). The rate of landward migration slowed drastically around 4,000 years ago when the rate of eustatic sea-level rise declined to approximately modern rates (Horton et al., 2009).

Onslow Beach is situated midway between Cape Lookout and Cape Fear on the coast of North Carolina (Figure 1-1). Bordered by Brown's Inlet to the northeast and the New River Inlet to the southwest, the island is approximately 12 km in length and covers an area of about 5 km<sup>2</sup>. An 1872 US Coast and Geodetic Survey topographic sheet shows that Onslow Beach was connected to the mainland by a marshy habitat containing narrow, sinuous channels (Figure 1-2). In 1932, the landward boundary of the barrier island was drastically altered with the construction of the Atlantic Intracoastal Waterway (AIWW) (Cleary & Riggs, 1999), which separated the island from the mainland with a 60-m wide linear channel. The modern AIWW averages 130 meters in width and is maintained to a depth of approximately 3.7 m (12 ft mean low water) by the US Army Corps of Engineers (<http://www.saw.usace.army.mil/nav/aiww.htm>). The island and surrounding lands were purchased by the US Department of the Navy in 1941 for use as an

East Coast amphibious training facility and are now part of Marine Corps Base Camp Lejeune (MCBCL). Although the barrier island and its shorelines are impacted by military training activities, the island provides an excellent study area because it is largely undeveloped, and the military activities that do occur are much more regulated and documented in comparison to the anthropogenic impacts on more highly populated and developed neighboring barrier islands.

Onslow Beach is microtidal, with a mean tidal range of approximately 1 m. Hourly wave data for 2008 from the National Oceanographic and Atmospheric Administration's offshore buoy (station 41035 in 10-m water depth), reports a mean significant wave height of 0.91 m and a dominant wave period of 7.4 seconds (<http://www.ndbc.noaa.gov>). A 20-year wave hindcast (1980-1999) performed by the US Army Corps of Engineers ([http://www.frf.usace.army.mil/cgi-bin/wis/atl/atl\\_main.html](http://www.frf.usace.army.mil/cgi-bin/wis/atl/atl_main.html)) estimates a similar long-term mean significant wave height of ~1 m in this vicinity, placing Onslow Beach in the mixed energy/wave-dominated classification of Hayes (1979) (Figure 1-3). The dominant wave direction is from the southeast during the spring and summer and from the northeast during the winter, although the impact of winter storm waves approaching from the northeast is limited due to partial sheltering provided by Cape Lookout.

Tropical and extratropical cyclones approaching from the east or south are episodic but can have a large impact. Based upon trends over the past 100 years, Barnes (2001) predicts that some portion of North Carolina will be affected by a hurricane about once every four years. Predicted wave heights computed for nearby Topsail Island range from 3.3 m for a one-in-50 year tropical storm to 3.8 m for a one-in-100 year case (Cleary & Riggs, 1999). To put this into perspective, Hurricane Fran (Class III) struck Onslow Beach on September 5<sup>th</sup>, 1996, with a reported maximum storm surge of 2.9 m on nearby North Topsail Beach (Cleary et al., 2001). This storm resulted in extensive barrier island overwash along the southern portion of the study area and a reported \$3.2 billion in damages for the state of North Carolina (Barnes, 2001).

Onslow Beach is located centrally within the cusp of Onslow Bay at a transition zone between the lower energy flank of Cape Lookout to the northeast and the higher energy flank of Cape Fear to the southwest. In general, barriers to the north of Onslow Beach are regressive and characterized by higher topography and multiple sets of beach ridges in all stages of modification. In contrast, barriers to the south tend to be transgressive, low-lying, characteristically unstable, and contain abundant overwash features (Cleary & Pilkey, 1996; Cleary & Riggs, 1999). This trend was illustrated in the work of Cleary and Hosier (1979) which depicts areas of moderate to severe overwash from south of Onslow Beach to Cape Fear and little to no overwash north towards Cape Lookout (Figure 1-4). A similar trend in morphology and shoreline behavior is also present on Onslow Beach itself. The northern half of the island is characterized by well-developed dune ridges (approximately 8-9 m in height in the proximity of Brown's Inlet) and a stable to accretionary shoreline with few overwash fans (Figure 1-5). In contrast, the southwestern half of the island (from New River Inlet to Riseley Pier) is characterized by poorly-developed segmented dunes, experiences chronic, long-term erosion ( $>3$  m/yr near New River Inlet) (Morton & Miller, 2005) and is the site of extensive active and historical overwash, making it an ideal focus site for this research.

Onslow Beach is severely limited in nearshore sediment volume. The elongate shoals at Cape Fear and Cape Lookout limit exchange from adjacent embayments (McNinch & Wells, 1999), and with no significant local fluvial inputs, the accumulation of recent nearshore sediment which is well-developed elsewhere on the southeastern US Atlantic shelf is essentially absent here (Cleary & Pilkey, 1968). Over 200 box dredge samples collected on the continental shelf of Onslow Bay reveal a patchwork of primarily relict or residual sediments (Cleary & Pilkey, 1968). Recent work by Wadman et al. (2008) affirms this is a sediment-starved nearshore system. The only significant nearshore sand is found as a narrow wedge approximately 4-m thick just offshore of Brown's Inlet that tapers both offshore and towards the southwest. Sidescan and sub-bottom

data indicate that the rest of the nearshore (water depths up to 11 m) is characterized by either a thin (<20 cm) veneer of sand overlying indurated hard bottom; or relict sediments.

#### **1.4 Barrier Island Formation and Geomorphology**

A barrier island is “an elongate, essentially shore parallel, island composed dominantly of unconsolidated sediment, which protects the adjacent land mass and is separated from it by some combination of wetland environments” (Davis, 1994). Barrier Islands make up approximately 6% of the global open ocean shoreline, the majority of which, (roughly 73% by length) are located along trailing edge margins where the broad, gently sloping continental shelf is most conducive to barrier-island development (Stutz & Pilkey, 2001). Theories of the primary mechanism driving barrier island formation have been debated for over 150 years, beginning with Elie de Beaumont’s hypothesis that wave action in shallow waters pile up sediment to form a bank or barrier that parallels the original shoreline (de Beaumont, 1845). Forty years later Gilbert (1885) asserted that barriers result from agitation in the breaker zone stirring up sediment which is transported down-drift, forming a spit which is subsequently breached and converted to a barrier island. Shortly thereafter, McGee (1890) shifted the emphasis towards the influence of changing sea levels with the hypothesis that barriers result from rising sea level and the drowning of former beach ridges. The debate over which of these three dominant competing theories: (1) emergent bar, (2) spit elongation, or (3) drowning of beach ridges is the primary mode of origin continues to some degree to this day. There is, however, a greater acceptance that under various conditions each of these mechanisms may, and likely do, take place.

The principal factors affecting barrier island morphology are sea energy (waves, wave-generated and tidal currents), wind energy (wind-driven currents and aeolian transport), sediment supply, substrate gradient and composition, sea level, and anthropogenic activities (Leatherman, 1979; Davis, 1994). Early classification of barrier islands followed Davies’ (1964) classic



distinction between micro, meso, and macro-tidal coasts (Hayes, 1979). Hayes (1979) began to emphasize the role that waves play (in addition to tidal range) in shaping barrier islands and thus developed the current classification of barrier islands as either wave-dominated, mixed-energy, or tide-dominated (Figure 1-6). Wave-dominated islands are long (typically tens of kms or greater) and narrow, with few, relatively unstable inlets, large flood tidal deltas and relatively small or absent ebb tidal deltas. Mixed-energy islands are generally shorter (only a few kms in length) and have numerous, relatively stable inlets with more prominent ebb tidal deltas. Hayes (1979) presented the barrier island drumstick model for islands (typically found in mixed-energy settings) where the refraction of waves around an ebb tidal delta results in the reversal of the sediment transport direction on the island downdrift of the inlet. The sediments deposited in the lee of the delta produce an island with one wide, prograding end and one narrow, transgressing end resulting in the characteristic “drumstick” shape. Although rare, tide-dominated barriers do exist in places such as the Bay of Fundy and along the coast of Georgia.

## **1.5 Overwash Processes and Morphologies**

The process of barrier island overwash occurs when wave run-up and/or storm surge exceeds dune crest height, resulting in the unidirectional flow of sediment-laden water over the beach crest towards the back of the island (Schwartz, 1975; Leatherman, 1979; Davis, 1994; Donnelly et al., 2006). Recent work (Morton et al., 2000; Sallenger, 2000; Donnelly et al., 2006) has further refined this basic definition to distinguish between two overwash regimes: 1) run-up overwash, and 2) inundation overwash. Run-up overwash occurs under conditions of excess wave run-up and is generally associated with lower-magnitude events where water is funneled either through a local discontinuity or gap in the beach or dune crest and spreads laterally on the backbarrier. Inundation overwash occurs when mean water level exceeds the beach crest and is most likely to occur during extreme storms or on low-lying barrier islands with poorly developed

dune crests. These regimes are not mutually exclusive and may occur together either during different phases of a storm or simultaneously over varying distances alongshore.

Although the terms overwash and washover are sometimes used interchangeably, Donnelly et al. (2006) distinguishes “overwash” as the physical process by which water and sediment is carried over a dune crest across land or in reference to the mass of water itself, while “washover” refers to the actual material deposited inland of a beach by the action of overwash. The degree to which overwash occurs is dependent upon multiple factors, including storm surge, magnitude and duration, wind strength and direction, wave height and period, tide, height of the dune crest, presence or absence of vegetation, beach topography, and nearshore bathymetry (Donnelly et al., 2006). It therefore follows that the morphology of individual washover deposits will vary with location and from storm to storm as well as with changes in slope and percolation rates of the underlying sediments.

Three common washover morphologies are the washover fan, washover terrace, and sheetwash (Figure 1-7). Washover fans generally result from run-up overwash where a gap in the dune or beach crest is exploited, funneling the sediment-laden water mass through the throat or neck of the overwash. As the water mass spreads laterally on the back barrier, percolation and friction slow the flow velocity, and the entrained sediment is deposited as a lobate or fan-shaped feature. If adjacent fans are close enough in proximity that they begin to merge laterally, the deposits can form a washover terrace (also known as a washover apron). Sheetwash is formed under the inundation regime and dominates a wide lateral extent of beach with a more expansive washover deposit. Sheetwash most commonly occurs on low-lying barriers or spits with poorly developed beach or dune crests, although it may also occur on islands with large dunes, which as a result of persistent wave attack, have become susceptible to sheetwash (Donnelly et al., 2006).

## 1.6 Objectives, Hypotheses, and Outline

The primary objectives of this research are to:

1. Calculate the volume of sediment contained on the island above a geologically-defined base.
2. Determine if GPR can successfully distinguish sub-surface washover deposits.
3. Approximate the volume of sediment within the active overwash complex composed of sedimentologically distinct washover deposits.
4. Characterize changes in subaerial expressions of overwash from 1938 to 2008 and relate this to spatial and temporal trends in shoreline change.

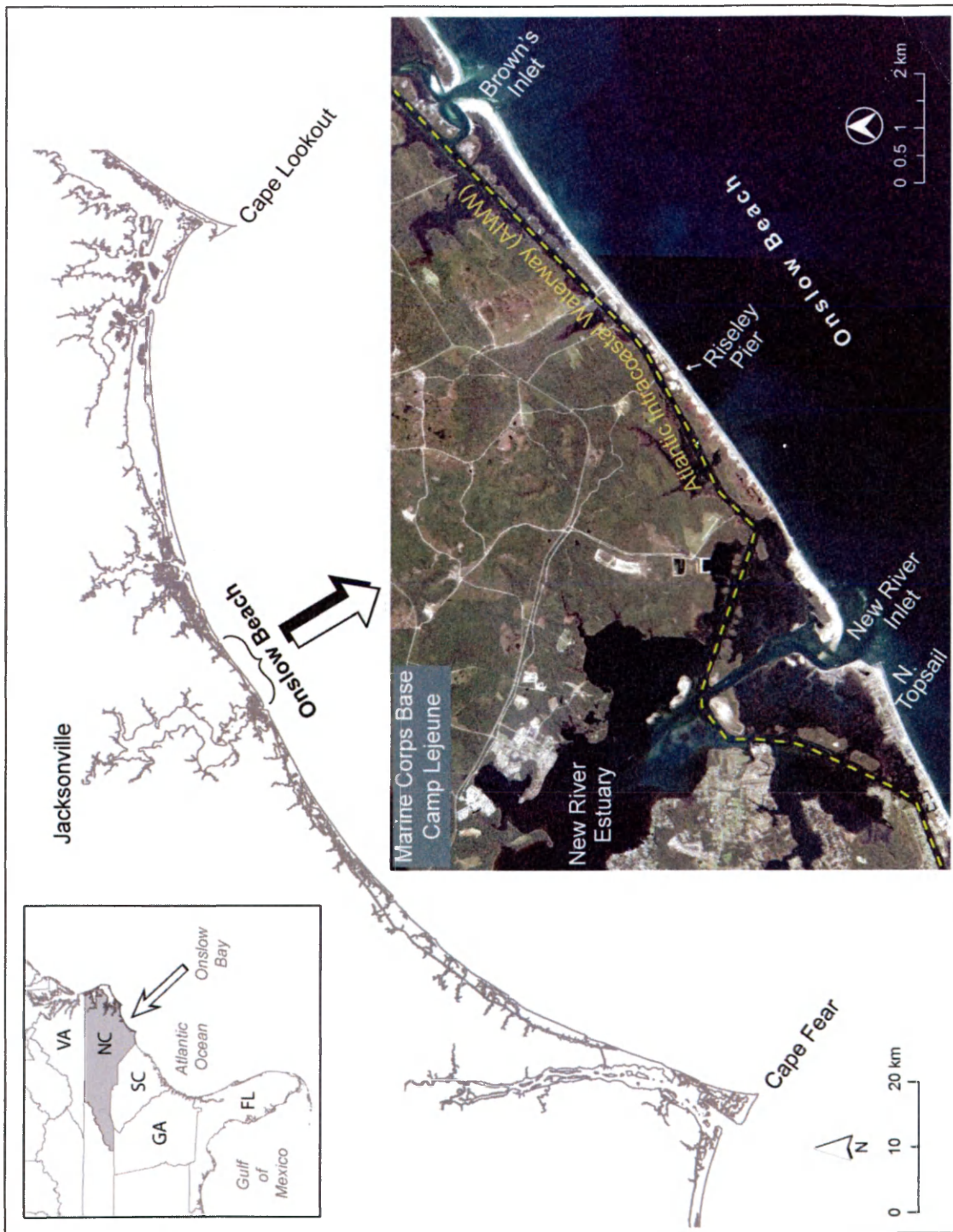
The hypotheses being tested include:

1. Longshore variations in the volume of the geologically-defined sand prism is inversely correlated with long-term shoreline erosion rates (i.e., smaller prism = more erosion).
2. Volume of washover deposits is positively correlated with beach erosion.
3. Surficial overwash expression has increased in area from the 1938 to 2008.

Chapter 2 focuses on the use of GPR and sedimentary analyses to quantify the relevant-sand prism and washover component of southern Onslow Beach (addressing Objectives 1-3 and Hypotheses 1-2). The third chapter evaluates spatial and temporal trends in shoreline position and overwash extent (addressing Objective 4 and Hypothesis 3). Chapter 4 provides an overall discussion, plans for future work, and conclusions. Chapters 2 and 3 have been written in the format of articles for submission to peer-reviewed journals. Thus additional background and motivation for the specific objectives listed above are provided in the introductory sections of each of these chapters.

## 1.7 Chapter 1 Figures

Figure 1-1.



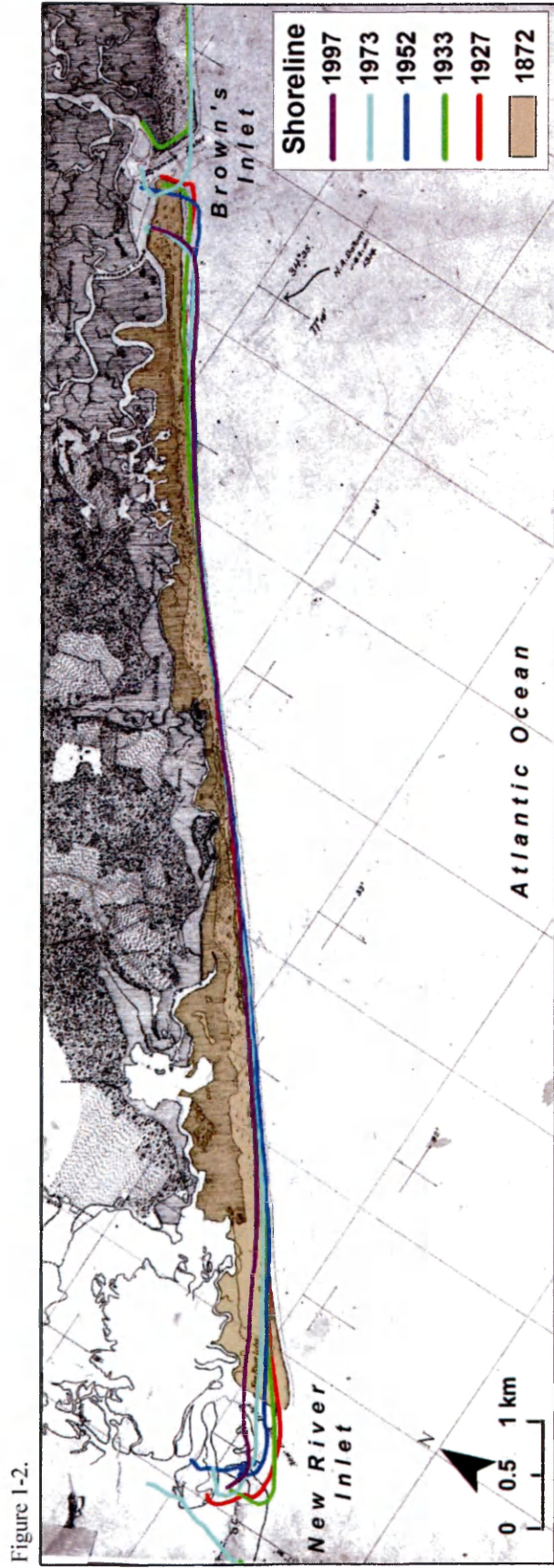


Figure 1-2.

Figure 1-3.

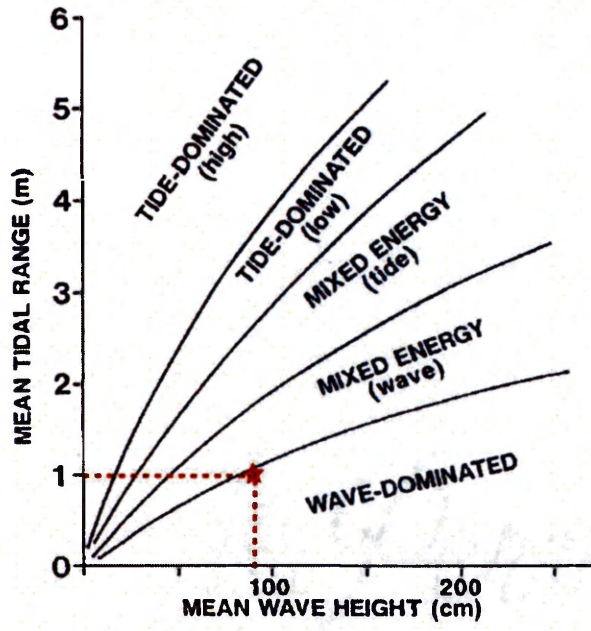




Figure 1-4.

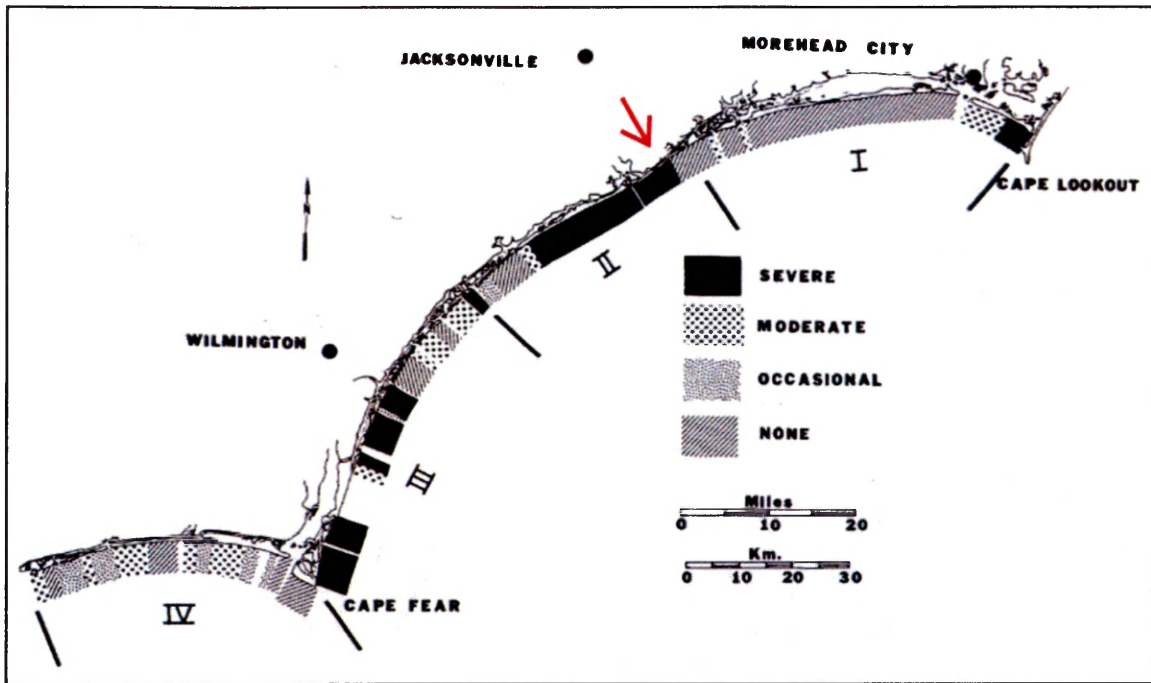




Figure I-5.

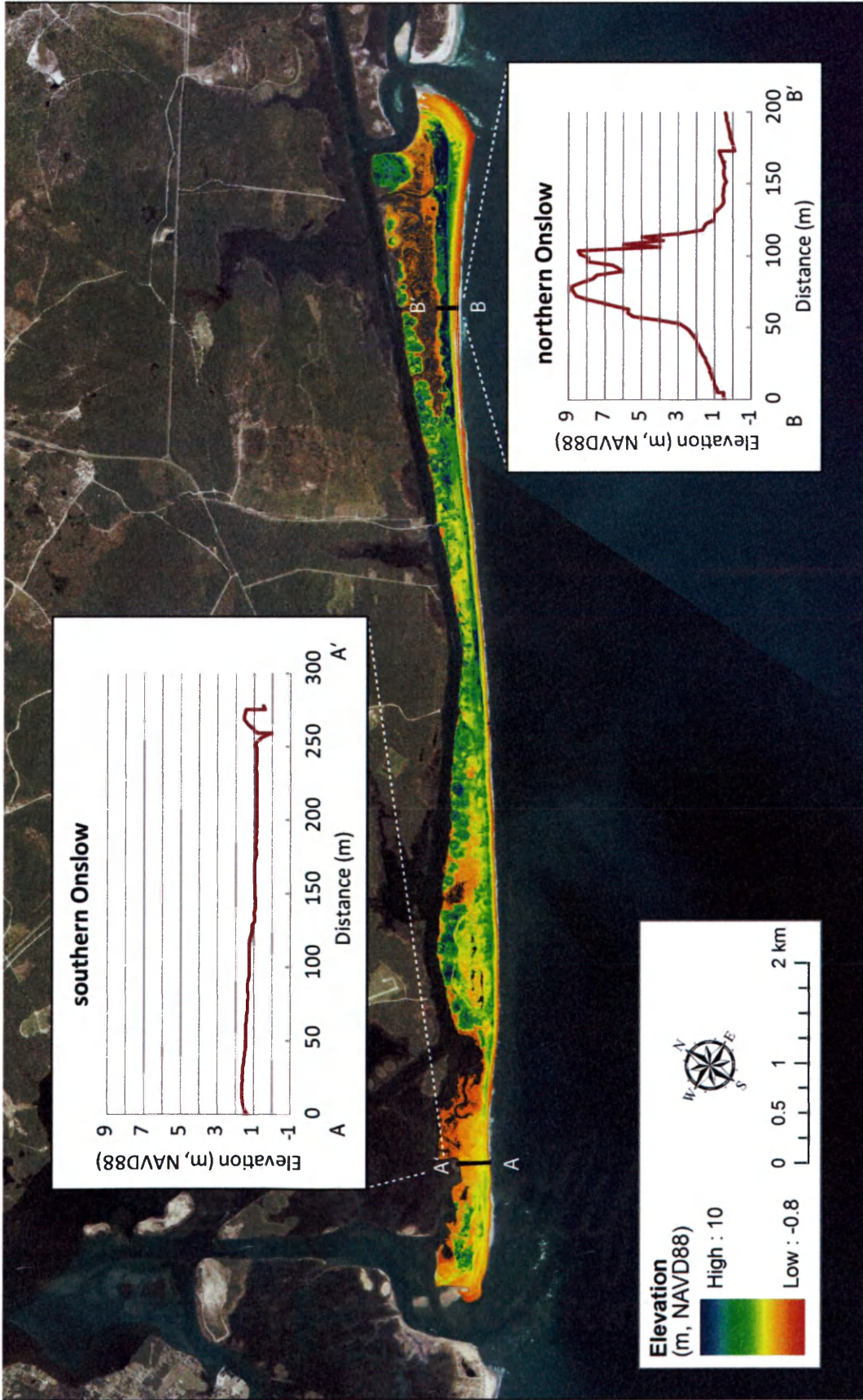


Figure 1-6.

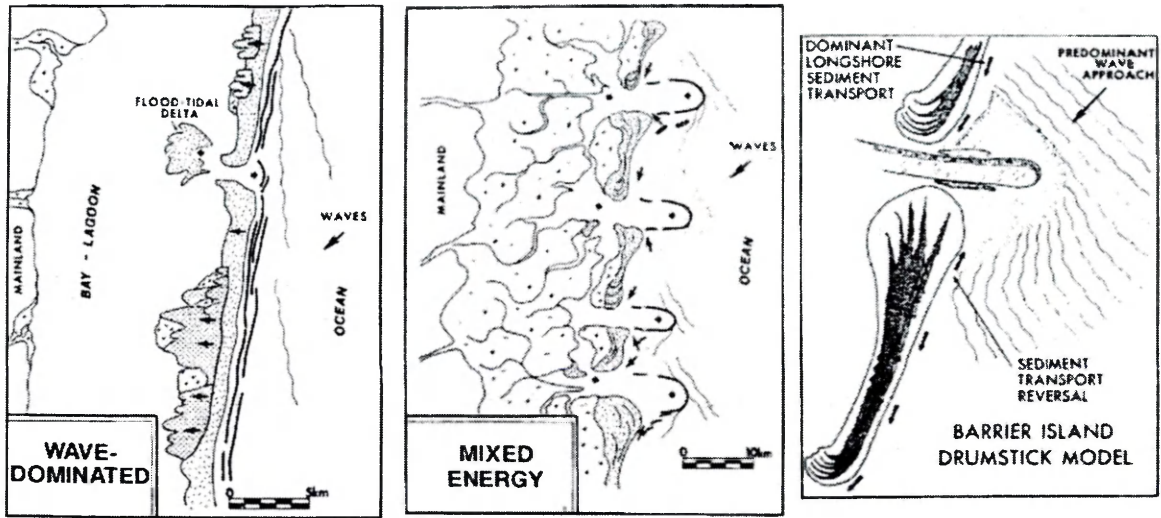
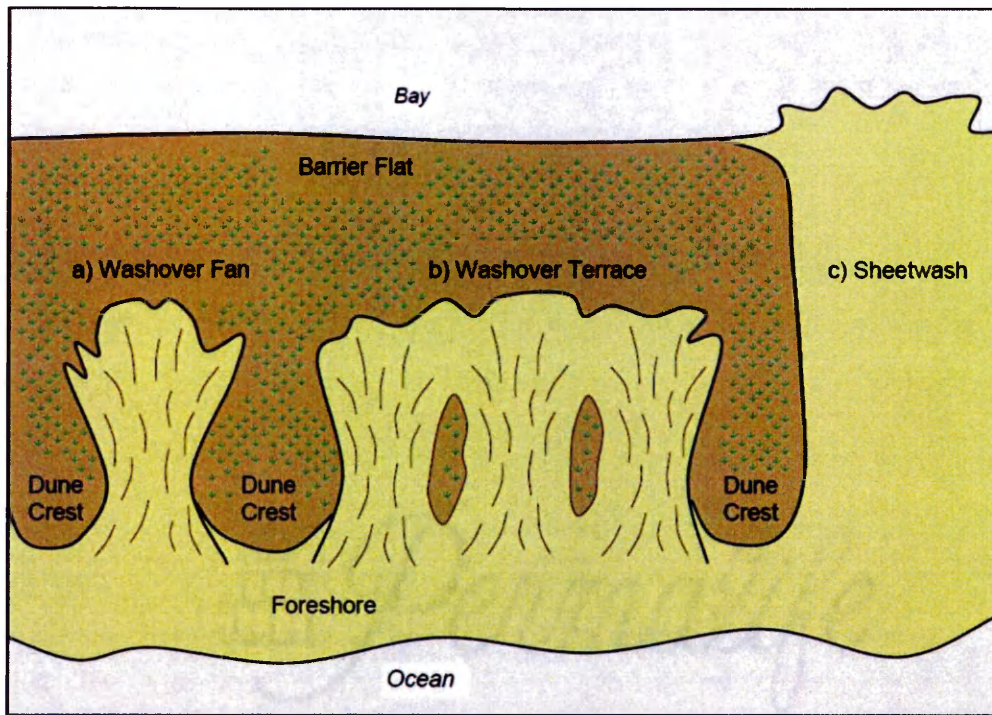


Figure 1-7.



**CHAPTER 2**  
**WASHOVER VOLUME AND SEDIMENTARY CHARACTERISTICS**

## 2.1 Introduction

Numerous scientific studies recognize the importance of barrier island overwash as an important mechanism for transporting sediments onto and/or behind the barrier surface, supporting backbarrier marsh habitats, and maintaining barrier islands in the face of rising sea level (Godfrey, 1970; Dolan, 1972; Leatherman, 1983; Kochel & Dolan, 1986; Davis, 1994). Despite the fact that washover may be a substantial loss term in the calculation of littoral budgets and a potential gain term in the sediment budget of the island itself, limited quantitative data exist on total washover volume retained within barrier islands and its net influence on the coastal sediment budget remains largely unknown. While traditional field techniques provide reliable measures of washover sediments transported via individual storm events or multiple events over a small area, they lack the spatial and temporal scope necessary to evaluate the role of overwash in island evolution over the time span of years to decades.

This research improves upon traditional coastal-sand prism estimates by determining a geologically-defined base as opposed to simply applying a fixed-depth boundary. The island's underlying stratigraphy was mapped using Ground-Penetrating Radar (GPR) and ground-truthed by sediment vibracores, enabling a precise measurement of the depth of the underlying silty/peat contact. This innovative approach not only provides a more accurate constraint on sediments readily available for transport, but also captures the spatial variability of the underlying base, which has been largely neglected in previous studies. The volume of sediments within this prism exhibiting sedimentary characteristics directly attributable to overwash events is estimated from sediment cores. The analysis of washover deposits preserved within the sediment column provides the long-term perspective necessary to accurately quantify the importance of overwash as a mechanism for barrier island migration at Onslow Beach, NC. This information is valuable on both local and regional scales for advancing the understanding of how barrier islands respond to changes in external forcings (e.g., sea-level rise, storms, etc.) and, in turn, will enable further refinement of models that forecast shoreline behavior.



## **2.2 Background**

### **2.2.1 Hurricanes Bertha and Fran**

The most recent storm to cause extensive overwash on Onslow Beach was Hurricane Fran (Class III) which made landfall on September 5, 1996, and generated a storm surge of 2.9 m on nearby North Topsail Beach (Cleary et al., 2001). The effects of Hurricane Fran were amplified by the fact that Hurricane Bertha hit the same region just two months prior (July 12, 1996) as a Class II Hurricane. This was the first time in 41 years that two hurricanes struck the North Carolina coast during the same season (Barnes, 2001). Figure 2-1 shows the expansive sheetwash created along the southern portion of our study area resulting from the delivery of significant amounts of sediment to the backbarrier. Channels that previously meandered through marsh along the back of the barrier were buried in washover sediments, creating drastic alterations to the topography.

### **2.2.2 Geologically-Defined Sand Prism**

Calculating sediment volume of a barrier island or coastal region necessitates the identification of an underlying surface that represents the base of the sand prism. Traditional studies use cross-shore and alongshore uniform depth of closure-based baselines, which often overestimate nearshore-sediment prism volumes and neglect any spatial variability in baseline morphology. Recently, Miselis and McNinch (2006) illustrated that in the subaqueous environment the use of geologically-defined baselines, which may vary in depth both alongshore and cross-shore, provides a more accurate estimate of the active nearshore sand prism than the depth-of-closure method, and more closely corresponds to long-term trends in shoreline movement. On transgressing barrier islands, the geologically relevant baseline is most-likely the relict underlying marsh platform upon which landward migration occurs. Underlying peat deposits exposed on beaches, such as those visible at low tide on Onslow Beach, are indicative of this marsh surface and a clear indication of the sand-prism base (Figure 2-2). The volume of

sediment above this geologically-defined base, henceforth referred to as the relevant-sand prism, represents the sediment that can be actively transported via wind or sea energy and thus provides a much more realistic measure of sediment readily available for barrier island migration. Over longer geologic timescales the lower-lying depth of ravinement, an erosional transgressive surface, could be considered the base of the sand prism. For the scope of this project, however, and for timescales of most concern to coastal managers (years to decades) we are focusing only on readily available sediments above the upper-most peat layer. In this study, the approach that Miselis and McNinch (2006) applied to the subaqueous environment is being applied to the barrier island itself by mapping this underlying peat contact using GPR ground-truthed by sediment cores.

### **2.2.3 Previous Overwash Studies**

To the best of our knowledge, there are no prior studies of wave-dominated barrier islands in the US that have directly measured the cumulative volume of washover sediments within the context of the island's sediment budget. Research conducted on a barrier spit in the northern European Wadden Sea (Christiansen et al., 2004) estimated that washover sediments comprise 51% of the spits' sediment budget above present sea level. Research by Inman and Dolan (1989) used aerial extents of washover deposits calculated by Dolan et al. (1979) in combination with measurements of washover thickness (Kochel & Dolan, 1986) to estimate overwash transport rates along the Outer Banks, North Carolina, but focused only on the flux of sediments without respect to the standing volume of the island itself. For the stretch of coast between Cape Henry and Cape Hatteras Inman and Dolan (1989) estimated overwash transport rates ranging from 1 – 10 m<sup>3</sup> per linear meter of beach annually, but readily admitted that transport rates associated with overwash processes and windblown sands were “probably the least accurately known components of the budget.”

Prior field studies aimed at determining the relative importance of overwash vs. aeolian transport in the vertical accretion of barrier islands have generated conflicting results (Leatherman, 1976; Fisher & Stuable 1977; Rosen, 1979; Cloutier & Hequette, 1998) which is likely due to the spatial and temporal limitations of traditional field measurements. Kochel and Wampfler (1989) asserted that variations in overwash fan surfaces depend primarily upon the frequency and magnitude of overwash and precipitation, as well as local topography. The influence of temporally variable climatic factors upon sediment dynamics of washover fans documented by Kochel and Wampfler (1989) underscores the need for long-term observation periods (10+ years) and highlights why long-term budgets derived from short-term observations may produce misleading results.

Without pre and post-storm elevation data, this study is unable to discern if the amount of washover preserved in the sediment column equals the original volume of net sediment aggradation, and/or if this volume has been decreased via scour or aeolian deflation. This analysis does, however, provide the long-term assessment of washover deposits that Kochel and Wampfler (1989) found to be critical in minimizing bias associated with observations spanning less than 10 years. This research provides a more spatially and temporarily expansive approach to quantifying washover, which cannot be obtained by traditional monitoring efforts, and when used in conjunction with geospatial analyses, will aid in the development of algorithms or models to quantify overwash occurrence and deposited sand volume.

#### **2.2.4 Sedimentary Characteristics of Washover Deposits**

Washover deposits are often preserved in backbarrier sedimentary sequences and can be distinguished by alternating layers of peat and sand or by specific sedimentological characteristics such as grain size and mineralogy (Heron Jr. et al., 1984; Davis, 1994; Hippensteel & Martin, 1999; Buynevich et al., 2004; Donnelly et al., 2004). Washover can extend landward up to a few



hundred meters, and estimates of the thickness of individual washover units range from a few tens of centimeters (Davis, 1994) up to a meter thick (McCubbin, 1982). Multiple overwash episodes may result in a composite fan that is meters thick (Davis, 1994). In undeveloped settings, washover sequences are likely superimposed upon vegetated backbarrier surfaces, dunes, or previously deposited washover sequences, which may have been altered since initial deposition by aeolian transport. Identifying the base of washover deposits is essential for isolating the boundaries of a single storm deposit. Schwartz (1975) found the occurrence of thin, dark, organic-rich sandy or silty sediments, occasionally containing vegetation, a useful indicator marking the top of the pre-storm surface.

Washover deposits may include transported shells, mud clasts, and other oceanic debris concentrated at the base of each unit, decreasing in abundance and average size upward in the unit (McCubbin, 1982). Internal structure of the strata consists of rhythmic alternations of fine and coarse sediments and occasional heavy mineral-rich laminae, with the sedimentation units typically exhibiting a scour base (Schwartz, 1982). Textural trends reveal normal and inverse grading between the sub-units and a coarsening or fining in the direction of flow (Schwartz, 1982).

Schwartz (1982) analyzed washover deposits from three sites in the US, each with very different geomorphic settings: (1) a North Carolina barrier island; (2) a southern California mainland beach; and (3) a spit on the shores of Lake Erie. Despite the different physical conditions and forcings, common sedimentary structures were found at each location. Two distinct stratigraphies reflect the environment at the time of deposition (Figure 2-3). Fans that develop overlying what is normally a subaerial surface tend to be dominated by sheetflow. The resultant washover stratigraphy consists of a plane bed and sub-horizontal to low-angle ( $< 5^\circ$ , landward dipping) planar stratification (McCubbin, 1982). In instances where overwash flow continues across the subaerial terrain and terminates into a standing body of water, such as a pond

or lagoon, delta foreset stratification develops due to slipface migration of the advancing front (Davis, 1994). Foreset stratification may either exhibit sigmoidal topset-foreset-bottomset forms or truncation by overlying topsets (McCubbin, 1982).

### **2.2.5 Ground-Penetrating Radar in Geologic Studies**

GPR is quickly becoming one of the most important geophysical instruments used in coastal barrier studies (Jol et al., 1996). Although the use of pulsed electromagnetic waves in subsurface investigations began as early as the 1920s, it was not until the 1980s that commercial GPR systems capable of digital acquisition became readily available, and by the mid-1990s, their use in geologic studies skyrocketed (Neal, 2004). The basic principles of GPR are analogous to seismic data in terms of wave propagation, reflection, and refraction in response to subsurface discontinuities. GPR, however, can obtain much higher vertical resolutions, on the order of 20 cm versus > 1 m for traditional seismics (Neal, 2004). The frequency of GPR systems range from 10 to 1000 MHz, and systems consist of either a single antenna that alternates between transmitting and receiving modes, or separate transmitting and receiving antennas.

The GPR system emits a short pulse of very high-frequency electromagnetic energy into the ground. When the pulse intersects differences in dielectric properties within the subsurface, some of the energy is reflected back to the surface and is detected by the receiving antenna. The amplitude and two-way travel time, measured in nanoseconds, of the reflected pulse is recorded. Horizontally sequential reflection traces build up a radar reflection profile. The signal propagation velocity through the ground can either be calculated using a common mid-point survey, correlated with geological logs, or estimated based upon published velocities for given substrates (Neal, 2004) to estimate depth of the reflection surfaces. The most common method of GPR collection is known as “common offset” where the transmitting and receiving antennae are

moved in unison along the survey line (Neal, 2004; Woodward et al., 2003). Data can either be collected continuously or triggered at fixed distances in a stepwise fashion.

GPR reflections can result from: 1) changes in the amount and type of fluid occupying pore spaces; 2) minor differences in porosity; and 3) changes in sediment mineralogy, shape, or orientation (Neal, 2004). The basic premise of using GPR in sedimentary analyses is that the majority of the aforementioned properties also change with transitions between distinct sedimentary facies, resulting in a direct relationship between the primary radar reflections and underlying stratigraphy (Neal, 2004). As with all geophysical instruments, it is important that interpretations of GPR reflections are well supported through ground-truthing and evaluated critically.

A drawback of using GPR in coastal environments is the likely attenuation of the electromagnetic signal by layers of salt-marsh peat, silts, clays, and saline water, thereby limiting the depth of penetration (Van Heteren et al., 1998; Bristow & Jol, 2003). Despite these potential interferences, a number of GPR studies have shown excellent results in coastal settings and barriers where a freshwater aquifer exists (Jol et al., 1996; Van Heteren et al., 1996; Moller & Anthony, 2003; Buynevich et al., 2004). Moore et al., 2004; GPR offers great advantages over traditional methods for determining the depth and internal structure of washover deposits (such as digging pits and trenches or collecting numerous sediment cores), in that GPR offers a nondestructive means of producing high-resolution, continuous images of underlying sedimentary structures in a time and cost-effective manner.

### **2.3 Methods and Materials**

The focus of this study is the southwestern half of Onslow Beach, south of Riseley Pier, which is where overwash is most predominant and also encompasses the area where military amphibious training drills take place. GPR was collected in a shore-parallel transect running the

length of our study area to map the location of the geologically-defined base, and additional transects were collected, along with sediment vibracores, in four overwash sites. The sites are denoted in Figure 2-4, each representing a different environment: (1) a large sheetwash deposit at the southern end of island that is largely undisturbed by human activity; (2) a single fan with a narrow throat and recovering dune crest, not exposed to vehicular traffic; (3) two adjacent overwash fans, or an overwash apron, experiencing some foot/automobile traffic; and (4) an overwash fan heavily subjected to regular military training activities and vehicular traffic.

The zone of active overwash was defined based upon 80 cm resolution IKONOS satellite imagery collected in 2008. For the purpose of this study, the region of active overwash refers to the area seaward of the vegetation line and landward of the dune toe but excludes vegetated foredune habitat that has been separated from the backbarrier as a result of a shore parallel beach access road. Any such isolated vegetation clusters with an area  $> 20 \text{ m}^2$  have been excluded from calculations of the zone of active overwash. The dune toe was delineated based upon satellite imagery and the change in slope captured by 1-m resolution bare earth lidar collected in 2007 for the National Geospatial-Intelligence Agency or NGA. The vegetation line was selected because it is easily distinguishable in aerial imagery and based upon ground surveys, provides a good approximation of the landward extent of recent overwash events. Any historic overwash sites, however, which have revegetated prior to 2008 are not included in our estimates. Calculations of total island area extend from the wet/dry line on the seaward edge to the point where land intersects water on the landward edge, which for the majority of the study area coincides with the AIWW.

### **2.3.1 Sediment Samples**

Twelve sediment vibracores ranging from 102 – 182 cm in length were collected from four overwash sites both to ground-truth GPR records and to document the sedimentological

signatures of washover deposits (Figure 2-4). The majority of cores captured peat deposits, and in all but one instance, penetrated to a depth where the sediments transitioned from sand to darker, more organic-rich, silty or clayey sediments. This contact is indicative of a depositional environment different from the overlying sediments and was identified as the base of the relevant sand prism. From here on, this contact will be referred to as the sand/silt contact; more detailed sedimentological information is provided in Appendices I and II.

Sediment cores were collected using a beach vibracore system with 7.6 cm diameter aluminum barrels. Cores were split lengthwise, photographed, and described. The cores were sub-sampled at 2 cm intervals and placed in air tight bags for archiving. Grain-size analyses were performed upon samples at 10 cm intervals down to the depth of the onset of the non-sand dominated (i.e., silt or peat) substrate. The fine fraction was removed by wet sieving the bulk sample through a 62  $\mu\text{m}$  mesh (ASTM No. 230), and the gravel fraction was extracted by dry sieving the resultant sample through a 2,000  $\mu\text{m}$  mesh (ASTM No. 10). The proportion of gravel, sand, and fine-sized sediments were calculated through comparison to the dry weight of the initial bulk sample. The sand-sized fraction ( $-1\phi - 4\phi$ ) was run through a Rapid Sediment Analyzer (RSA) settling tube. A Matlab<sup>TM</sup> script was developed to analyze the weight distribution of each sample to derive hydraulically equivalent grain size distributions based upon the Ferguson and Church (2004) hybrid equation. This unique approach reduces to Stokes' Law for finer sand-sized particles and a constant drag for coarser sands where Stokes' Law no longer accurately predicts settling rates. Water density and eddy viscosity values were assigned based upon water temperature within the settling column at the time each sample was processed and the particle density of quartz ( $2.65 \text{ g/cm}^3$ ) was assumed. Weight distributions of hydraulic size equivalents (in psi) were generated for each sample. Psi is a logarithmic velocity scale equal to  $\log_2 \times$  velocity (in cm/sec) (Middleton, 1967) which serves as a better representation of sedimentary behavior in hydrodynamic environments than do sieve-determined size distributions (Reed et al.,

1975). Due to the fact that there is not uniform agreement on which formula to use in the conversion of settling velocities recorded by the RSA into equivalent particle diameters (Syvitski et al., 1991), as well as the inherent assumptions with such formulas, results are presented in psi.

Settling-velocity distributions were calculated for all samples and standard descriptive statistics (mean, median, standard deviation, skewness, and kurtosis) computed using the method of moments. Settling velocities computed using the RSA data assume a grain density of quartz ( $2.65 \text{ g/cm}^3$ ) and although the carbonate shell hash present in some samples may slightly bias the data towards a finer grain size, we chose not to selectively remove carbonate from our RSA samples because it is a valid component of a hydraulically representative washover deposit. For reference, 12 samples were soaked overnight in a dilute (10%) hydrochloric acid solution to calculate an approximate range of carbonate content. Five surface sediment samples were collected from active dune sites and processed using the same RSA approach to aid in distinguishing between different depositional environments.

The grain-size analyses described above were used in combination with visual inspection of the split cores to discern facies exhibiting sedimentary characteristics consistent with washover deposits. The cumulative thickness of distinct stratigraphic layers from within each core representative of washover deposits was recorded and used as the basis for volumetric calculations of washover. Typical distinguishing characteristics included: poorly-sorted sediments, which may have contained shell fragments and/or heavy mineral laminae. The basal contact tended to be sharp and may have exhibited scour, often coarser sediments were concentrated at the base of the deposit which is consistent with prior washover studies (Schwartz, 1975; McCubbin, 1982; Schwartz, 1982; Kochel & Dolan, 1986). The argument could be made that since Onslow Beach formed offshore thousands of years ago and arrived at its present day location through barrier island rollover, the entire island is composed of washover deposits. For the context of this research, however, we are concerned with more recent overwash events and

the modes of sediment transport actively shaping the barrier island today. Thus said, the term “washover deposits” refers to the sedimentologically distinct facies within the active overwash zone as described above. A first-order estimate of total washover volume was calculated by multiplying the average thickness of washover deposits determined from sediment cores by the surface area of the island falling within the active overwash region.

To examine changes in sediment water content, ten short cores (from 54 – 107 cm in length) were collected using a small jackhammer corer with 3.8 cm diameter plastic barrels. These cores were collected in conjunction with the 200 MHz GPR surveys, sliced open in the field, and sampled immediately to detect changes in percent water content which aid in the interpretation of GPR data. Sediments were sub-sampled at an approximate 10 cm interval and placed into pre-weighed scintillation bottles. Water content was determined by weighing the samples before and after drying to determine the mass of water lost.

To expand depth measurements of the sand/silt contact seaward, elevations of the contact from the foreshore and backshore were provided by colleagues on the DCEPR project for an additional seven cores collected using a jackhammer corer. In addition, Real-Time Kinematic (RTK) Differential GPS (DGPS) measurements of peat exposed in the foreshore were collected to provide additional control points for interpolating the baseline of the relevant-sand prism seaward of GPR measurements.

### **2.3.2 Ground-Penetrating Radar**

A pulseEKKO PRO™ GPR was used to examine the underlying stratigraphy of Onslow Beach. The resolution of GPR systems, or the finest feature the instrumentation is able to resolve, varies depending upon the frequency of the transmitting antennas. Both 100 MHz and 200 MHz antennas were used in this study. The vertical resolution of the 100 MHz antenna (20-25 cm) was sufficient for defining the base of the geologically-defined sand prism and was used

to collect a shore-parallel transect running the length of the study area as well as a select number of shore-normal transects. GPR surveys within overwash fans were also collected using the 200 MHz antennas with a vertical resolution of 13-15 cm (Jol, 1995; Sensors & Software, 2003) in order to differentiate between small scale (order of 10s of cm) variations in sedimentary characteristics indicative of washover. The accuracy, or closeness of GPR measurements to true values, and the precision, or repeatability of the GPR measurements are addressed in Section 2.3.4.

The GPR units were mounted to custom sleds with the 100 MHz antennas fixed at a distance of 1 m apart, and the 200 MHz spaced 0.5 m apart. The GPR was set to collect continuously while towed along the surface either by hand or by a Kubota all-terrain vehicle (Figure 2-5). Effort was made to maintain a steady walking/driving pace that would result in recorded traces approximately every 25 cm with the 100 MHz, and every 10 cm with the 200 MHz antennas. A RTK DGPS survey with a vertical and horizontal accuracy of up to 2 cm was collected in conjunction with the GPR survey to tie transects to real-world coordinates. The beginning and end coordinates of each transect were taken from the GPS and, based upon the total length of each transect, the position of individual GPR traces were linearly interpolated and the profiles shifted to account for variations in topography. A total of over 15 km of GPR transects were collected throughout the study area (Figure 2-4).

Standard processing steps were applied including the application of a DEWOW filter to remove low-frequency noise resulting from electronics saturation at the surface, a trapezoidal bandpass filter (10-40-140-280 MHz and 10-40-325-650 MHz for the 100 and 200 MHz surveys, respectively) to remove noise at the high and low end of the amplitude spectrum, and automatic gain control (AGC) to compensate for the rapid decrease in radar-signal amplitude from deeper depths. The conversion from two-way travel time to depth was calculated by assuming a uniform velocity for the propagation of electromagnetic energy of 0.1 m/ns. This value falls within the



published range of velocities for unsaturated sand of 0.1 - 0.2 m/ns (Neal, 2004). Since profile depths were not adjusted to account for the slower travel of electromagnetic energy through the deeper, water-saturated sediments, depths beneath the water table only represent an approximate elevation, and are likely slightly overestimated.

To enhance geologic interpretation, the GPR profiles were hung in 3D space using Interactive Visualization Systems' (IVS 3D) Fledermaus<sup>TM</sup> software. Each transect was georeferenced and assigned proper elevation values (relative to NAVD88) to create fence plots of the entire GPR survey. Figures 2-6 and 2-7 demonstrate how sediment cores were used to aid interpretation of the GPR record. The coordinates of the sand/silt contact as obtained from sediment cores and DGPS measurements at locations where peat is exposed within the surf zone, were also imported into the Fledermaus<sup>TM</sup> scene. The measured elevations of the sand/silt contact were combined with the GPR reflection profiles to facilitate in the identification of the reflector representative of the sand/silt contact. Due to the large surface area of the southern sheetwash site (Site 1), interpretation of the sand/silt contact was dependent largely upon the morphology of the GPR reflection surfaces. The GPR revealed a number of buried channels within this site, and these reflection surfaces, indicative of past fluvial features, were selected to indicate the base of the relevant-sand prism (Figure 2-8). Reflection surfaces were not always continuous across the entire length of the sheetwash, and therefore, fluvial surfaces at the southern end of the site were not necessarily the same facies as those observed on the northern end. Overall, the best reflection surface at any one location was presumed to be representative of the sand/silt contact, and its elevation recorded (Figure 2-9).

The generation of 3D fence plots not only aided in visualization and facies interpretation, but also enabled us to trace individual reflection surfaces and export coordinate data as x, y, z ASCII text files. Since the GPR profiles were all georeferenced to common horizontal (NAD83) and vertical (NAVD88) datums, the reflection surfaces were exported directly to a GIS for

volumetric calculations. The traced GPR reflections were combined with the elevation point data of the underlying sand/silt contact from beach vibracores and DGPS measurements of peat exposed within the swash zone, and the combined datasets were interpolated into a continuous raster surface depicting the elevation of the contact throughout the study area. To improve the ability of the gridding algorithm to capture the complicated buried channel features at Site 1, contours were added at the edges of the channels seen in March 1996 aerial photographs (Figure 2-1) and assigned an elevation consistent with the nearest GPR reflection surfaces. Due to the lack of GPR or core measurements along the back side of the island, a contour was added at a distance of 50 m landward of the island boundary, and elevations assigned in accordance with the nearest GPR data. A similar contour was added 50 m seaward of the wet/dry line (Figure 2-10). These contours were added to force the gridding algorithm to interpolate elevations from the seaward side of the island across the width of the island to the AIWW. The extrapolated elevations in regions distant from field measurements are less reliable, but since the underlying peat surface that we're mapping is not likely to experience large variations in topographic relief, a linear extrapolation was acceptable. A 1-m resolution grid representing the depth of the sand/silt contact was generated using the ArcGIS™ "Topo to Raster" tool which utilizes both point and contour data in an iterative finite difference interpolation algorithm to generate a continuous elevation model (Figure 2-11). Subtracting this sand/silt contact elevation model from bare earth lidar (collected in 2007 for the National Geospatial-Intelligence Agency or NGA) provides an estimate of thickness of the relevant-sand prism throughout the study area (Figure 2-12). The southernmost km of the island is known to be dominated by inlet dynamics, based upon an 1872 T-sheet, and as a result, was excluded from analyses.

### **2.3.3 Spatial Correlation with Shoreline Change**

To compare how our measurements of sand prism thickness and washover volume vary in the alongshore with long-term trends in shoreline position, GIS data layers from the USGS National Assessment on Shoreline Change (Miller et al., 2005) were used. The same shore-normal transects (spaced at a 50-m intervals) used by Morton and Miller (2005) to calculate long-term (1872-1997) and short-term (1973-1997) shoreline change rates were used to calculate alongshore variations in the relevant-sand prism and washover volumes. Volume to the depth of the sand/silt contact was calculated per square meter of surface area ( $\text{m}^3/\text{m}^2$ ) along each cross-island transect. A first-order estimate of alongshore variations in washover volume was calculated by multiplying the average thickness of washover deposits determined from sediment cores by the surface area of the cross-island transects falling within the active overwash region (the area exhibiting signs of overwash discernable by 80 cm resolution satellite imagery collected in 2008).

### **2.3.4 Uncertainties and Errors**

Sediment prism calculations must take into account error introduced through uncertainties in horizontal positioning (x, y) as well as vertical (z) errors in surface elevations and/or depth within the sediment column. Table 2-1 lists the components accounted for in error assessment and an explanation of how they were estimated is provided below.

The error associated with delineating the vegetation line and wet/dry line from a 2008 IKONOS satellite image was minimized through the use of a GIS-based tool (BeachTools) developed by the US Army Corps of Engineers (Hoeke et al., 2001). BeachTools performs a clustered supervised classification based upon mean pixel values within an image and outputs a vector polygon encircling pixels of similar values. Although this minimizes human-induced error, some variability still remains due to which pixels are selected as the basis for classification.

The precision of the digitized vegetation line was assessed by repetitively tracing the same regions and computing the standard deviations of the output (5.6 m). Variability in the position of the shoreline must also account for the excursion of the wet/dry line over the course of a tidal cycle. Dolan et al. (1980) found that for medium-size sand beaches with slopes similar to the study area, the high water line (HWL) migrates within an average of 1-2 m over a 12-hour 25 minute tidal cycle. An average of uncertainty in the vegetation line (5.6 m) for the landward boundary in combination with the 2 m variability in position of the HWL for the seaward boundary equates a width of uncertainty of  $\pm 3.8$  m. Surface area uncertainty was approximated by calculating the area contained within a swath 3.8 m wide around the perimeter of the region of interest.

Vertical errors include accuracy of the elevation data obtained from lidar (RMSE = 15 cm) and the offset between the elevation of the GPR surface reflector (calculated based upon two-way-travel time) and the elevation as recorded by the DGPS. The latter was assessed by differencing surface elevations derived from the GPR profiles, from the DGPS measurements recorded at the time of data collection. The difference showed a mean offset of 25 cm (SD = 8) and 32 cm (SD = 6) for the 100 and 200 MHz GPR surveys, respectively. The appropriate offsets were applied to each GPR transect to better fit the GPR traces to the same vertical datum as the lidar survey (NAVD88). The average standard deviation of the offset between the GPR and DGPS elevations (7 cm) is used in error assessment. The precision with which the GPR reflection surfaces were traced in Fledermaus<sup>TM</sup> was estimated by repetitively tracing the same GPR profile and calculating the standard deviation between the outputs (2 cm).

The depth of the sand/silt contact within the sediment cores provides an excellent means of ground-truthing the elevation of the sand/silt contact as determined from the GPR profiles. The difference between the core and GPR-derived elevations were compared for 15 locations where sediments cores were collected within 8 meters of a GPR transect (Table 2-2). The majority of

measurements ( $n = 11$ ) show very good agreement between the sediment cores and GPR with a mean difference of 6 cm ( $SD = 15$ ). Four sediment cores collected towards the southwestern landward extent of Site 1 exhibit sand/silt contact depths within the sediment cores that are up to 2.5 m shallower than the GPR reflection. This could be the result of core compaction when vibracoring through the distal portion of a large sheetwash where increased pore spaces may lead to sediment compaction. In addition, three of these cores (ONSV25, ONSVC26, and ONSVC40) are instances where an actual peat layer was not captured. It is possible that there are sediments higher in silt content and/or peat layers deeper than we were able to penetrate with the vibracorer, and that the minor silty sediments that we captured in the cores were not significant enough to result in a distinct GPR reflection. Due to these reasons, the excessive offset between the sand/silt contact depth in the GPR and the sediment cores for this cluster of samples is not considered a reasonable representation of the error of the GPR and as a result, these values were not included in the calculation of survey error. The RMSE between the GPR versus core-derived depth of the silt/sand contact for the remaining 11 cores (53 cm) was used in error approximations.

An additional source of uncertainty that has not been quantified is the interpolation error, or the potential error in the elevation of the sand/silt contact in regions poorly constrained by field measurements. This is namely of concern over the landward side of the island, and along the northern third of the study area where the sand/silt peat contact could not be traced along the beach access road due to chaotic, discontinuous reflectors in the GPR record. A limited number of cores were collected along the back side of the island and in the AIWW by Sproat (1999) but since the topographic elevation of the cores was not recorded at the time of collection, we could not accurately georeference them to the same vertical datum as our measurements. In future field efforts we hope to collect measurements of the depth of the sand/silt contact along the back side of the island to minimize this interpolation error, however, it is unlikely that the underlying peat

surface varies greatly in elevation across the island, thus a linear interpolation provides a sufficient approximation. It is also important to note that the active washover volume calculations provided are likely underestimates of total island washover volume because they are restricted to the unvegetated surface of the study area in 2008, derived from 80 cm resolution IKONOS satellite imagery. Historic overwash sites which have revegetated are not included in these estimates.

## **2.4 RESULTS**

Interpretation of the GPR record demonstrates that it is possible to identify large-scale washover deposits overlying lagoonal or marsh sediments. The foreset stratification captured in the southern sheetwash region corresponds to sequences documented when a washover fan builds into shallow standing water (McCubbin, 1982) (Figure 2-13). Additionally, GPR reflections in the individual washover fans at Sites 2, 3, and 4 exemplify the planar sub-horizontal stratification consistent with overwash deposited on a subaerial surface (Figure 2-14). In response to Objective 2, however, we were unable to conclude with any certainty that the GPR could consistently distinguish the subtle variations that occur between overwash facies and those deposited by aeolian transport (i.e., sand-on-sand deposits), and we were unable to consistently tease out reflections that may be the result of changes in water content (Appendix III). As a result, the GPR was used to delineate the depth of the sand/silt contact throughout our study area, but the thickness of sedimentologically distinct washover facies within the overwash complex was calculated directly from sediment cores.

### **2.4.1 Sedimentary Characteristics of Washover Deposits**

Samples within each core comprised of sedimentologically distinct washover deposits were distinguished based upon RSA data (Figure 2-15) (Appendix II) and visual inspection of the cores for specific characteristics such as those documented by Schwartz (1982), McCubbin

(1982), and Kochel and Dolan (1986). Sorting (standard deviation) provided a good indication of differences between depositional environments and values greater than 0.5 were generally presumed to be representative of washover sediments. The calculated mean grain-size for washover sediments is 1.71 phi (n = 70, SD = 0.38) and the non-washover sediments 2.38 phi (n = 59, SD = 0.17) (Table 2-3). A two-sided T-test shows there is a significant difference in mean grain size between the two populations at the 95% CI with a P-value of <<0.05. A plot of mean grain size versus standard deviation (sorting) begins to separate samples into distinct populations where washover and dune sediments represent two end-members (Figure 2-16). The washover sediments have a higher standard deviation (less sorting) and a larger mean grain size than dune sediments. A similar trend is revealed in a plot of skewness versus kurtosis (Figure 2-17) where overwash sediments have lower values of skewness and kurtosis relative to the dune samples. Mason and Folk (1958) found similar results in a comparison between beach and dune sediments on a barrier island on the south Texas Gulf Coast. It is not surprising that there is a large degree of overlap between the washover and non-washover sediments since washover is comprised of a combination of offshore, beach, and dune sediments that have been altered since deposition by aeolian transport and anthropogenic activities (particularly at the sites close to active military egress points).

#### **2.4.2 Relevant-Sand Prism and Washover Volumes**

Subtracting the elevation of the interpolated sand/silt surface from 2007 bare earth lidar gives a total relevant-sand prism volume of  $1.8 \pm 1.1 \times 10^6 \text{ m}^3$ . The prism thickness ranges from 0 to 6 m and averages approximately 90 cm in thickness. This is consistent with depth estimates made by Cleary and Riggs (1999) of < 0.5 m to 2 m along Onslow's mean high tide line and on the same order of magnitude as Sproat's (1999) estimate of 1 to 2.5 m along the backbarrier. The thickness of the relevant-sand prism calculated from the 12 sediment cores is 96 cm (SD = 18)

and serves as an additional check on accuracy of the interpolated sand/silt contact. The study area was divided into three geomorphic settings: (1) from the dunetoe to the vegetation line, excluding isolated clusters of dune vegetation covering an area  $> 20 \text{ m}^2$  (i.e., the active overwash region); (2) landward of the vegetation line (i.e., backbarrier); and (3) seaward of the dunetoe (i.e., beach). The backbarrier contains the largest proportion of the relevant-sand prism volume at 52%, followed by the active overwash region, 39% and the beach, 6% (Table 2-4).

Further analyses were performed to assess alongshore variability of relevant-sand prism and washover deposit volumes. The thickness of the relevant-sand prism was calculated for 96 cross-island profiles (50 m spacing) to produce an estimate of volume of sediment per square meter of surface area ( $\text{m}^3/\text{m}^2$ ) along each transect (Figure 2-18). These shore-normal transects were further divided into the three environments described above: (1) the active overwash region, (2) backbarrier, and (3) beach (Figure 2-19). The area-normalized relevant sand-prism volume over the entire study area averages  $0.9 \text{ m}^3/\text{m}^2$  ( $\text{SD} = 0.5$ ). The prism volume within the region of active overwash averages  $2.3 \text{ m}^3/\text{m}^2$  ( $\text{SD} = 2.4$ ), while the beach portion averages  $1.0 \text{ m}^3/\text{m}^2$  ( $\text{SD} = 0.5$ ), and the backbarrier  $0.7 \text{ m}^3/\text{m}^2$  ( $\text{SD} = 0.4$ ). T-tests reveal a significant difference ( $P\text{-value} \ll 0.05$  at 95% CI) between area-normalized volumes in the active overwash region in comparison to both the beach and backbarrier environments. The estimates for the backbarrier, however should be taken only as a rough approximation since field measurements were only collected in beach and overwash areas.

The total thickness of sedimentologically distinct washover deposits above the sand/silt contact was estimated for each core based upon the aforementioned sedimentary characteristics. An average cumulative washover thickness of 52 cm ( $\text{SD} = 23$ ) (Table 2-5) and a surface area of active overwash in 2008 of  $383 \pm 62 \times 10^3 \text{ m}^2$  equates a volume of  $199 \pm 88 \times 10^3 \text{ m}^3$  of washover sediments. In other words, sedimentologically distinct washover deposits make up



approximately 29% of the active overwash complex or 11% of the entire study area's relevant sand-prism.

To assess alongshore variability in the volume of washover deposits, an estimate of the volume of washover sediments at each transect was calculated by multiplying the average cumulative washover thickness determined from the sediment cores (52 cm) by the length of transect falling within an active overwash region (Appendix IV). Linear regression indicates that there is a moderately significant relationship ( $R^2 = 0.54$ ) between increased long-term shoreline erosion rates and increased washover volume, supporting Hypothesis 2, however, Figure 2-20 shows that this trend is driven in part by the cluster of data from the large sheetwash at Site 1 and not necessarily representative of behavior of the island as a whole. Figure 2-21 shows the variation in cross-island volume of the relevant sand-prism with distance alongshore. Figure 2-22 compares alongshore variations in relevant-sand prism volume to long-term (1872-1997) and short-term (1973-1997) shoreline change rates calculated by the US Geological Survey (Morton & Miller, 2005). A scatterplot of long-term (1872-1997) shoreline change versus area-normalized volume of the relevant-sand prism reveals that a simple linear relationship does not exist between the two (Figure 2-23). As a result, the proposed hypothesis that alongshore variation in the volume of the geologically-defined sand prism is inversely correlated with long-term shoreline erosion rates, Hypothesis 1, is rejected. To determine if relevant-sand prism volume estimates were biased by the use of the back of the barrier island as the landward extent, a somewhat arbitrary feature in terms of geomorphology and largely controlled by the location of the AIWW, shoreline change rates were also compared directly to volume within the beach and overwash regions. The trend is similar to that of the overall sand prism and no significant correlation is seen between the volumes of beach or overwash prism sediments versus shoreline change (Figure 2-23).

## 2.5 Chapter 2 Tables

Table 2-1.

<b>Sources of Vertical Error</b>	<b>Approximate Error (m, ±)</b>
	<i>Surface Elevation</i>
vertical accuracy of 2007 lidar	0.15
offset of GPR surface reflector from lidar	0.07
	<i>Sand/Silt Contact</i>
precision of tracing GPR reflection surfaces	0.02
measured offset between GPR reflections and core facies	0.53
<b>Total Vertical Error</b>	<b>0.56</b>

<b>Sources of Horizontal Error</b>	<b>Approximate Error (m, ±)</b>
	<i>Landward Limit</i>
precision of tracing vegetation line using BeachTools	5.6
	<i>Seaward Limit</i>
variability in position of wet/dry line	2.0
<b>Error in Surface Area Calculations</b>	<b>area ± 3.8 m buffer</b>

Table 2-2.

## Core Coordinates

Core ID	UTM X (m)	UTM Y (m)	Distance from core to GPR transect (m)	Elevation of cored sand/silt contact		Difference (cm)
				NAVD88 (m)	NAVD88 (m)	
ONSVC04	289262.4	3825909.9	0.7	0.56	0.46	10
ONSVC05	289254.6	3825918.8	0.1	0.53	0.62	-9
ONSVC06	289232.7	3825940.5	0.4	0.68	0.29	39
ONSVC09	288910.0	3825641.7	6.2	0.3	0.29	1
ONSVC14	288219.0	3825153.5	0.1	0.50	0.38	12
ONSVC18	287682.6	3824749.0	4.7	0.95	1	-5
ONSVC25	286283.4	3824093.3	3.8	0.17	-2.29	246
ONSVC26	286290.5	3824098.1	2	0.27	-1.8	207
ONSVC29	286221.7	3824082.0	4.9	-0.05	-2.44	239
ONSVC40	286250.5	3824014.3	2.7	0.37	-0.76	113
ONSPC02	289256.0	3825915.8	1	0.70	0.58	12
ONSPC04	288238.6	3825133.5	2.9	0.61	0.78	-17
ONSPC07	286610.8	3824320.0	3.5	0.07	-0.12	19
F1-2	286884.9	3824296.3	7.6	0.62	0.51	11
F2-5	287351.8	3824557.1	0.7	0.50	0.54	-4

Table 2-3.

	<b>n</b>	<b>Mean (M1)</b>	<b>SD (M2)</b>	<b>Median</b>	<b>Skewness (M3)</b>	<b>Kurtosis (M4)</b>
<b>Washover</b>	70	1.71 (0.38)	0.77 (0.17)	1.91 (0.43)	19.24 (9.60)	63.46 (52.79)
<b>Non-Washover</b>	59	2.38 (0.17)	0.40 (0.10)	2.43 (0.14)	43.16 (24.32)	266.95 (243.84)
<b>Dune Surface</b>	5	2.35 (0.20)	0.30 (0.05)	2.34 (0.17)	105.32 (36.93)	778.43 (415.07)

Table 2-4.

Region	Surface Area	Percent of Total	Relevant-Sand	Percent of
	( $\times 10^3 \text{ m}^2$ )	Surface Area	Prism Vol ( $\times 10^3 \text{ m}^3$ )	Relevant-Sand Prism
Entire Study Area <sup>1</sup>	1,985 ± 63	100%	1,755 ± 1,112	100%
Backbarrier	1,454 ± 63	73%	909 ± 814	52%
Active Overwash	383 ± 62	19%	680 ± 215	39%
Beach	122 ± 40	6%	102 ± 68	6%

<sup>1</sup>Totals for the entire study area also include clusters of vegetated foredunes that have been isolated due to a beach access road. These "vegetation islands" account for a combined surface area of ~26,000 m<sup>2</sup> and a prism volume of ~64,000 m<sup>3</sup>.

Table 2-5.

<b>Core ID</b>	<b>Cumulative Washover Thickness (cm)</b>	<b>Depth of Sand/Silt Contact (cm)</b>	<b>% Washover</b>
		<i>Site 1</i>	
ONSVC25	77	93	82.8
ONSVC26	66	83	79.5
ONSVC29	57	115	49.6
ONSVC40	72	93	77.4
ONSPC07	56	73	76.7
ONSPC05	88	N/A	N/A
		<i>Site 2</i>	
ONSVC18	38	105	36.2
		<i>Site 3</i>	
ONSPC04	23	122	18.9
ONSVC14	12	110	10.9
		<i>Site 4</i>	
ONSVC04	64	104	61.5
ONSVC05	39	97	40.2
ONSVC06	29	62	46.8
<b>Average:</b>	<b>51.8</b>	<b>96.1</b>	<b>52.8</b>
<b>Standard Deviation:</b>	<b>23.4</b>	<b>18.0</b>	<b>25.0</b>

## 2.6 Chapter 2 Figures



Figure 2-1.

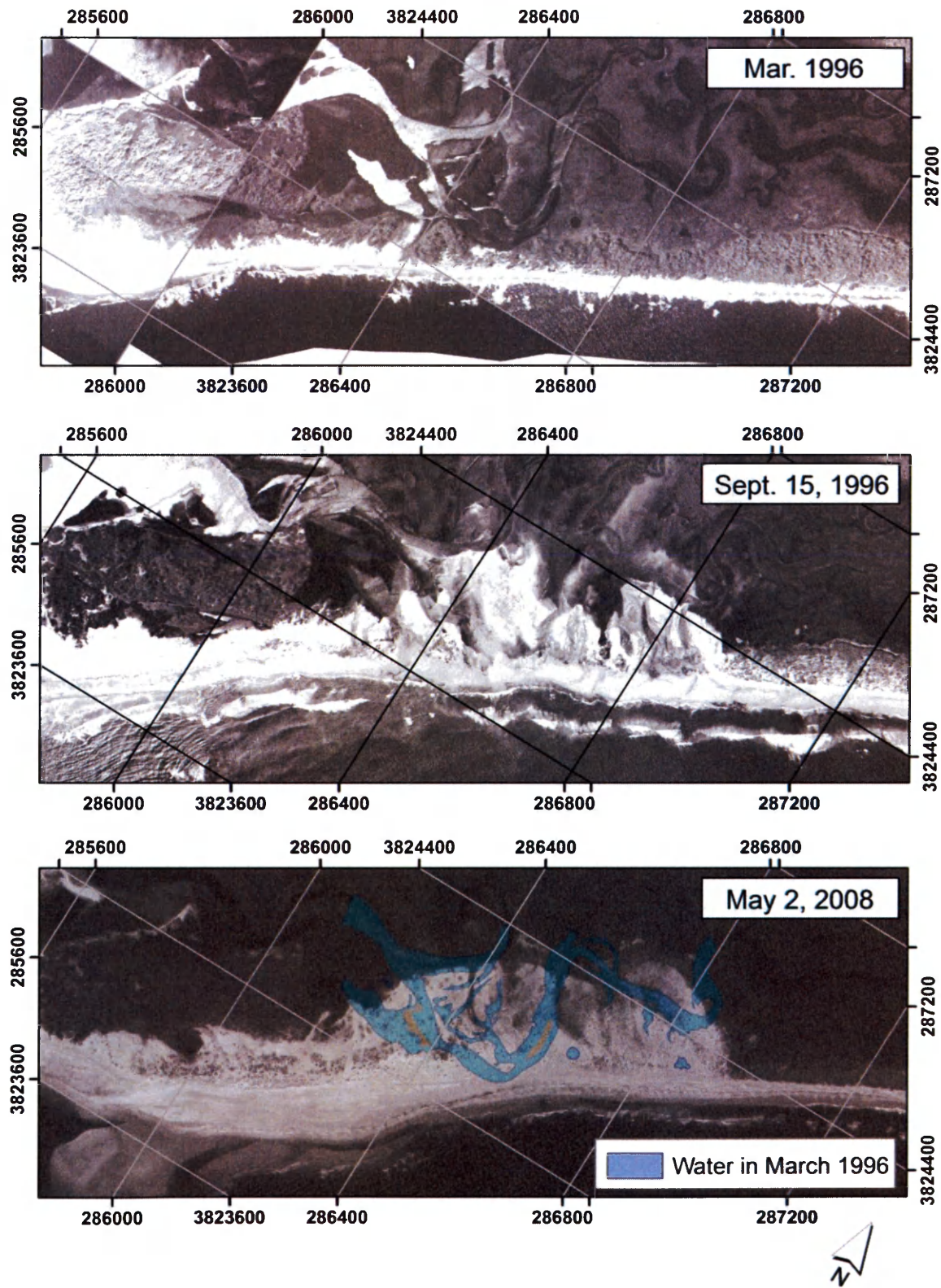


Figure 2-2.

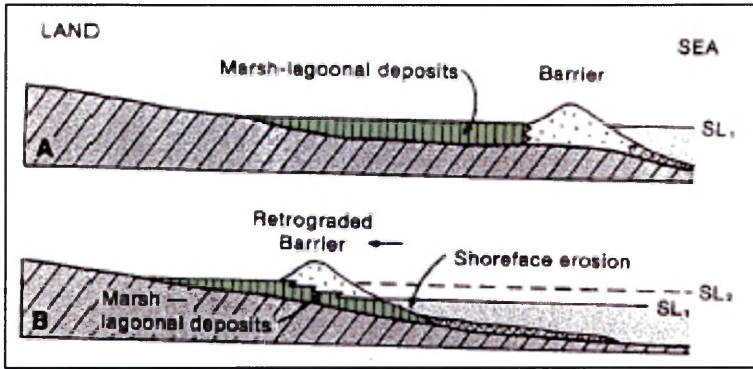


Figure 2-3.

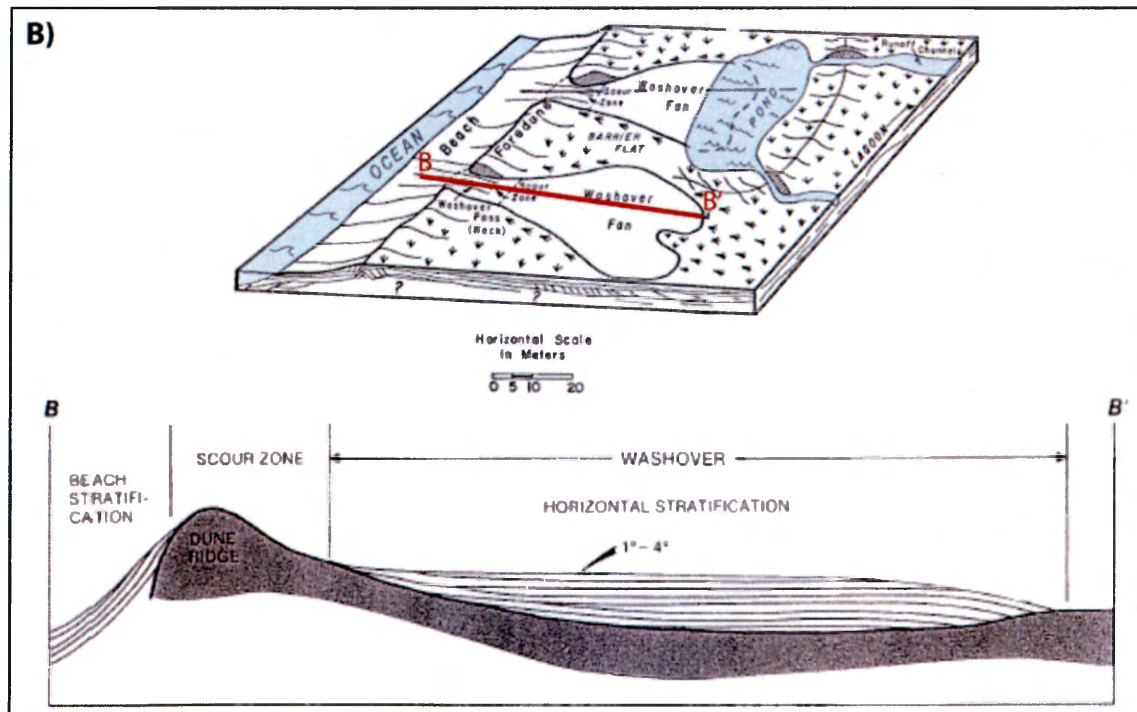
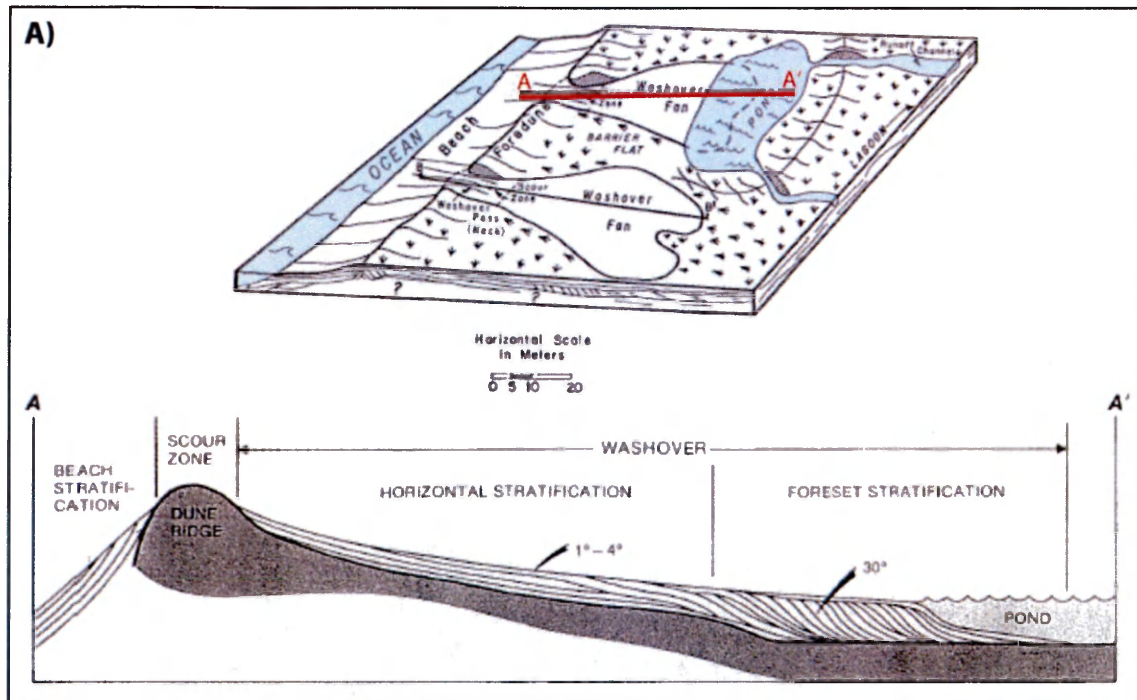




Figure 2-4.



Figure 2-5.





Figure 2-6.

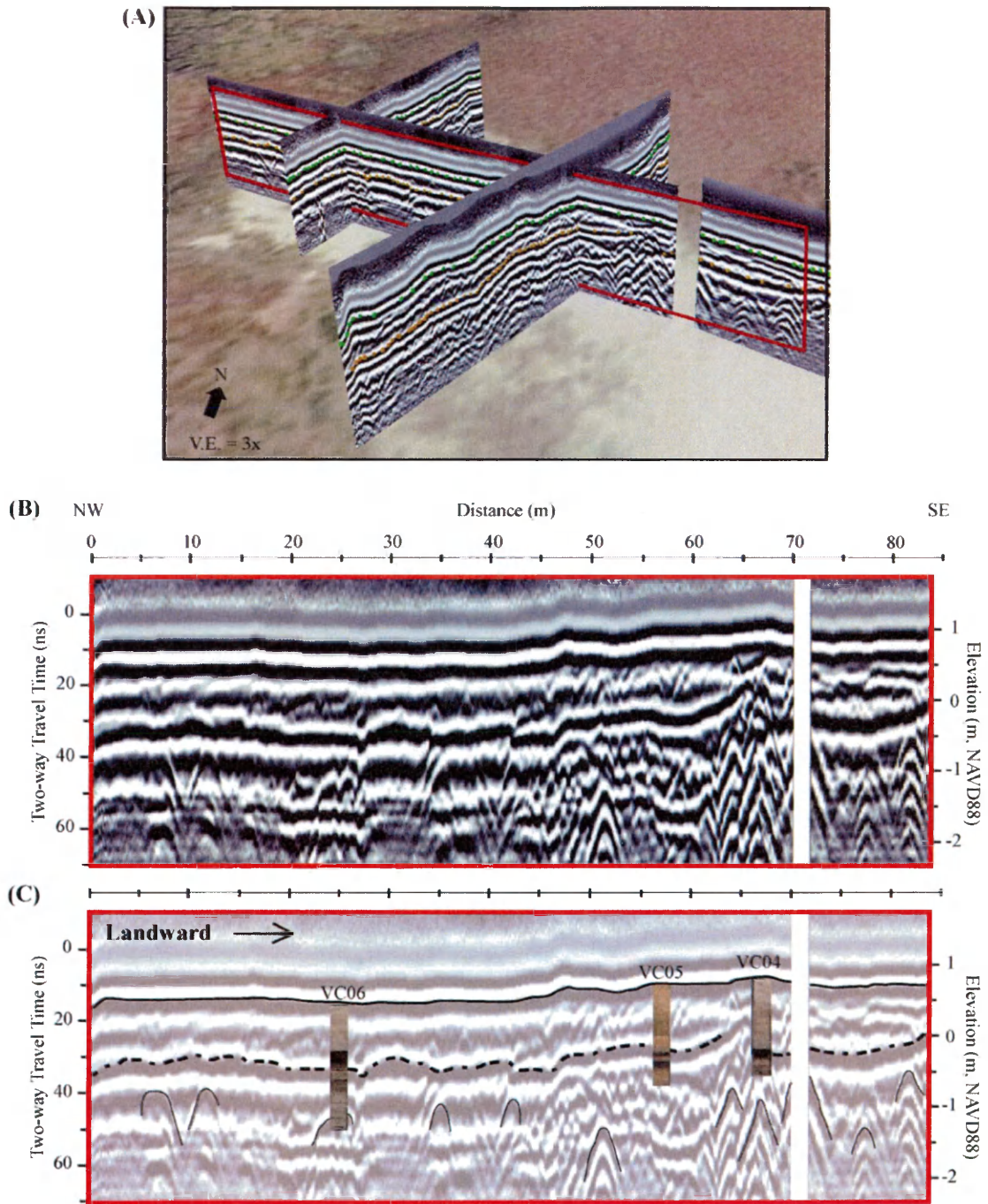


Figure 2-7.

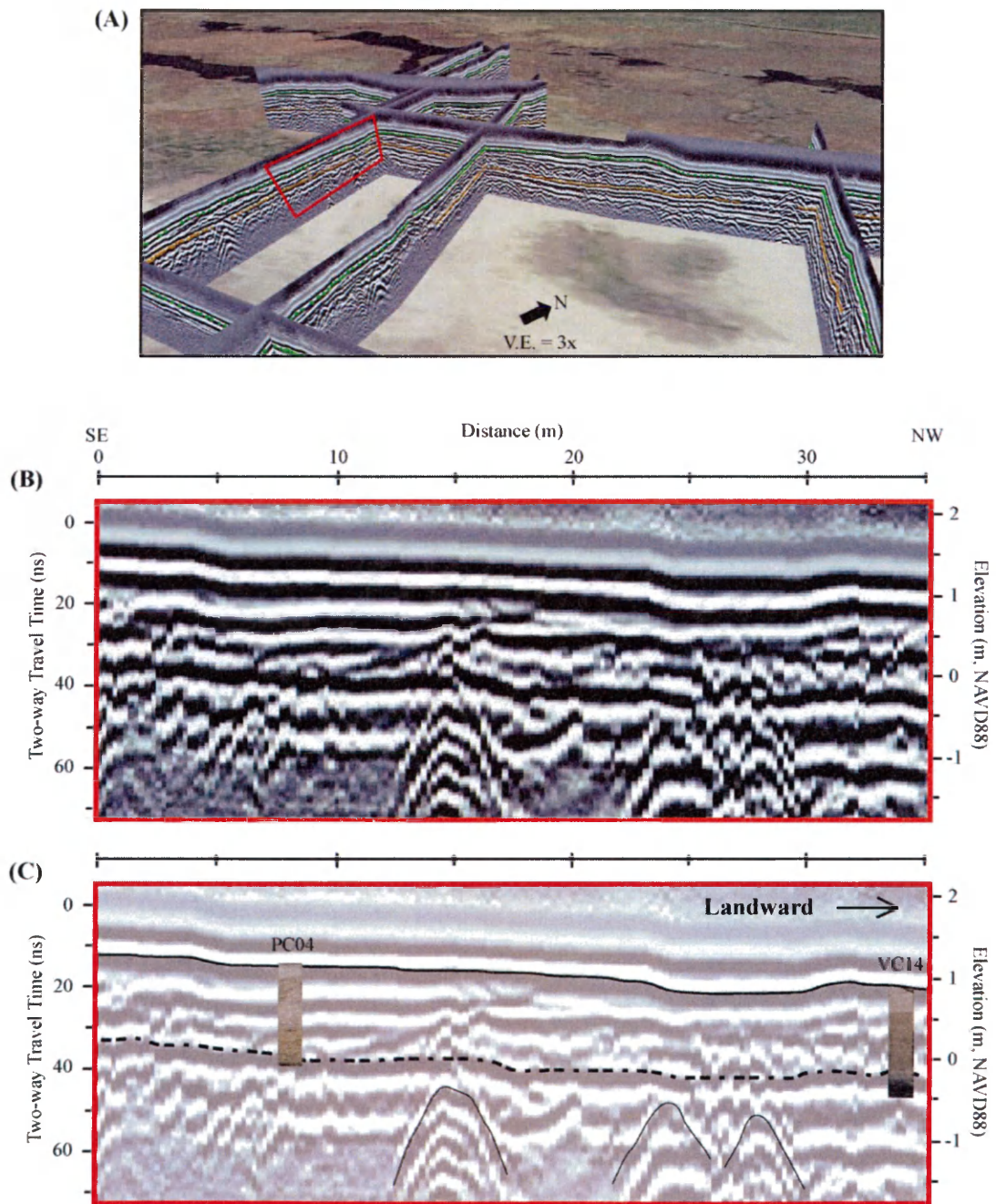




Figure 2-8.

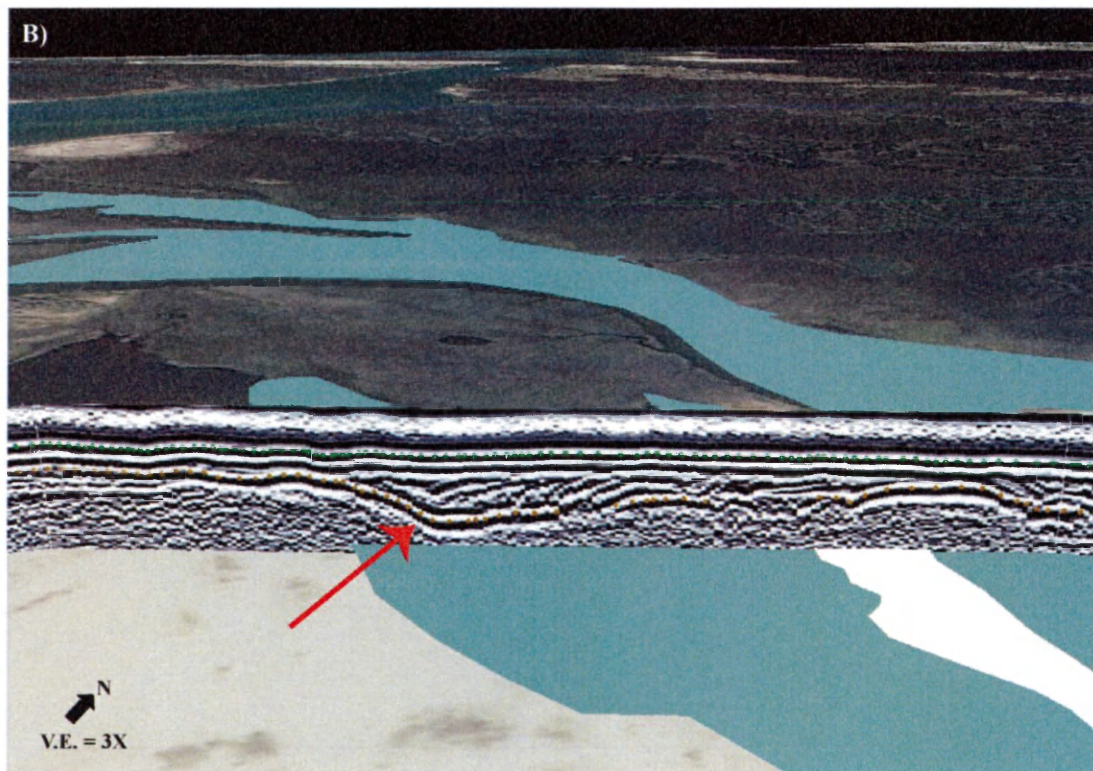
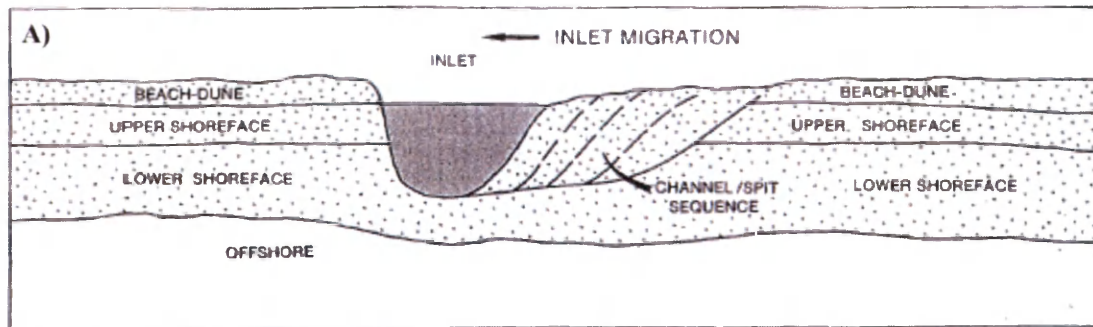




Figure 2-9.

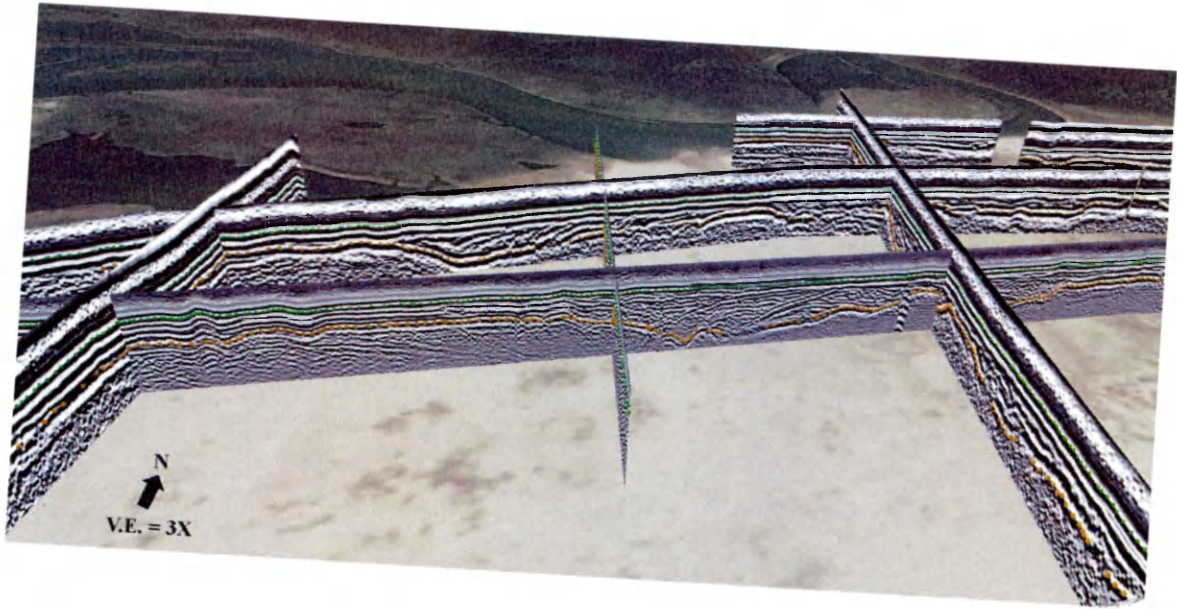






Figure 2-11.

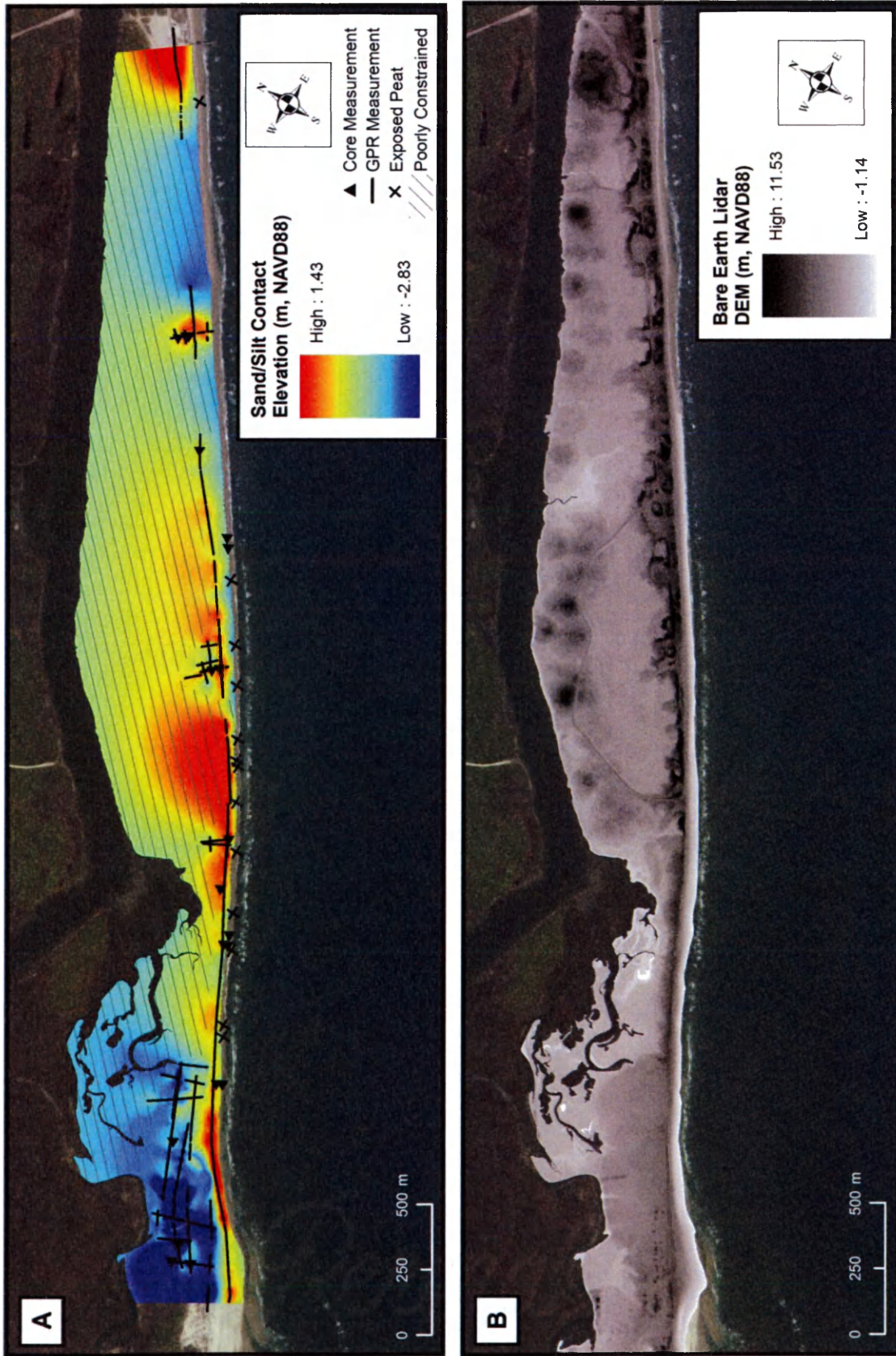


Figure 2-12.





Figure 2-13.

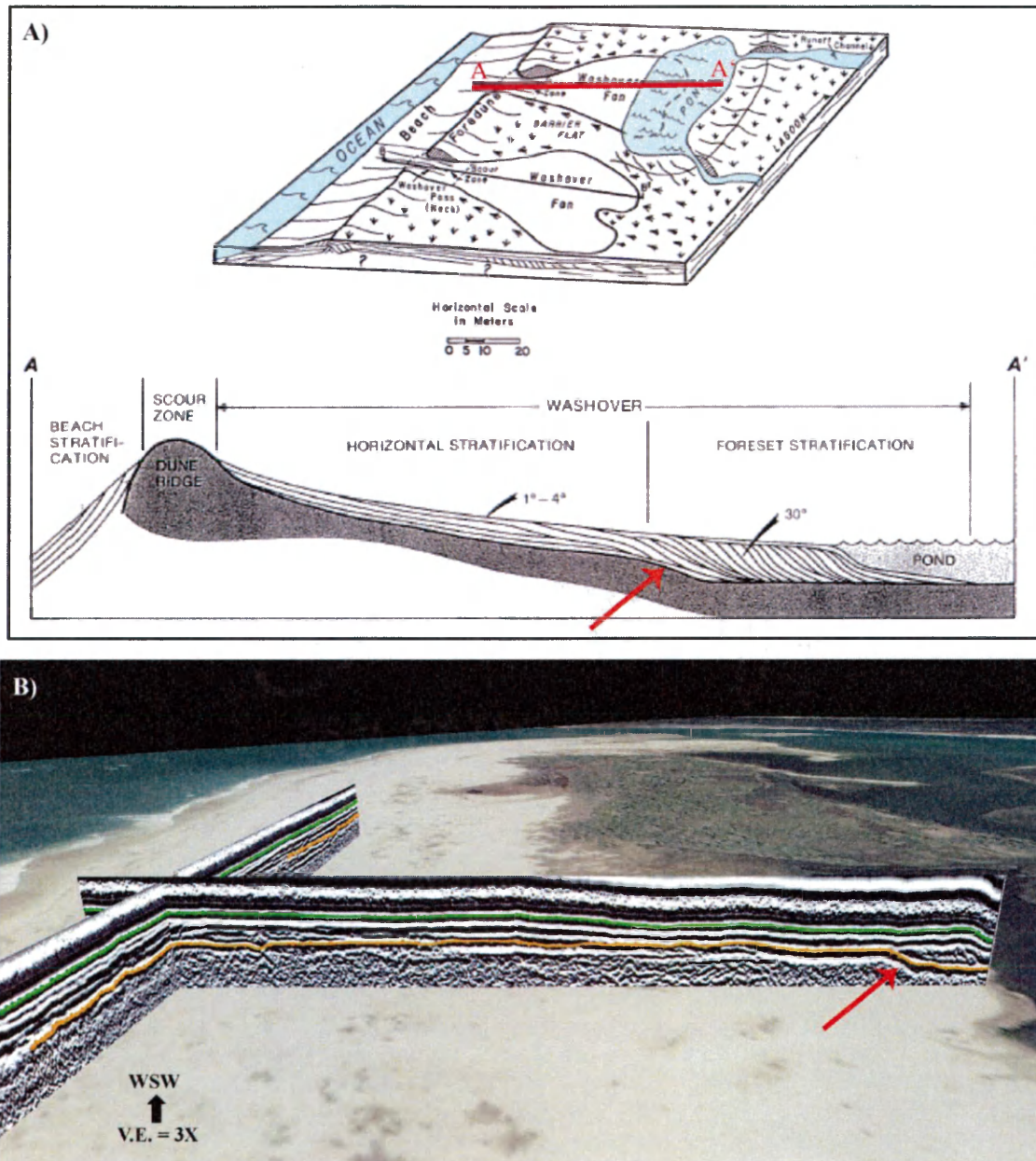


Figure 2-14.

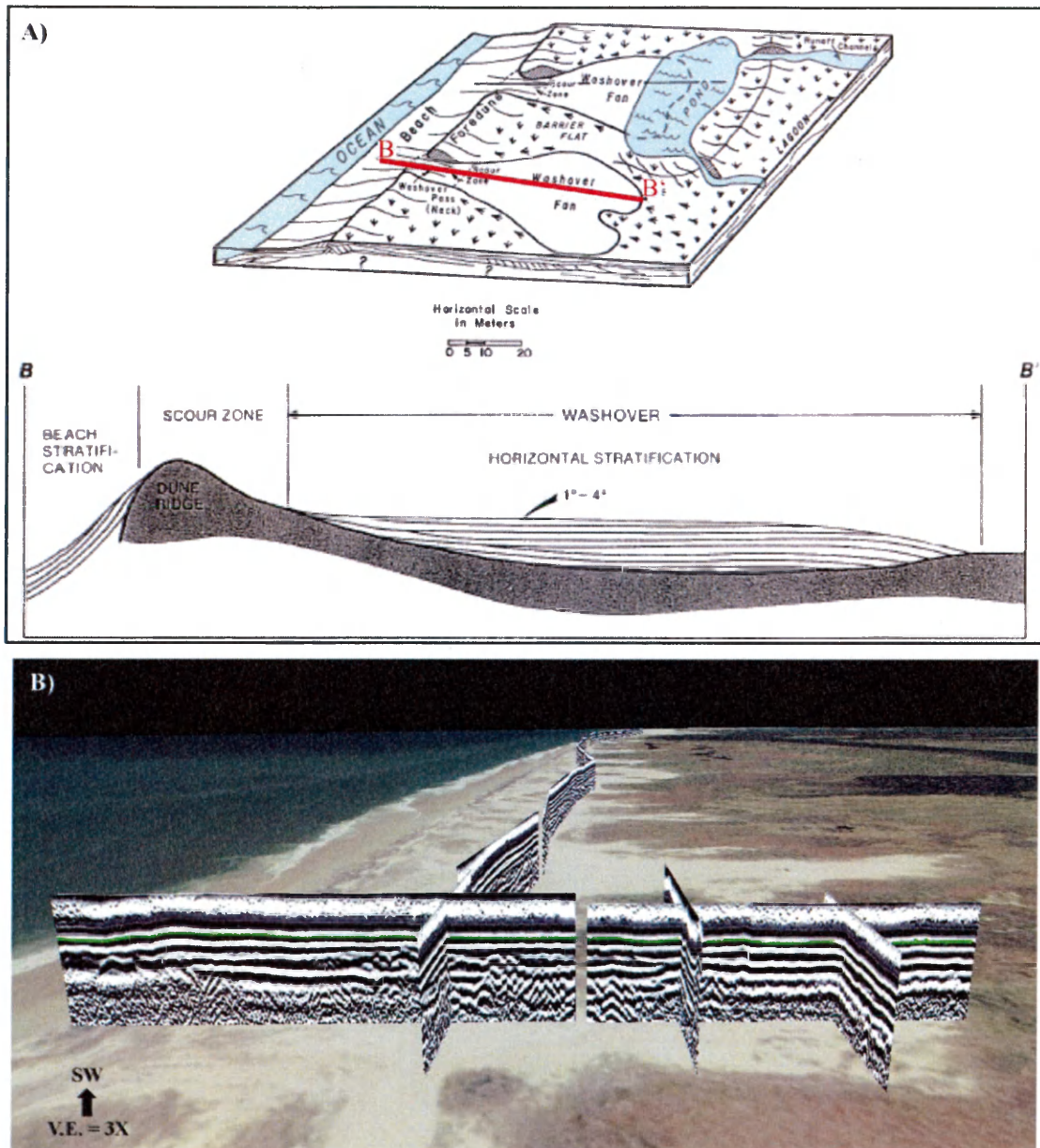


Figure 2-15.

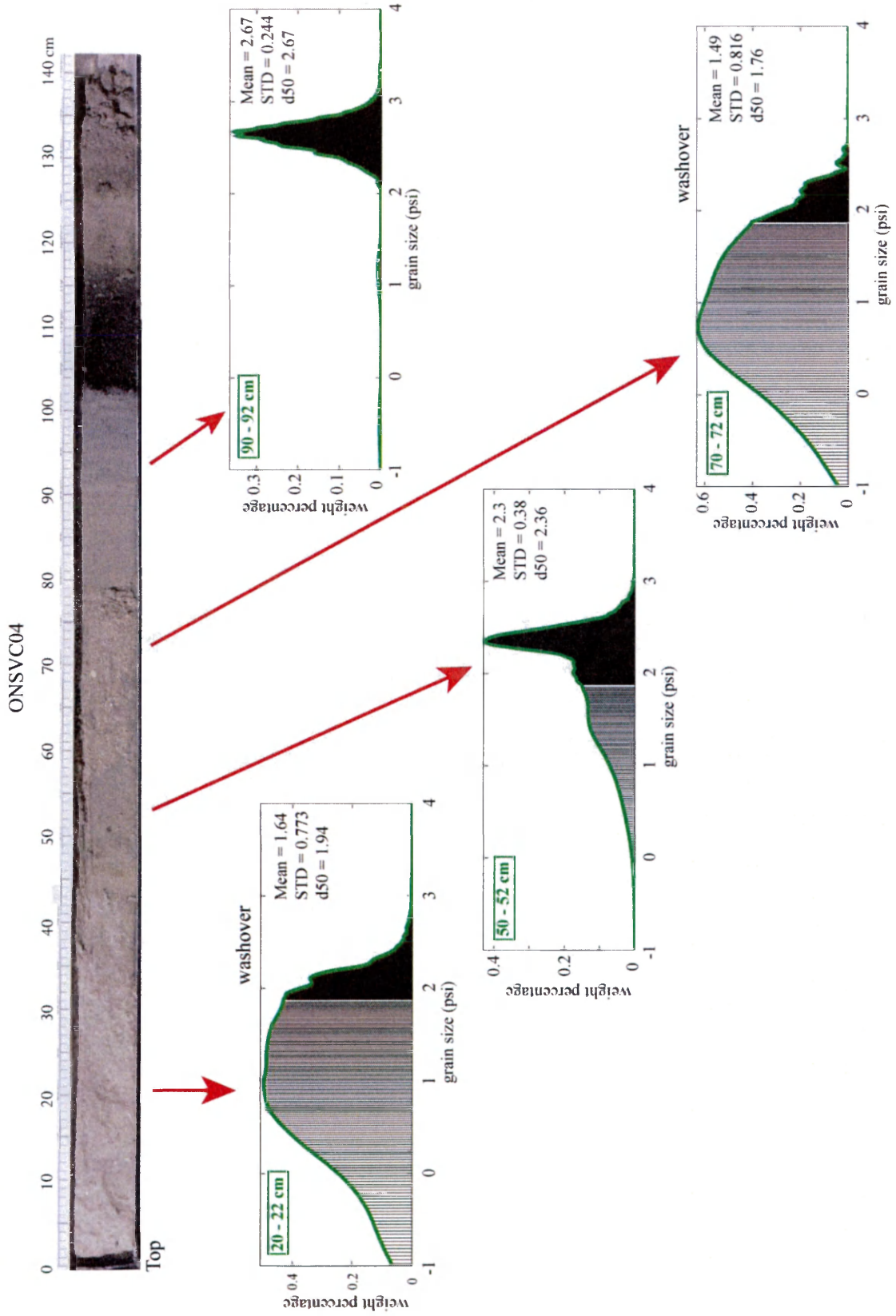


Figure 2-16.

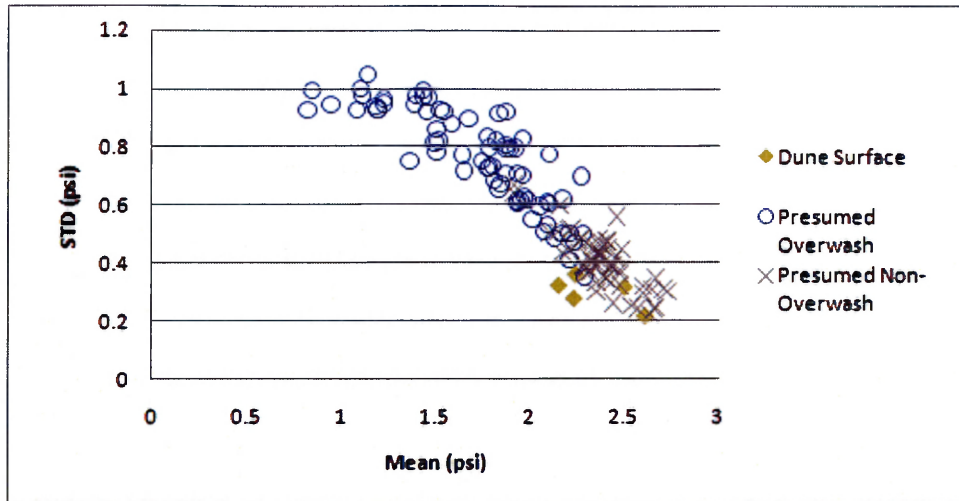




Figure 2-17.

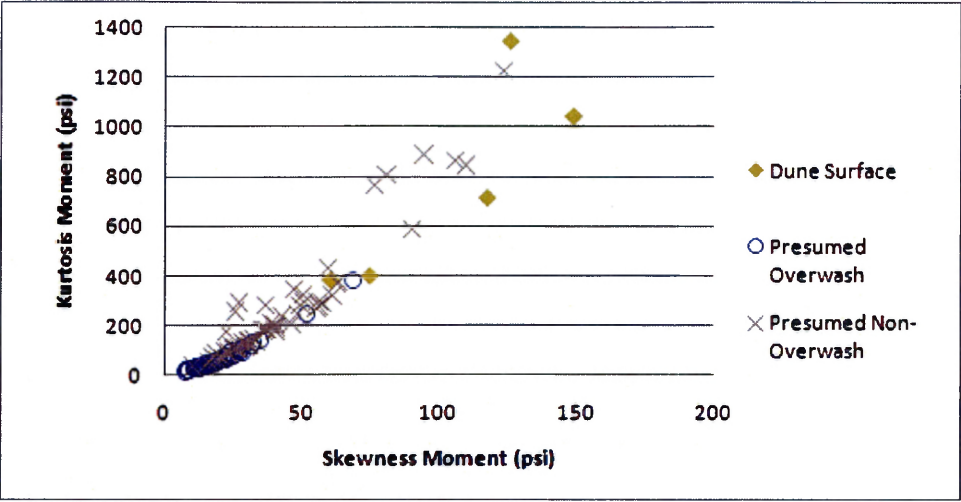


Figure 2-18.

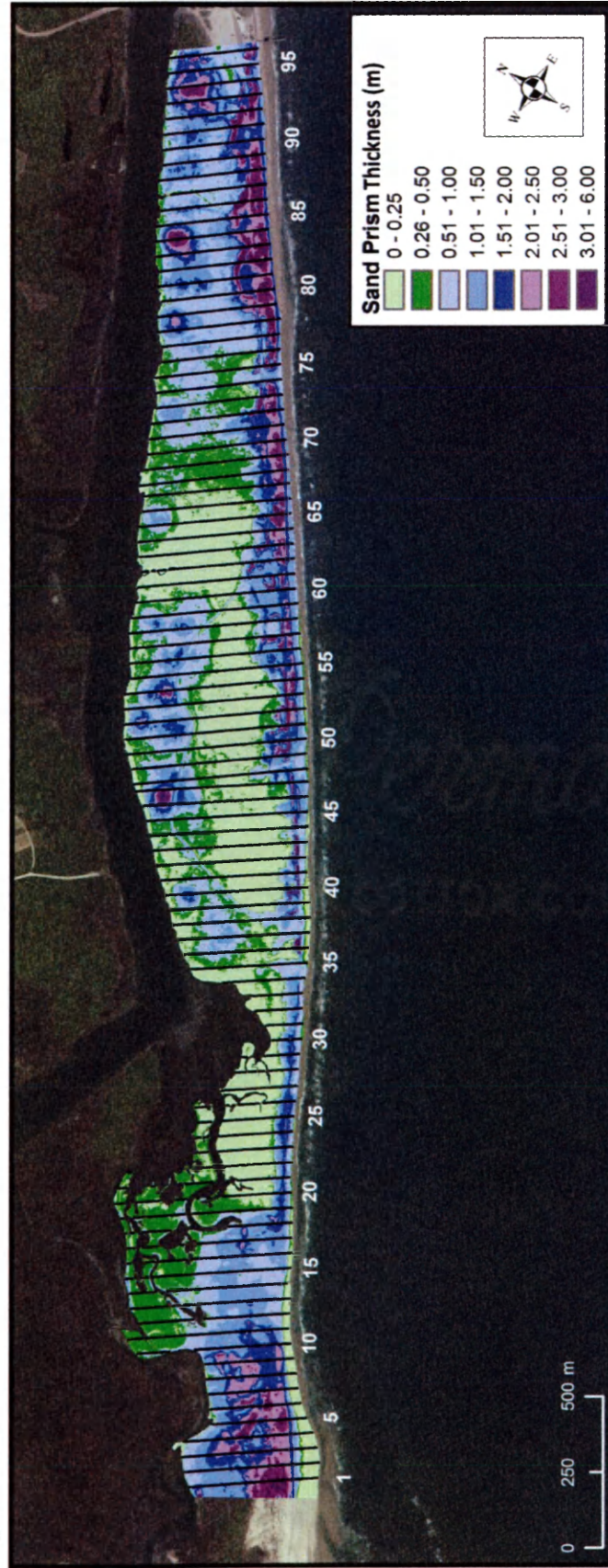


Figure 2-19.

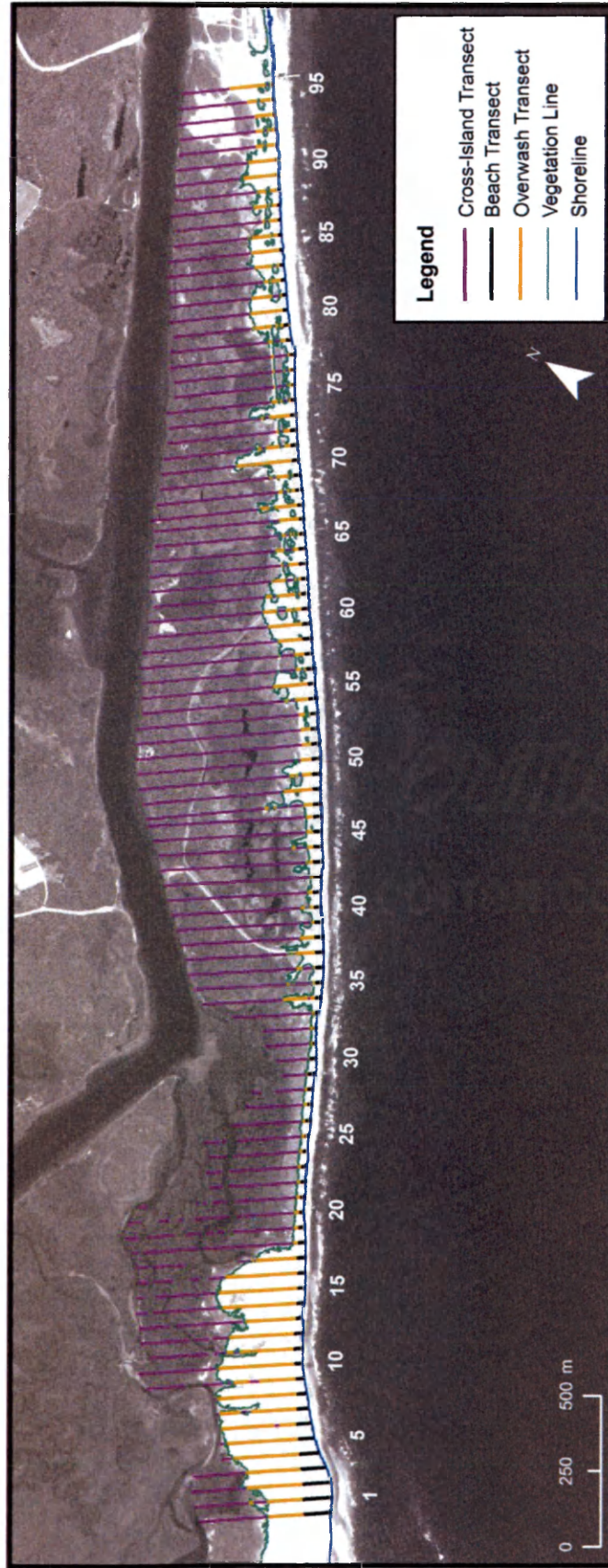


Figure 2-20.

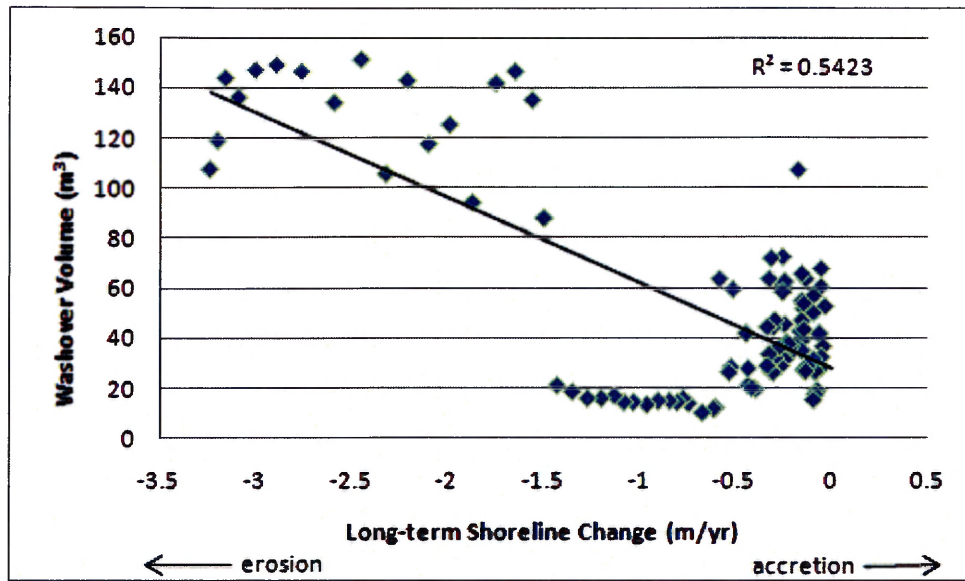




Figure 2-21.

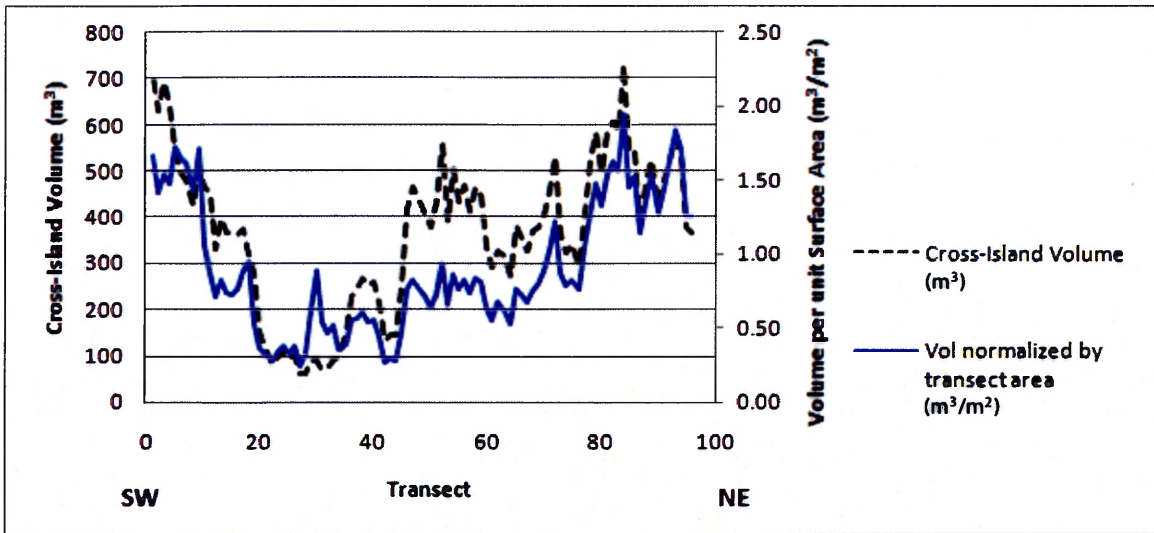
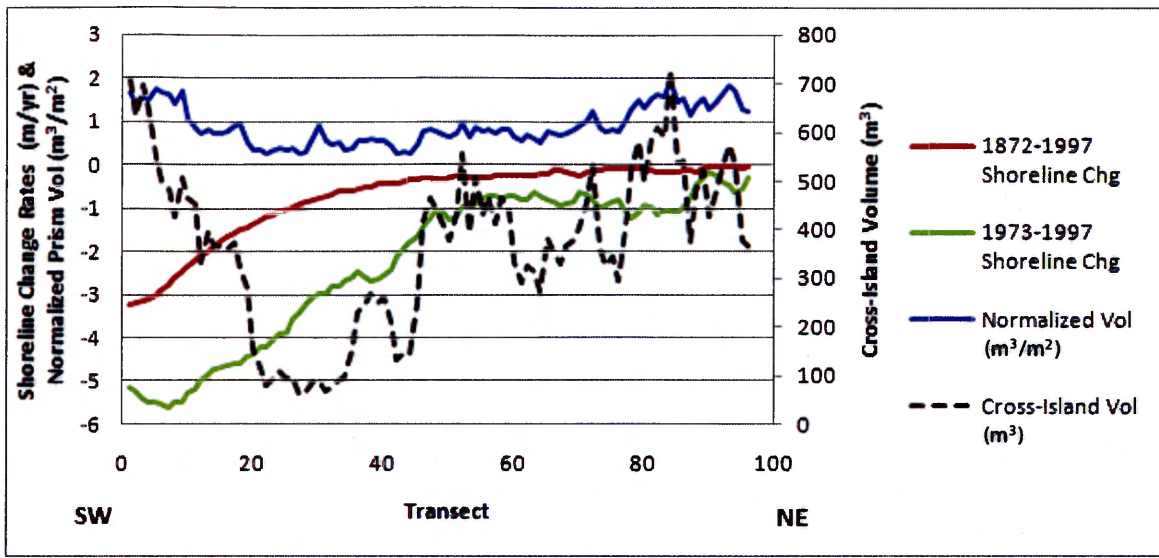


Figure 2-22.





**CHAPTER 3**  
**SPATIAL AND TEMPORAL TRENDS IN SHORELINE**  
**MIGRATION AND OVERWASH OCCURRENCE: 1938-2008**



### **3.1 Introduction**

Barrier island overwash is a natural mechanism by which an island migrates in response to changes in sea level. Overwash benefits the coastal environment by supplying the necessary sediments to backbarrier marsh habitats supporting vegetation growth and providing preferred nesting habitat for threatened and endangered birds (Godfrey, 1970; Donnelly et al., 2006). At the same time, overwash can result in significant beach erosion, a lowering of the dune crest, and a complete reworking of the topography damaging any structures in its path. The occurrence and extent of overwash on a given environment varies due to natural forcings (tide level, wave set-up, wind) as well as the localized topography and composition (elevation, vegetation, degree of sediment saturation) and, as a result, varies both temporarily and spatially (Kochel & Wampfler, 1989; Donnelly et al., 2006). With heightened concerns of rising sea level and increased societal impacts of coastal storms, it is imperative that we improve understanding of the interplay between shoreline erosion and barrier island overwash. Assessing the variability of barrier island morphodynamics over time, (years to decades) and space, (meters to 10s of kms) will enable scientists to improve shoreline susceptibility models, thereby enabling coastal managers and residents to best prepare for future climate scenarios.

#### **3.1.1 Motivation**

Understanding the driving forces behind alongshore variability in shoreline behavior is of utmost importance for scientists working to forecast shoreline behavior and to resource managers working to adopt plans for future viability of coastal resources in the face of rising sea level and changing storm conditions. Approximately 30% of the US coast is lined by barrier islands (Stutz & Pilkey, 2001) which offer unique and valuable habitats in their own right while simultaneously serving as important buffers shielding the mainland from the full force of oceanic storms. Due to their high exposure and low topographic relief, barrier islands are especially susceptible to the impacts associated with sea level rise and storm activity. The morphodynamics of barrier islands

are shaped by a combination of natural factors such as sea and wind energy, sediment supply, substrate gradient and composition, sea level fluctuations as well as anthropogenic activities. How these forcings vary in time and space and the relative importance of each must be understood in order to develop reliable forecasts of shoreline trends and storm-susceptibility models.

### **3.1.2 Study Area Background**

Onslow Beach offers an ideal setting to evaluate the evolution of a barrier island over the past 80 years. The island has experienced alongshore variability in shoreline behavior as well as overwash occurrence over its recorded history. MCBCL is the largest Marine Corps amphibious training facility in the world, and high erosion rates (up to 3 m/yr) (Morton & Miller, 2005) coupled with the large overwash event at the southern end of the island during Hurricanes Bertha and Fran in 1996 (Figure 3-1) have heightened concerns of long-term sustainability. Although military training activities do impact the site, the island provides an excellent study area because it is largely undeveloped and the activities that do occur are much more regulated and documented in comparison to anthropogenic impacts on the highly populated and developed neighboring barrier islands. This setting offers a unique opportunity to evaluate the role of overwash as a mechanism for shaping barrier island morphology and influencing shoreline migration rates. In addition, evaluating spatial and temporal trends in conjunction with historic storm data and well-documented land-use practices will enable us to better distinguish between natural versus anthropogenically-induced change.

Figure 3-2 shows an 1872 topographic sheet depicting the island prior to the construction of the AIWW and prior to its purchase by the US Department of the Navy in 1941. The overlying shorelines published by the US Geological Survey (Miller et al., 2005) depict the long-term trend of erosion towards New River Inlet, stability in the central portion of the island, and slight

deposition near Brown's Inlet, suggesting that these general trends in shoreline behavior began prior to the AIWW or military activities. Although human activities have undoubtedly affected evolution of the barrier island, these data suggest that natural forces (e.g., wave climate, underlying geology, sediment availability, etc.) exert first-order control.

Onslow Beach exhibits distinct differences in morphology between the northern and southern portions of the island. The southwestern half of the island (from New River Inlet to Riseley Pier) is characterized by poorly developed, segmented dunes and is the site of extensive active and historic overwash. Dunes increase in elevation along the northern half with well-developed dune ridges approaching eight to nine meters in height in the proximity of Brown's Inlet (Figure 3-3). For a comparison between natural and anthropogenically-induced change, the study area was divided up into four zones which reflect the major beach activities within each zone (Figure 3-4). Zone 1 is difficult to access at high tide and is largely uninfluenced by anthropogenic disturbances barring some off-road vehicle usage in the vicinity of the New River Inlet. Zone 2 is where the majority of amphibious training activities take place. Zone 3 is largely used as a recreational area for Marines and their families. Lastly, Zone 4 which extends to Brown's Inlet, is a military impact zone which is completely off-limits to public access. Disturbances along this stretch of beach are very infrequent but have the potential to be quite large and this is also the location where dredge spoils from the AIWW are occasionally deposited. Morton and Miller (2005) calculated long-term (1872-1997) shoreline erosion rates greater than 3 m/yr for the southern portion of the island, while the central portion has remained relatively stable and the northern portion has been stable to slightly accretional.

### **3.2 Methods**

Geospatial analyses provide a valuable tool for evaluating the evolution of coastlines over seasonal to decadal or longer time periods. A series of aerial photographs and satellite images

depicting six time periods between 1938 and 2008 (Table 3-1) were used to track changes in shoreline position and overwash extent along Onslow Beach over the span of 80 years. For the purpose of this study, the active overwash region is the area seaward of the vegetation line and landward of the wet/dry line (a shoreline proxy) thereby including beach width in our calculations. In terms of geomorphology, the dune toe provides a better representation of the seaward boundary of overwash, however, it is often difficult to distinguish in aerial imagery. As a result, the wet/dry line was selected, which is visible in aerial imagery as a tonal change in sand color due to differences in water content and is the most commonly used proxy for shoreline position (Dolan et al., 1980; Smith & Zarillo, 1990) and closely approximates the High Water Line (HWL) (Dolan et al., 1980). The vegetation line is a feature that is consistently distinguishable in aerial imagery, and based upon a Real-Time Kinematic (RTK) Differential GPS (DGPS) ground survey, provides a good approximation of the landward extent of active overwash (Figure 3-5). A GIS-based tool (BeachTools) developed by the US Army Corps of Engineers for the purpose of delineating features such as the wet/dry line and vegetation line from aerial imagery was used to automate digitization of these features (Hoeke et al., 2001). The Digital Shoreline Analysis System (DSAS) (Thieler et al., 2005) was used to generate rates-of-change for the time series of shorelines and vegetation lines. Shoreline migration within 1 km of New River Inlet is known to be dominated by inlet dynamics (based upon an 1872 T-sheet) and as a result, the stretches of beach within 1 km of New River or Brown's Inlet have been excluded from analyses.

Uncertainty associated with deriving shoreline change rates from aerial imagery can be divided into two categories: 1) errors associated with the original source data; and 2) errors introduced in measurement techniques. A description of potential errors is provided below and an estimation of their cumulative effects upon our results is provided in Table 3-2. The values provided in Table 3-2 were also used within DSAS to generate accuracy statistics at the 90%

confidence interval for vegetation line and shoreline positions as well as change rate calculations. Imagery was georeferenced using what are referred to as secondary or supplemental control points. The points differ from primary ground control points in that the coordinate information is obtained from other maps, images, or field surveys as opposed to direct field measurements (Thieler & Danforth, 1994). An IKONOS satellite image collected in September of 2006 was used as the basis by which all other imagery was georeferenced to a common projection and horizontal datum (UTM zone 18, NAD83). The 2006 imagery has a resolution of 80 cm and a reported horizontal circular error of 2.2 m at the 90% confidence interval (CE 90%). Assuming that the National Map Accuracy Standards (NMAS) application factor of 2.146 was used, this equates to a horizontal positioning RMSE of approximately 1 m (FGDC, 1998).

A sparsely developed barrier island that has undergone significant alterations as a result of natural processes and human activities provides a challenging setting to locate well-defined points present in historical aerial photos as well as 2006 satellite imagery; however, a minimum of four control points were selected for each image. Points commonly used for georeferencing included the intersections of roads, corners of buildings, or distinct features in the marsh or meandering channel networks. A first-degree polynomial transformation was performed upon each image to estimate the best fit between all control points. The average RMS error for computed positions of control points is listed for each time series in Table 3-2. Thieler and Danforth (1994) stress that these map transformation residuals (RMS errors) provide unrealistically low error estimates that do not adequately reflect the accuracy of the image. Unfortunately, in the absence of proper ground control points (which provide accurate coordinate and elevation data obtained by field surveys for well-defined locations in aerial images) and without camera calibration reports or the fiducial marks from the original photos, we were unable to assess errors introduced through distortion of the camera lens and/or film or any tilt in the aircraft at the time of exposure. The majority of images used, however, have an adjacent overlap

of approximately 30%, and whenever possible, data from the center of the photo was used to limit the effects of radial or tilt distortion.

The line distinguishing between wet and dry sand (wet/dry line) is the most frequently used shoreline for digitizing because it is generally visible on aerial photographs as a significant tonal change (Theiler & Danforth, 1994). The wet/dry line serves as a proxy for the high water line (HWL) which is nearly equivalent to the mean HWL mapped as the shoreline on historical NOS T-sheets (Dolan et al., 1980). When using the wet/dry line to approximate shoreline position, a number of errors must be taken into account including variability of the position of HWL on the shoreface (due to changes in beach slope, waves, tide, and wind) interpretation of the wet/dry line on the aerial photograph, and the ability of the digitizer to accurately annotate this line.

The greatest error associated with using the wet/dry line as a proxy for shoreline position is the natural migration of the HWL with seasonal and tidal fluctuations (Moore, 2000). The position of the shoreline migrates due to: (1) tidal fluctuations; (2) seasonal changes in beach slope; (3) roughness of the beach face; (4) wave height and period; (5) storm impacts, and (6) wind set-up and set-down (Dolan et al., 1980). The natural migration of the shoreline must be taken into account when digitizing a wet/dry line from an aerial photograph which supplies only a snapshot of the water level at a given time. Errors due to seasonal variability were minimized by only using photographs collected between January and May, with the exception of November imagery from 1989 and post-storm imagery was avoided (Figure 3-6). To assess the excursion of the wet/dry line over the course of a tidal cycle Dolan et al., (1980) found that for medium-size sand beaches with slopes similar to the study area, the HWL migrates an average of 1-2 m over a 12-hour 25 minute tidal cycle. In accordance with the measurements of Dolan et al., (1980) and following Smith and Zarillo (1990) this study assumes an uncertainty of  $\pm 2$  m in the position of the HWL for our long-term assessment of shoreline change. This estimate does not account for

larger-scale tidal or seasonal fluctuations and may underestimate short-term variations in shoreline position, which based upon monthly beach profiles over a 13-month period (Smith and Zarillo, 1990) may reach up to  $\pm 20$  m.

Although the error associated with the limitations of an individual's ability to visualize and digitize minor changes in pixel values was minimized through the use of BeachTools, there remains variability due to differences in adjustments to the brightness and contrast applied to imagery as well as which pixels are selected as the basis for classification. BeachTools performs a clustered supervised classification based upon mean pixel values and outputs a vector polygon encircling pixels of similar values. This approach minimizes the subjectivity in delineating such features and provides highly detailed output. To assess the error associated with the individual's selection of pixels, a repetitive measurement of the wet/dry line was performed three times over a 600-m long stretch of beach. Each time, a different set of pixels were highlighted to perform the classification analyses and the differences in positioning between the three lines calculated every 10 m. Errors in an individual's ability to clearly distinguish a wet/dry line is significantly hindered when the contrast of the images is poor or if other shore parallel features such as tire tracks or erosional scarps are present, all of which could ultimately result in human misinterpretation of the HWL (Moore, 2000; Crowell et al., 1991).

Mapping the vegetation line also presents a degree of subjectivity in that the density of vegetation which the users defines as the vegetation line must be consistent, and due to variations in imagery, selecting an equivalent sample from each time period can be challenging. Due to fragmentation of the dunes in all post-1938 imagery, the vegetation line cannot be accurately represented by a single line but must also be augmented by a number of "vegetation islands" that occur seaward of a shore-parallel beach access road that intersects the dunes. The dirt road extends through Zones II and III and is only paved in Zone III. Since the aim of this research is to distinguish migration of the vegetation line due to overwash or natural processes, the

vegetation line that coincides with the landward side of the road was not traced. The pockets of dune vegetation seaward of the road were considered a better representation of a natural vegetation line and although they are somewhat difficult to distinguish in aerial imagery due to their limited size, vegetation islands with an area greater than or equal to 20 m<sup>2</sup> were encircled using BeachTools. The result is a segmented vegetation line that is totally absent from stretches of the beach where development has completely eliminated the natural vegetation line.

Shore-normal transects obtained from the USGS National Shoreline Assessment (Miller et al., 2005) with an alongshore spacing of 50 m were used to evaluate changes in location of the shoreline and vegetation line for each time period. For 201 transects DSAS was used to measure the location of each of these geomorphic boundaries relative to an offshore baseline so that the migration of each feature could be evaluated independently of one another or in relation to the other datasets. In areas where the shore-perpendicular transect intersects either the shoreline or vegetation line in more than one location (e.g. where there are multiple pockets of vegetation in the foredune), the intersection closest to the offshore baseline was selected for use in DSAS. DSAS also generated rate-of-change measurements in the form of linear regression or end-point rates as well as estimating the statistical uncertainty associated with each dataset and chosen method.

### **3.3 Results**

Figures 3-7 through 3-12 show each set of imagery overlain by the digitized vegetation line and shoreline. A visual, qualitative assessment of changes to the barrier island is provided from these data. A direct comparison of the location of the shoreline and vegetation line for each step in the time series is shown in Figure 3-13. The series of shoreline and vegetation line data was analyzed in DSAS to generate rate-of-change calculations based upon a linear regression, weighted linear regression, and end-point rates. In addition, for each shore-normal transect



DSAS output the distance from the predefined baseline and accuracy assessments of computed shoreline positions and erosion rates based upon the reported accuracy of the input data. Samples of data generated from DSAS are provided in Table 3-3, to receive digital copies of this information for our entire study area, contact Jesse McNinch (Jesse.McNinch@usace.army.mil).

From 1938 to 2008 Onslow Beach experienced an average shoreline erosion rate of 1.08 m /yr based upon a linear regression between all six time periods. A maximum depositional rate of 1.65 m/yr occurred near the northeast end of the island and a maximum erosion of 3.85 m/yr at the southwest end (Figure 3-14). These rates are similar to the average short-term shoreline change rate of 1.27 m/yr calculated by the USGS (Morton & Miller, 2005) based upon a 1973 Topo-Sheet and a 1997 lidar-derived shoreline. Morton and Miller (2005) estimated an average long-term (1872 – 1997) erosion rate of 0.39 m/yr. Figure 3-15 compares our shoreline change rates with those from the USGS on a transect-by-transect basis.

Tracking net movement of the shoreline and vegetation line (marking the landward extent of overwash) from 1938 to 2008 (addressing Objective 4) reveals that there is a significant positive correlation between the two (Figure 3-16;  $R^2 = 0.7$ , 95% CI). In addition, there is a positive correlation ( $R^2 = 0.7$ , 95% CI) between the rate of shoreline and vegetation line change (Figure 3-17). This quantitatively confirms what one may intuitively suspect, that the shoreline and vegetation line behave in concert with one another. If this were not the case, a divergence of the shoreline and vegetation line would result in an infinite widening of the beach, or a convergence in the total disappearance of the beach. Figure 3-18 demonstrates how increases in the distance between the shoreline (HWL) and the vegetation line serves as a good indication of regions where overwash occurs. Locations of the 4 zones of predominant beach activity (displayed in Figure 3-4) are overlain for reference. Distinct variations in the width between the shoreline and vegetation line can be seen between Zones 1 and 2 where overwash is dominant in comparison to Zones 3 and 4 where overwash is virtually non-existent. An increase in the

average distance between the shoreline and the vegetation line from 46 m (SD = 22) in 1938 to 63 m (SD = 63) in 2008, indicates an increase in overwash extent and supports Hypothesis 3. Figure 3-19 shows increased distances between the shoreline and vegetation line in both the 1956 and 1998 which correspond to periods of increased storm frequency (Figure 3-6).

### 3.4 Chapter 3 Tables

Table 3-1.

<b>Imagery</b>	<b>Date</b>	<b>Pixel Size (m)</b>
B&W Aerial Photo	04/24/1938	1 or 5
B&W Aerial Photo	02/15/1956 <sup>1</sup>	1
B&W Aerial Photo	01/22/1979	0.7
Color Infrared DOQ	11/25/1989	1
Natural Color Orthophotos	03/??/2008 <sup>2</sup>	0.3
IKONOS Satellite Image	05/02/2008	0.8

<sup>1</sup> Collection of the 1956 photos spanned three dates: Jan-25, Feb-1, and March-4. For consistency, a single date of Feb-15 is used in this table and all future references.

<sup>2</sup> The precise dates within March that the 2008 imagery was collected is unknown.

Table 3-2.

<b>Approximate Errors (m, ±)</b>	<b>Time Period</b>					
	<b>1938</b>	<b>1956</b>	<b>1979</b>	<b>1989</b>	<b>1998</b>	<b>2008</b>
2006 IKONOS Horizontal RMSE	1	1	1	1	1	1
Subsequent Georeferencing RMSE	1	2.2	3.5	5.1	1.8	0.8
Precision of Digitization	5.6	5.6	5.6	5.6	5.6	5.6
HWL Variability with Tidal Cycle	2	2	2	2	2	2
<b>Total Shoreline Position Error</b>	<b>6.1</b>	<b>6.4</b>	<b>7.0</b>	<b>7.9</b>	<b>6.3</b>	<b>6.1</b>
<b>Total Vegetation Line Position Error</b>	<b>5.8</b>	<b>6.1</b>	<b>6.7</b>	<b>7.6</b>	<b>6.0</b>	<b>5.7</b>

Table 3-3.

<b>Shoreline Change Rates &amp; Associated Errors</b>										
<b>Transect</b>	<b>EPR</b>	<b>WLR</b>	<b>WR2</b>	<b>WSE</b>	<b>WCI90</b>	<b>LRR</b>	<b>LR2</b>	<b>LSE</b>	<b>LCI90</b>	<b>LMS</b>
1	2.07	1.71	0.82	2.43	0.86	1.65	0.80	24.35	0.87	1.03
2	1.96	1.59	0.77	2.61	0.93	1.52	0.75	26.07	0.94	0.84
3	1.86	1.48	0.77	2.46	0.87	1.42	0.74	24.62	0.88	0.81

<b>Distance (m) of Shoreline from Offshore Baseline</b>						
<b>Transect</b>	<b>04/16/1938</b>	<b>02/15/1956</b>	<b>01/22/1979</b>	<b>11/25/1989</b>	<b>03/01/1998</b>	<b>05/10/2008</b>
1	190.7	254.1	370.0	405.8	471.4	364.4
2	190.8	258.1	359.8	400.7	466.1	358.3
3	186.9	258.6	359.0	392.8	468.4	360.9

<b>Net Movement (m) of Shoreline from Previous Survey (+ offshore, - onshore)</b>					
<b>Transect</b>	<b>1938-1956</b>	<b>1956-1979</b>	<b>1979-1989</b>	<b>1989-1998</b>	<b>1998-2008</b>
1	-63.4	-116.0	-35.8	-65.6	107.0
2	-67.3	-101.7	-40.9	-65.4	107.8
3	-71.7	-100.4	-33.7	-75.6	107.5

## 3.5 Chapter 3 Figures

Figure 3-1.

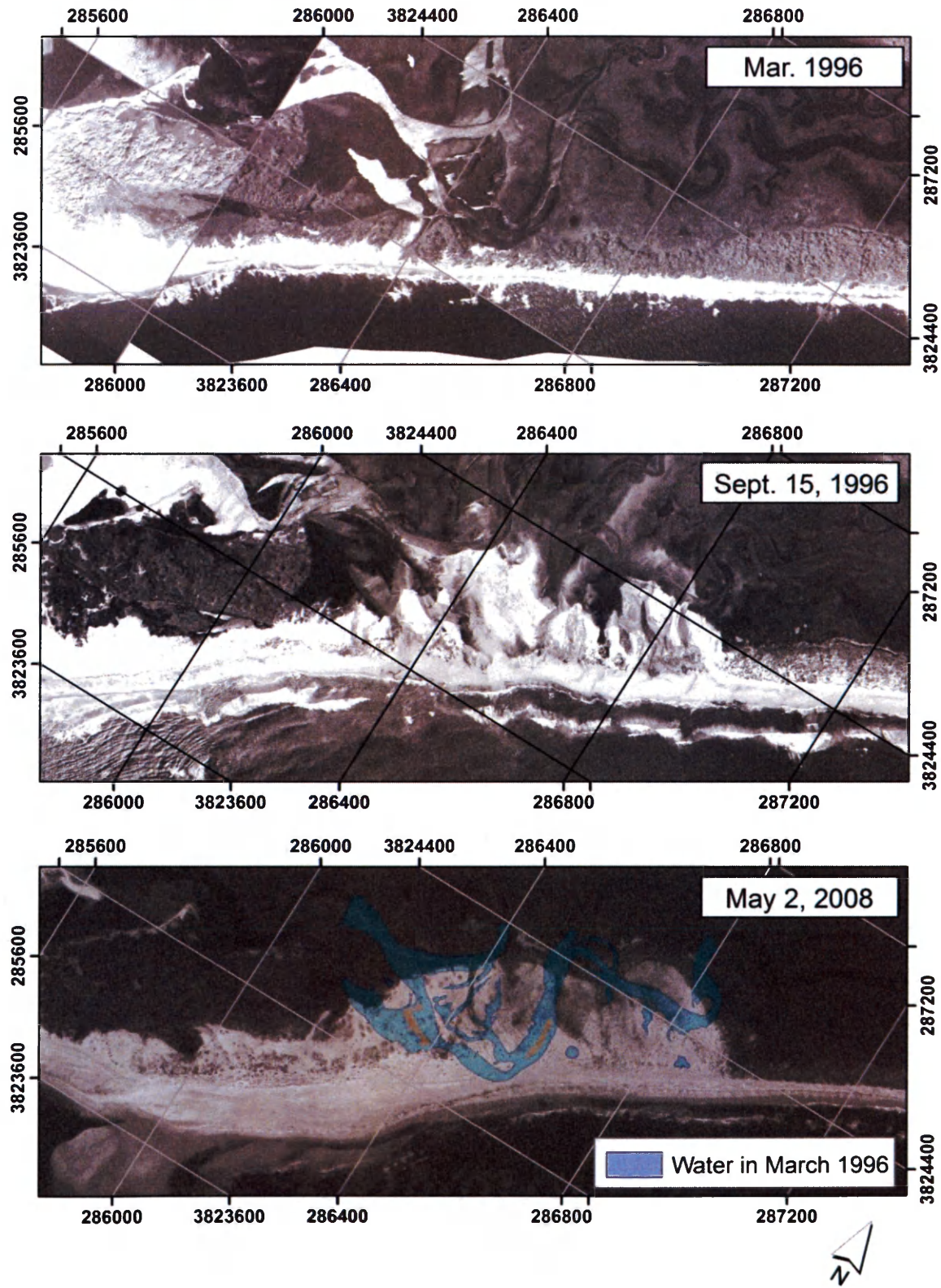




Figure 3-2.

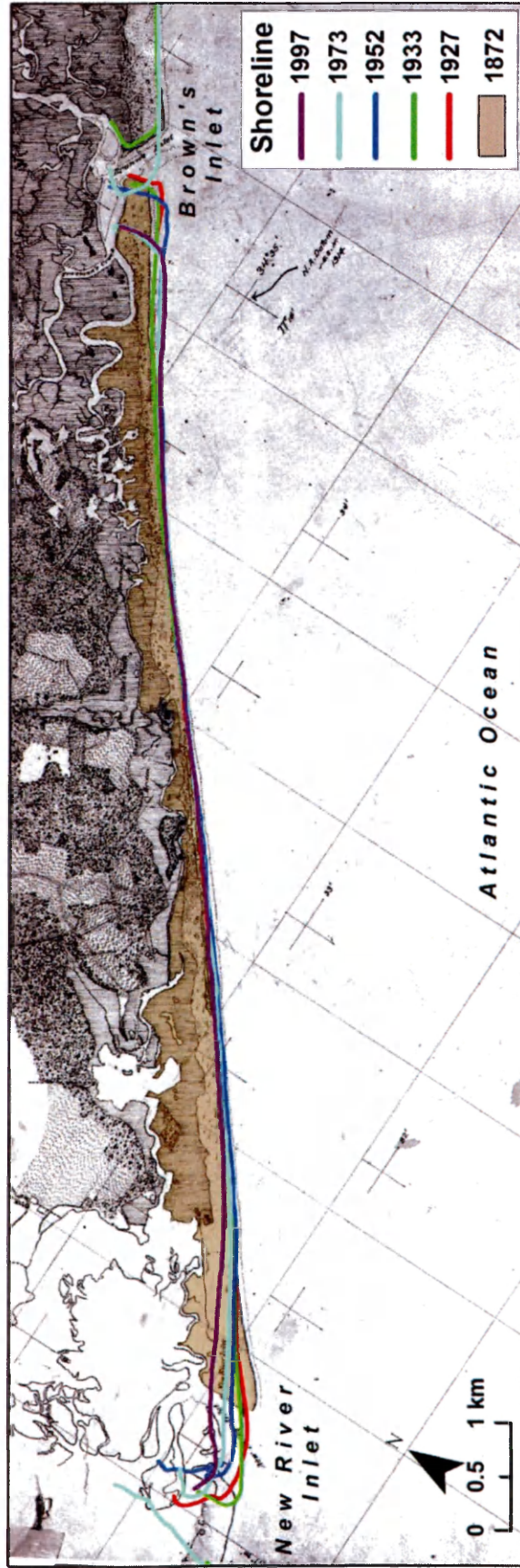


Figure 3-3.

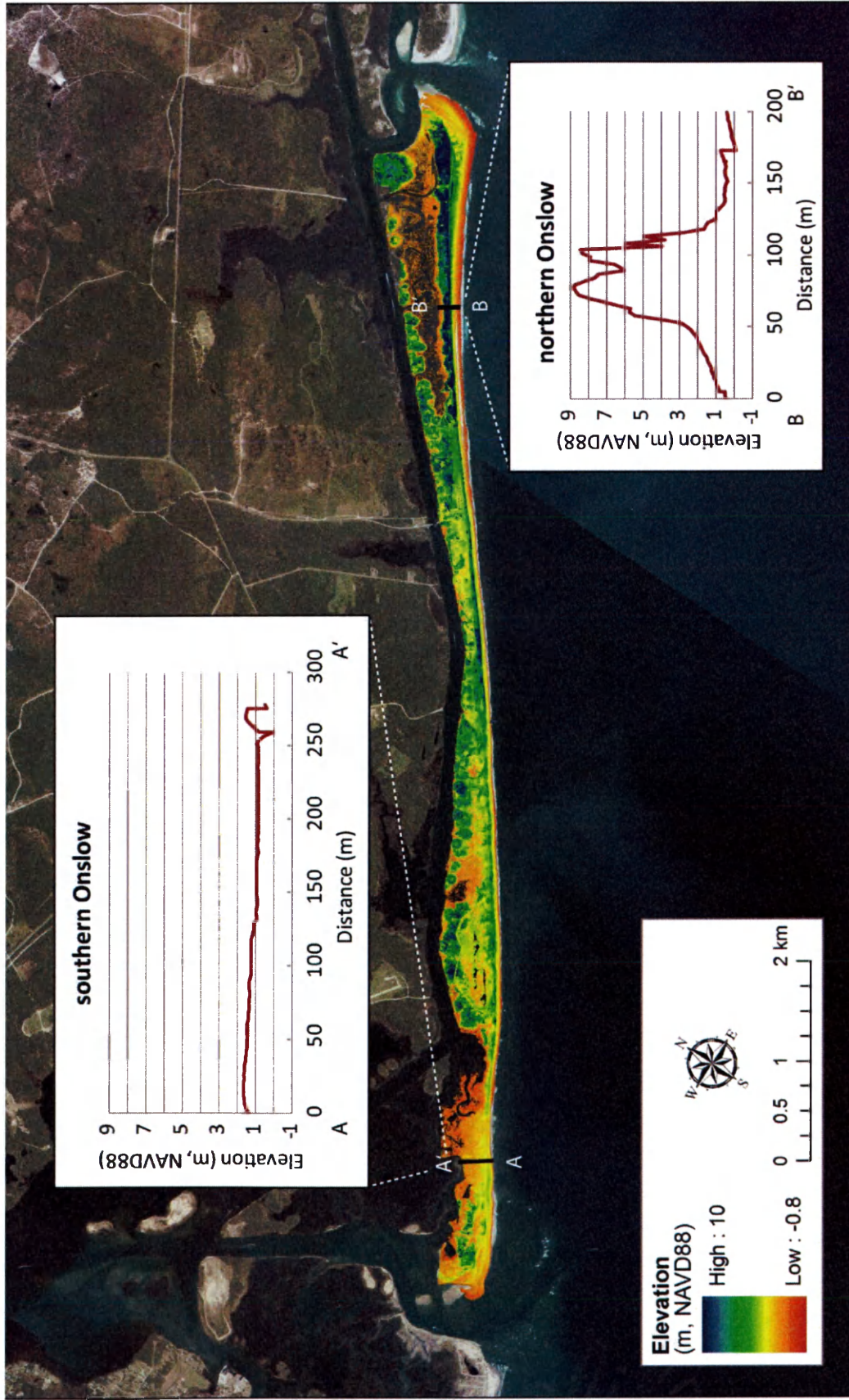




Figure 3-4.



Figure 3-5.

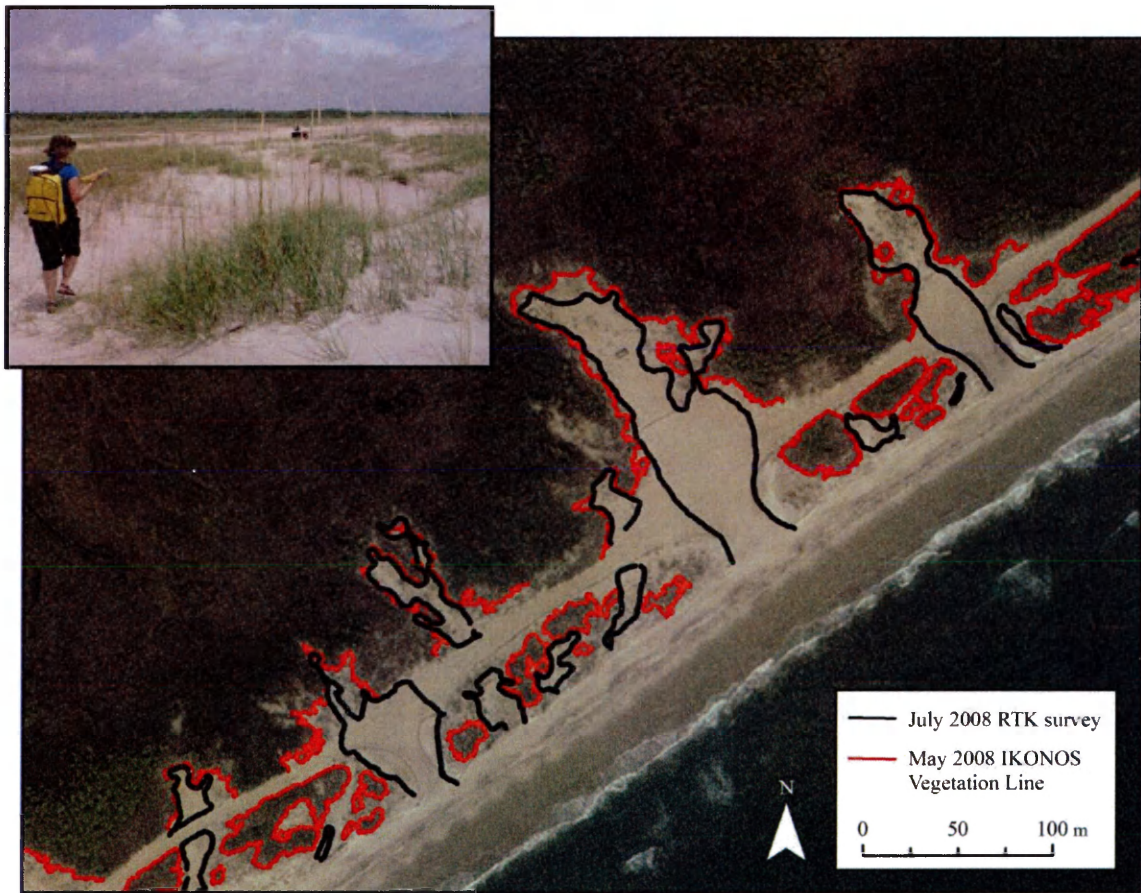


Figure 3-6.

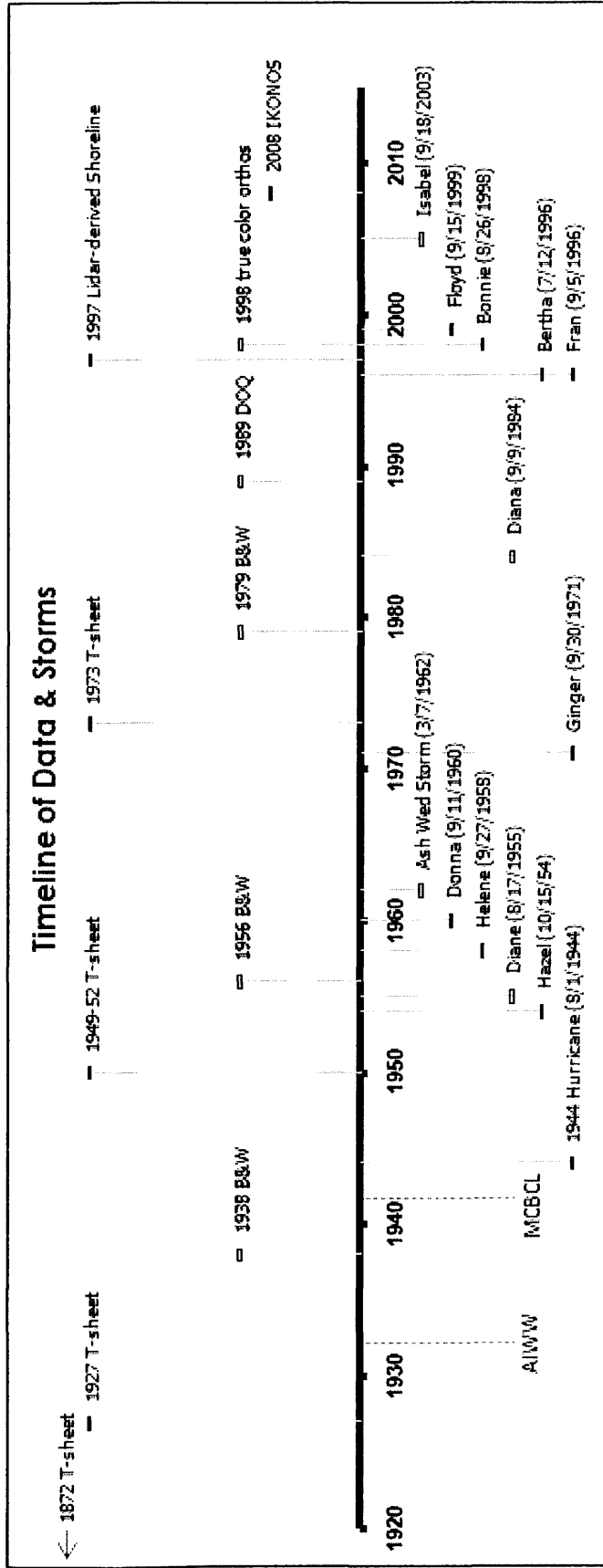




Figure 3-7.

1938

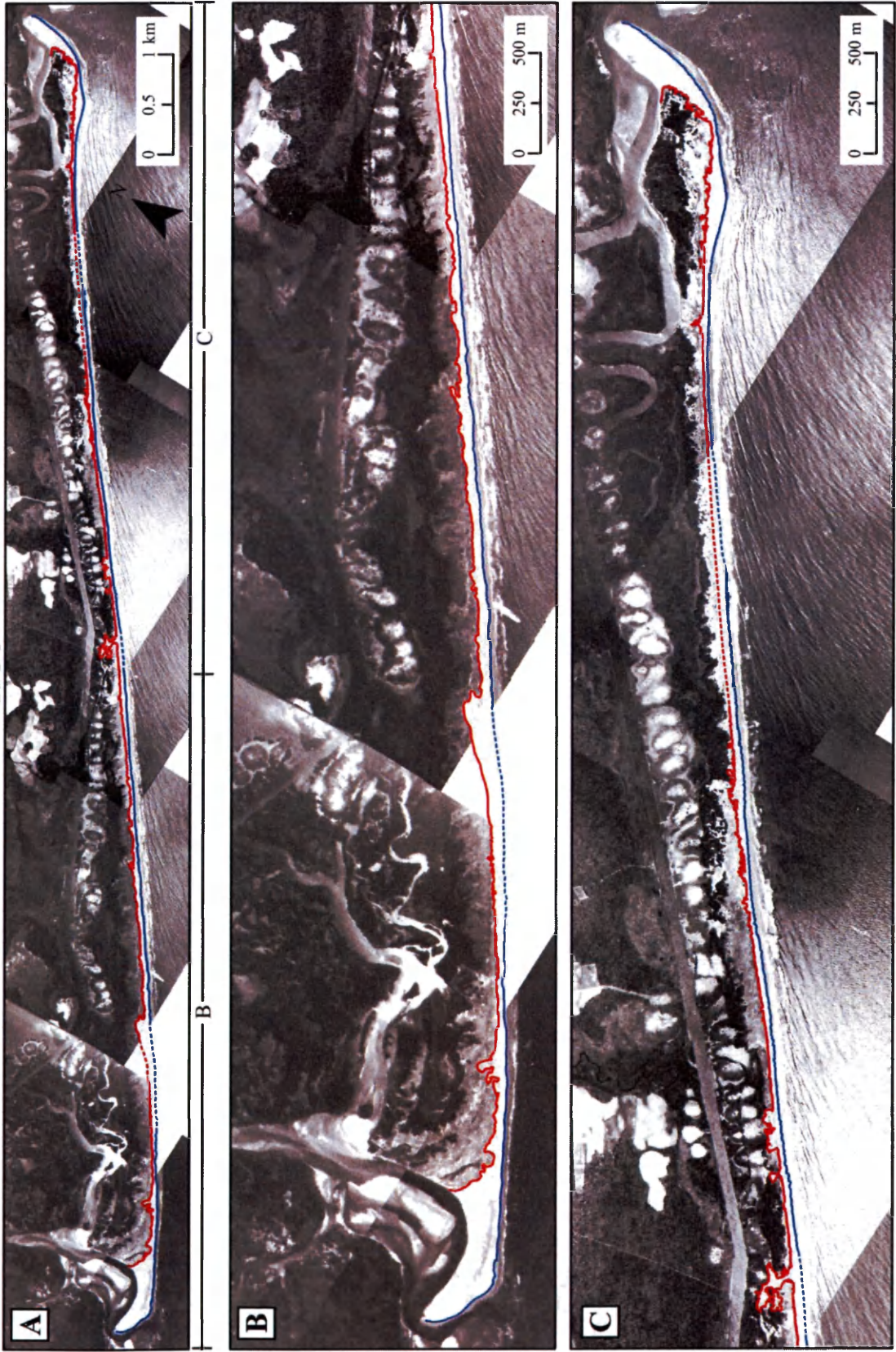




Figure 3-8.

1956

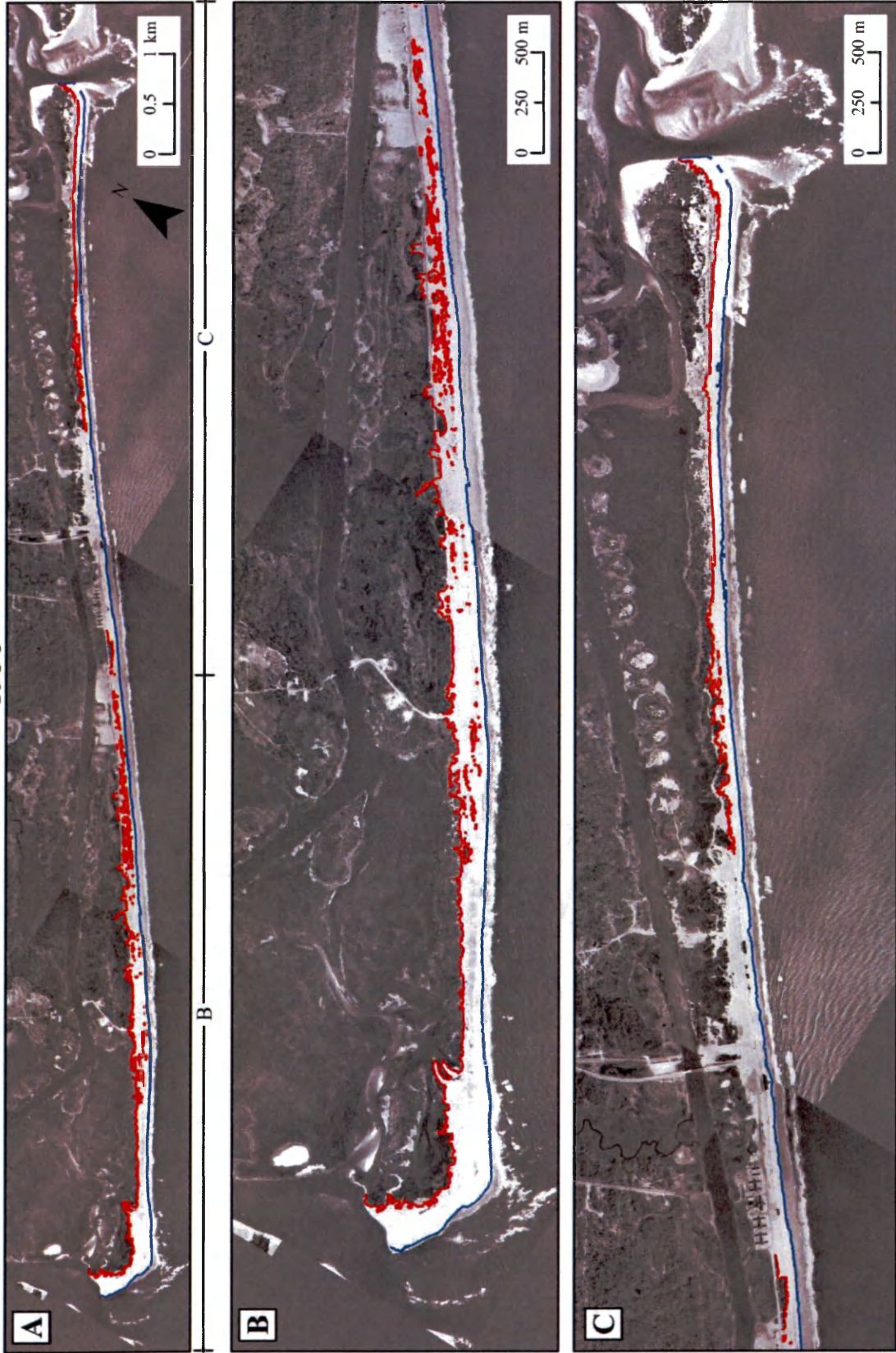




Figure 3-9.

1979

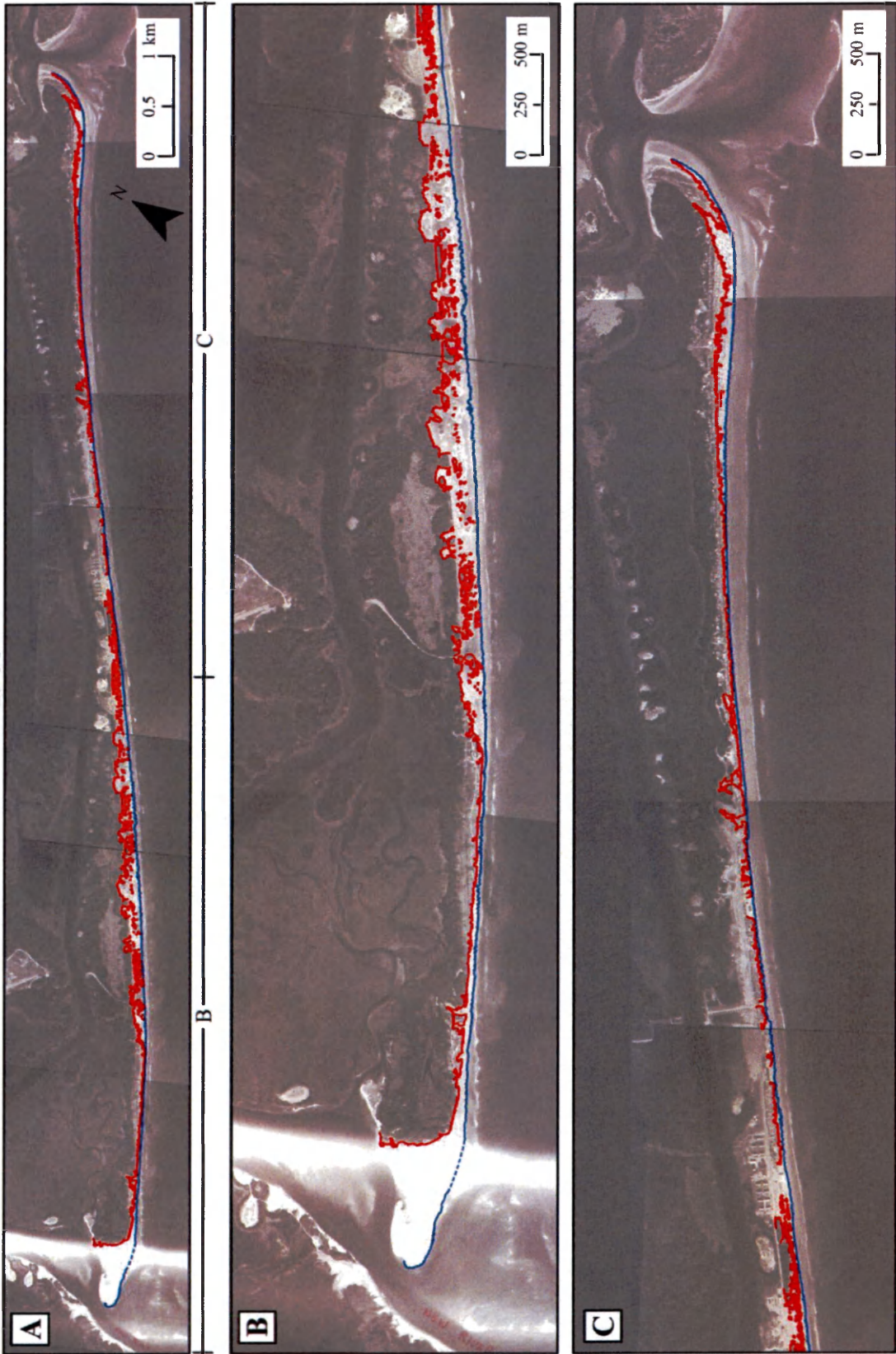




Figure 3-10.

1989

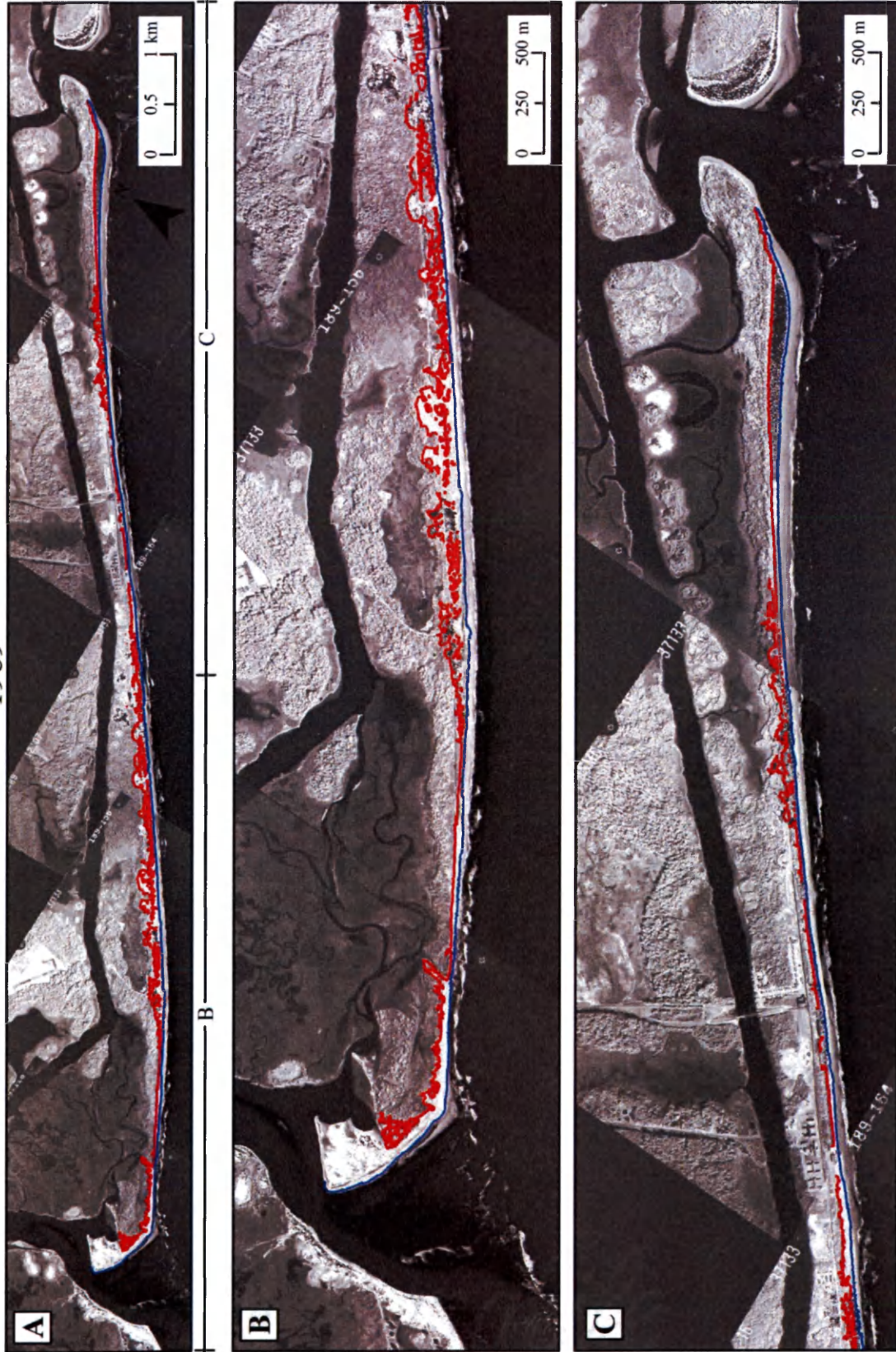




Figure 3-11.

1998

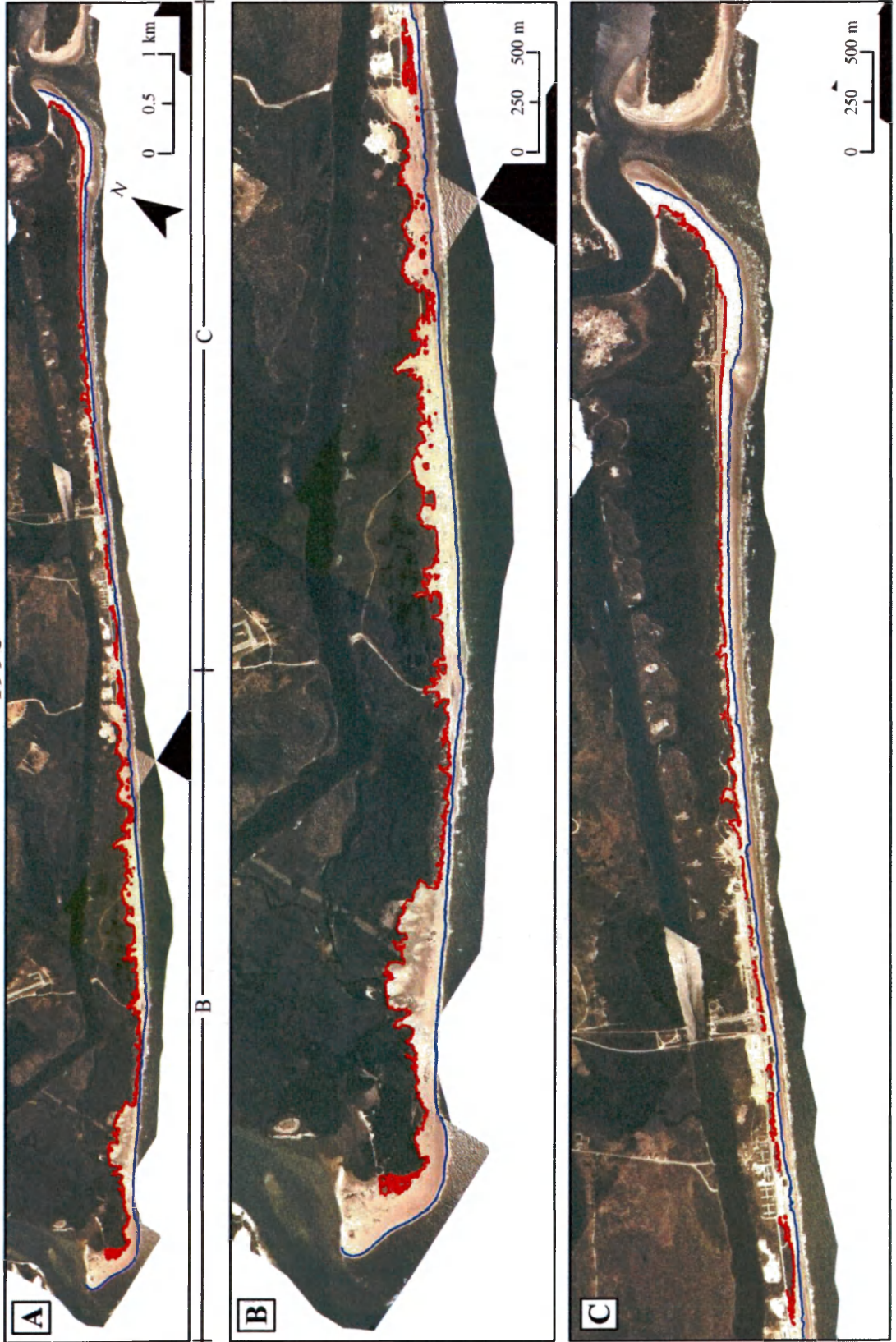




Figure 3-12.

2008

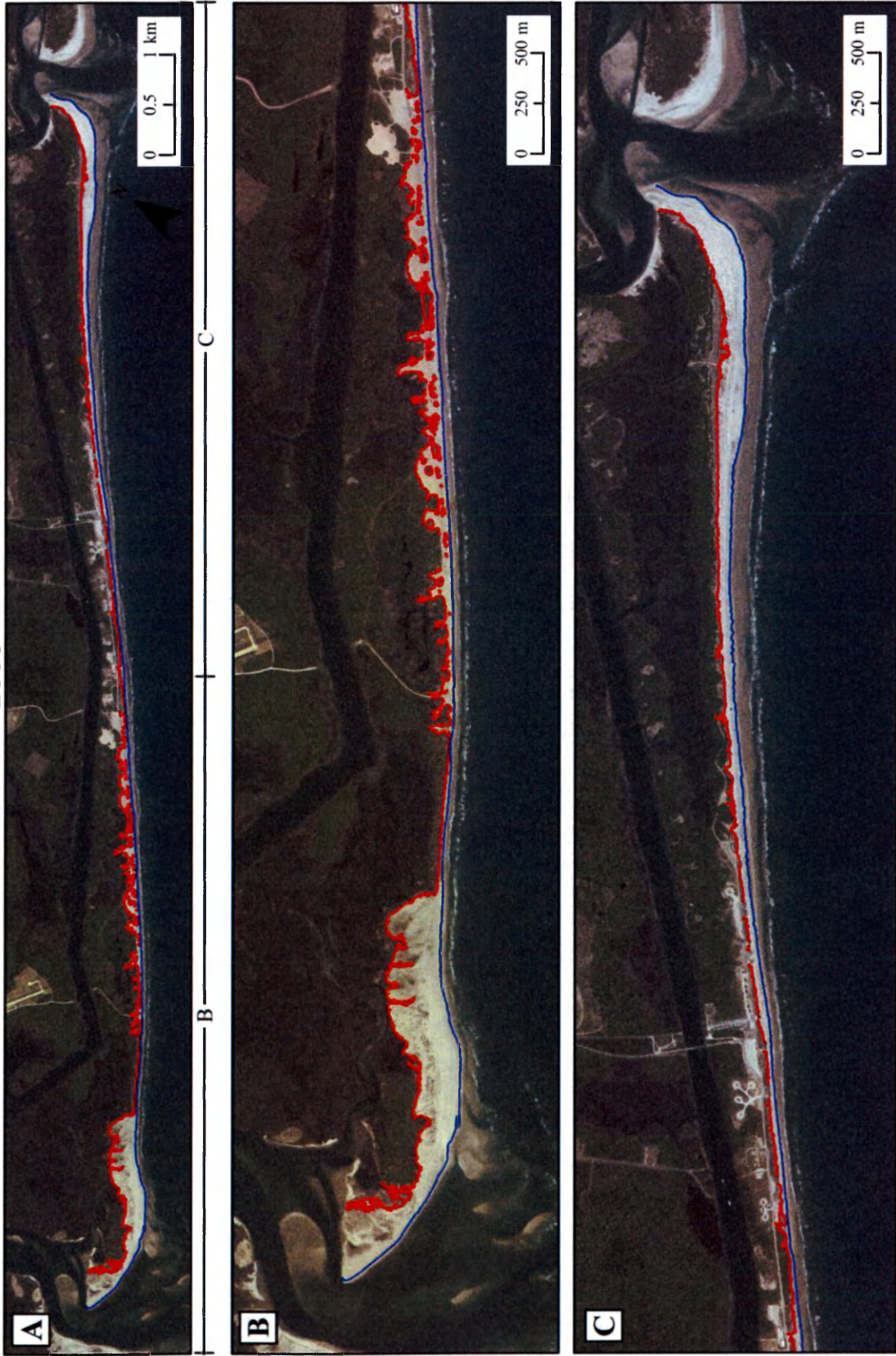


Figure 3-13.

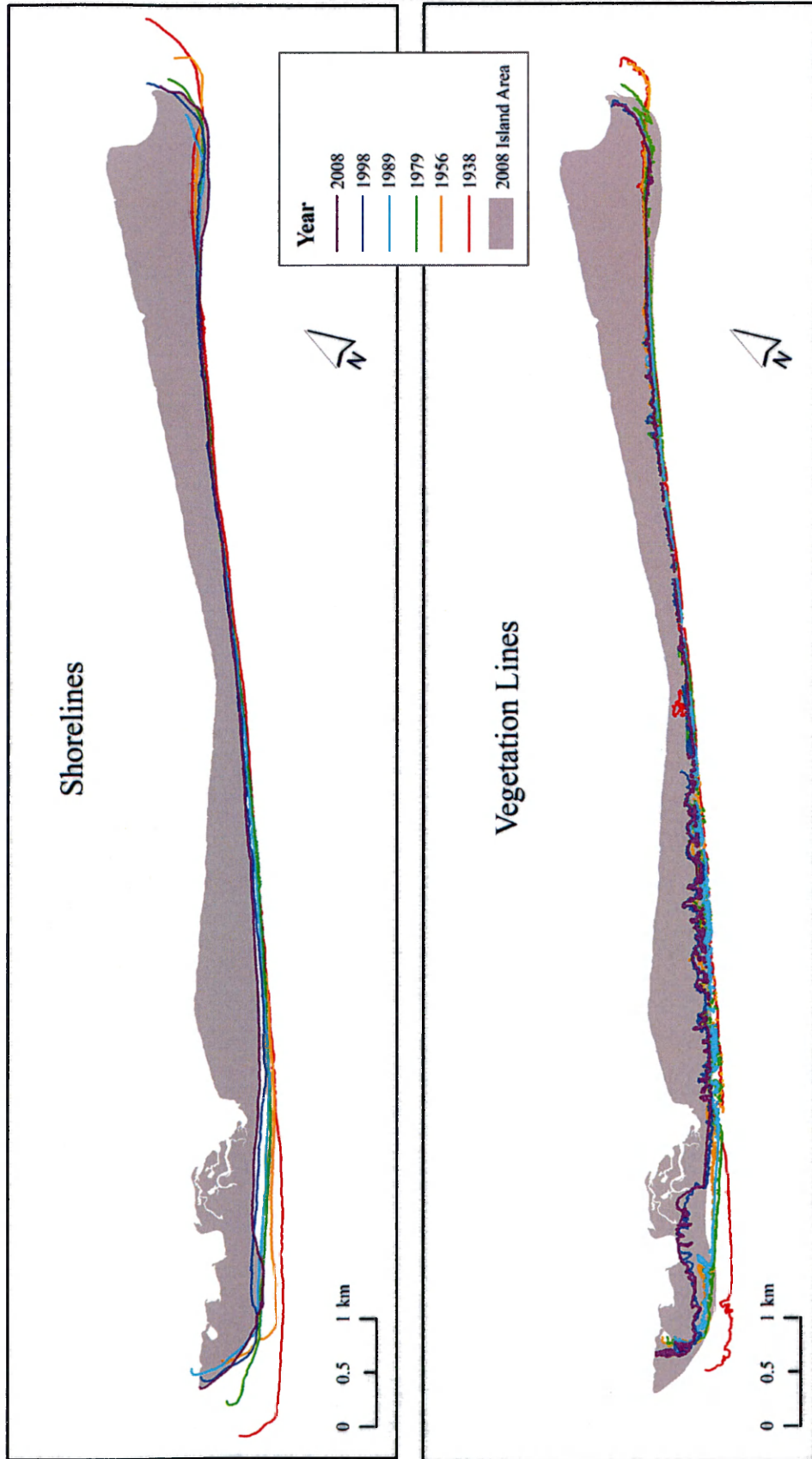




Figure 3-14.

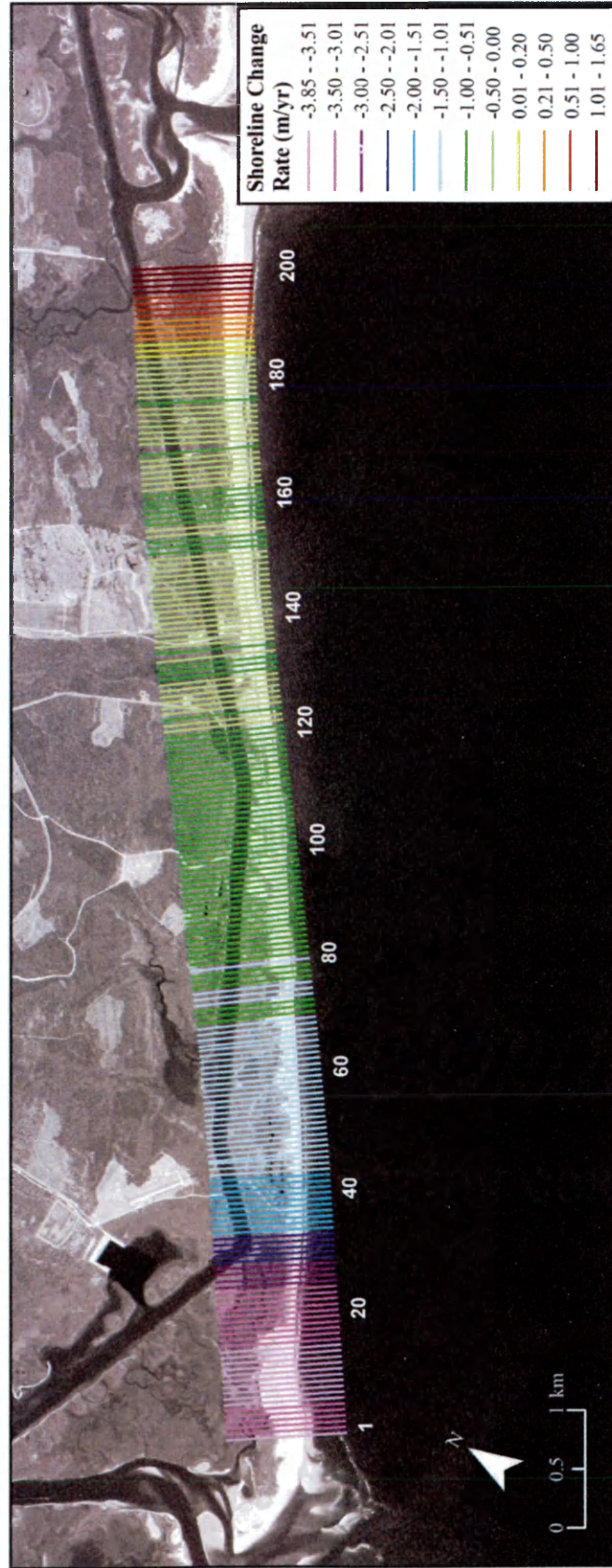


Figure 3-15.

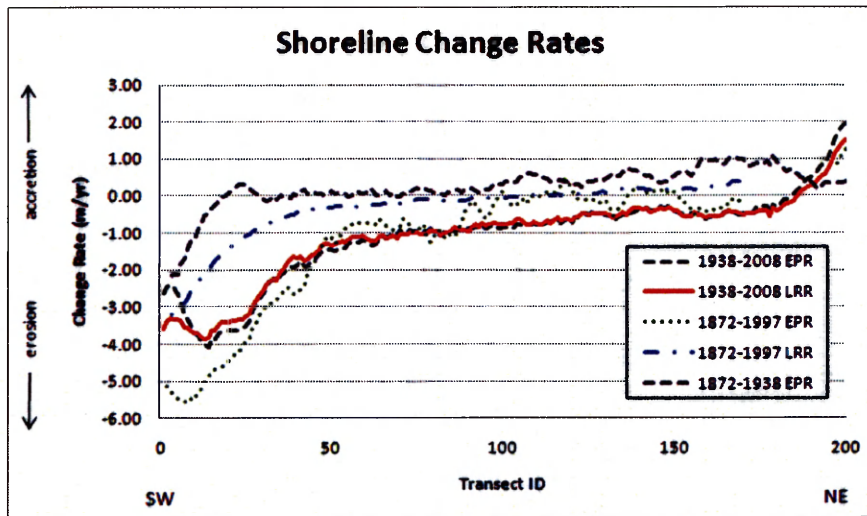


Figure 3-16.

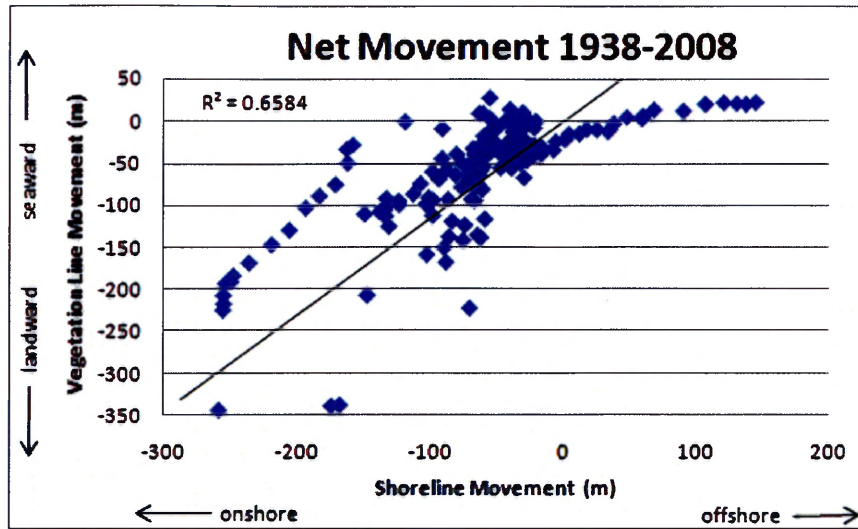


Figure 3-17.

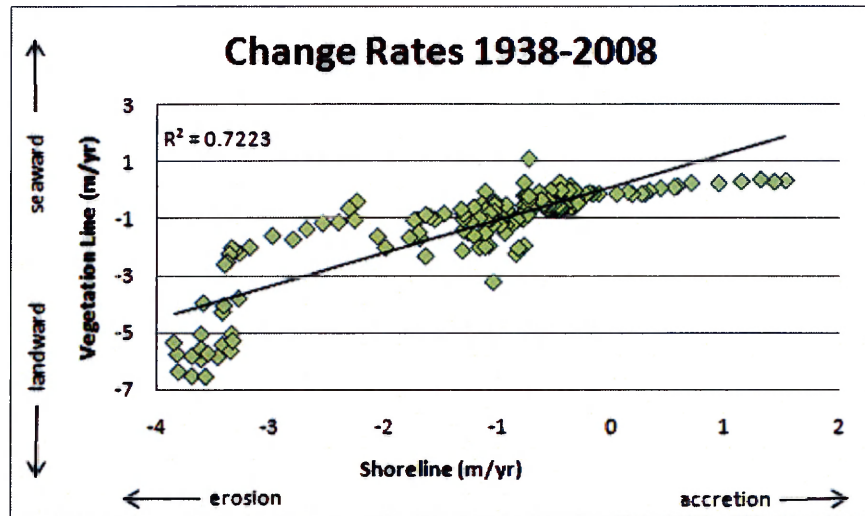




Figure 3-18.

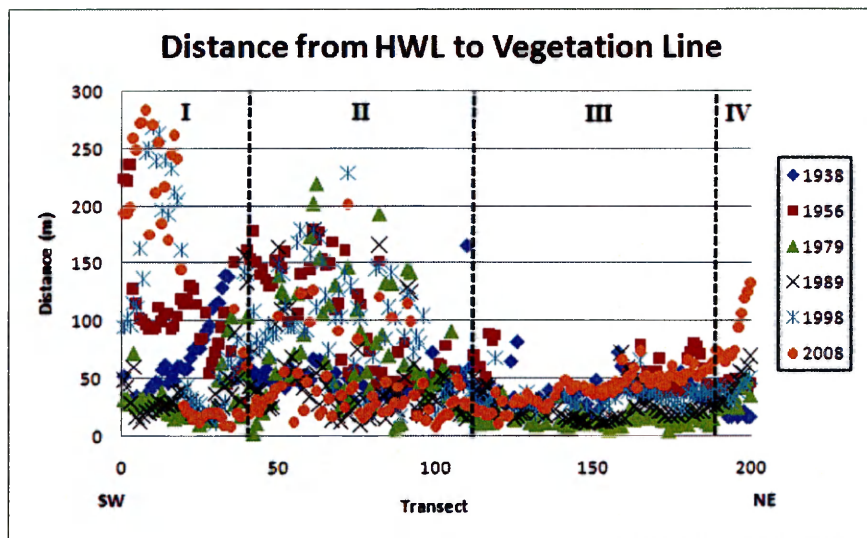
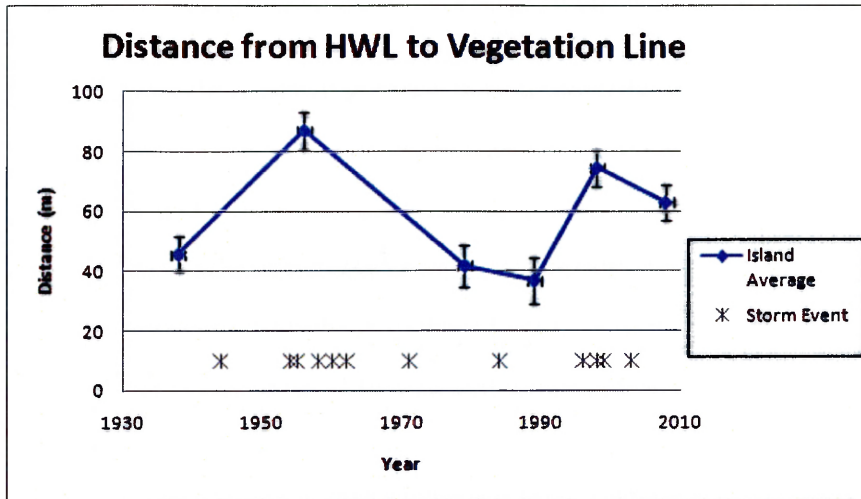


Figure 3-19.



**CHAPTER 4**  
**DISCUSSION, FUTURE WORK, AND CONCLUSIONS**

## 4.1 Discussion

A number of significant findings are presented in this research which not only quantify the role of barrier island overwash in the evolution of Onslow Beach, but also have broad-reaching implications for the importance of overwash as a mechanism for barrier island migration over seasonal to decadal timescales. The geophysical, geospatial, and sedimentological data presented here indicate that: (1) the relevant-sand prism of Onslow Beach is severely limited; (2) approximately 11% of the prism is comprised of sedimentologically distinct washover deposits; (3) the southern portion of Onslow Beach is actively undergoing barrier-island rollover; and (4) natural forcings have predominately shaped the evolution of Onslow Beach over the past 80 years.

The relevant-sand prism of southern Onslow Beach is severely limited. A volume of  $1.8 \pm 1.1 \times 10^6 \text{ m}^3$  equates an average thickness of only 90 cm of sand overlying the uppermost peat layer. The thickness of Onslow's relevant-sand prism is thinner than the prior estimate of 2-3 m for transgressive barrier islands provided by Heron et al. (1984) based upon drill holes collected along Core Banks and Portsmouth Banks, NC. This suggests that even in relation to other transgressive barrier islands of the eastern United States, Onslow Beach represents an end member in terms of sediment availability. Approximately  $199 \pm 88 \times 10^3 \text{ m}^3$  of sediment within the active overwash complex is comprised of sedimentologically distinct washover deposits. In other words, approximately 29% of the active overwash complex or 11% of the entire study area's relevant-sand prism consists of sedimentologically distinct washover deposits. To the best of our knowledge, there are no other such estimates of washover volume relative to barrier island prism to compare this estimate with. The closest comparison we can draw is with Skallingen barrier spit in the Danish Wadden Sea where Christiansen et al. (2004) estimated that overwash comprised 51% of the spits' standing volume above present day mean sea level. Although our research objectives are quite similar, the results are not directly comparable due to the different settings and primary modes of formation. Skallingen is a young barrier spit that formed

approximately 400 years ago through spit elongation ( Davis et al., 1997; Christiansen et al., 2004) as opposed to the barrier islands of the Outer Banks which originally formed offshore and translated landward over time reaching approximately their present day location around 4,000 years ago (Heron et al., 1984). Furthermore, Davis et al. (1997) and Christiansen et al. (2004) attribute the relatively high percentage of washover deposits found at Skallingen to the high-energy conditions that existed during the spits' initial formation (prior to any dune development).

The large sheetwash at the southwestern end of Onslow Beach is a textbook example of barrier island rollover. The sediments eroded from the nearshore during Hurricanes Bertha and Fran were deposited upon and behind the barrier island, enabling it to maintain mass while translating landward. As a first order approximation of how this sheetwash has evolved since initial deposition, full feature lidar collected in the fall of 1997 ([www.csc.noaa.gov/digitalcoast](http://www.csc.noaa.gov/digitalcoast)), one year after Hurricanes Bertha and Fran struck, was subtracted from 2007 NGA bare earth lidar. Figure 4-1 indicates that this unvegetated region has accumulated an average of 40 cm of sediment over the 12 years following Hurricane Fran. The sheetwash deposited by Hurricanes Bertha and Fran has, in essence, served as a platform upon which aeolian sediments and washover from minor events continue to aggrade.

The fact the sediments deposited on the island during storm events are retained within the sediment column over the long term demonstrates that overwash offers an important mechanism for island preservation in the face of rising sea-level and increased storm activity. This finding is particularly relevant for long-term sustainability of the island and demonstrates that although large storm events may result in shoreline erosion, a significant proportion of sediment removed from the nearshore is not lost from the system via offshore transport. Rather, it is deposited either on top of or behind the barrier island. This loss of sediment from the active littoral cells equates to a gain for the barrier island itself.

As is the case for the many coastlines, it is unlikely that the shoreline will be allowed to transgress landward indefinitely without some form of interference from coastal development. For the majority of Onslow Beach, if washover sediments were to reach the back side of the island, they would spill into the AIWW. If the position of the AIWW is held static into the future through dredging, and the barrier island is unable to transgress landward, an overall narrowing of the island will occur. Under the unlikely scenario that the trends in shoreline erosion that have occurred over the past 80 years (Figure 3-14) are projected into the future and all other conditions remain the same, the shoreline along the central portion of the island would erode to the present-day location of the AIWW in approximately 400 years. This research, however, exemplifies the dynamic nature of shoreline evolution, thereby highlighting the fundamental faults associated with applying linear projection rates, such as these, into the future. Forecast models that simply project historic shoreline trends into the future, or apply static models of inundation that do not take into account the effects of erosion and alterations in topography are likely to generate unrealistic predictions.

Regions experiencing an increase in the distance between the shoreline and the vegetation line, a likely indication of overwash, are shown to fluctuate through time in accordance with storm frequency. More research is necessary to examine overwash impact as it varies with storm intensity, tide level, wind and wave-setup, etc., but this reinforces the idea that trends in barrier island morphodynamics can be largely controlled by less frequent, high intensity events. This, in combination with knowledge that the area of highest shoreline erosion rates and overwash along Onslow Beach coincide with an undeveloped region that is largely uninfluenced by anthropogenic activities, underscores the fact that natural forcings (sea level, wind and wave energy, geology, etc.) exert first order control on the barrier island morphodynamics of Onslow Beach.

The fact that we document a moderately significant correlation between long-term shoreline change and washover volume (Figure 2-20), but do not see a linear trend between



shoreline change and volume of the relevant sand-prism (Figure 2-23) is somewhat conflicting and a bit puzzling. Furthermore, the latter is inconsistent with what Miselis and McNinch (2006) found in the nearshore subaqueous environment. This could indicate that the subaerial sediment volume of a barrier island may not be directly correlated with nearshore dynamics, at least in the case of severely sediment limited barrier islands such as Onslow Beach. Alternatively, the lack of correlation with alongshore variation in the relevant-sand prism may be a result of the landward and seaward boundaries used in this study. It is possible that the volume of sediment seaward of the shoreline plays a large role and that when our estimates of barrier island prism volume are combined with volume estimates from the nearshore, a stronger correlation may appear. Nevertheless, this is a point which warrants further investigation.

## **4.2 Future Work**

Although not addressed in this thesis, our GPR surveys also extended north of Riseley Pier in a shore parallel transect running the length of the beach access road to approximately 2.8 km southwest of Brown's Inlet (where public access is not allowed) along with three cross-island transects in the northern and central portions of the island. At the time this thesis was submitted, no vibracores had been collected to ground-truth the GPR north of Riseley Pier, thus we limited our volume calculations to the southern half of the island where we had good control. There were however, a number of interesting features discernable in the GPR including what looks like a historic river outlet ~ 3 km southwest of the present day location of Brown's Inlet. This could be of great importance when evaluating the long-term evolution of the island and explaining the dramatic differences in morphology between the two ends of the island. Given a bit more ground-truthing, we hope to extend our relevant-sand prism calculations to the entire island and to collect cores along the back side of the island for better landward constraint on the depth of the sand/silt contact. In addition, we plan to extend our volume calculations to include the nearshore environment by integrating submerged sediment volumes derived from multibeam bathymetry

and high-resolution sub-bottom (chirp) profiles that were collected offshore (in depths < 10 m) and along the back side of the island in the AIWW in September of 2007 (Wadman et al., 2008). These data will be used in combination with GPR collected along the barrier island, both ground-truthed by sediment vibracores, to develop a more comprehensive estimate of the volume of sediment available for transport via wind or sea energy.

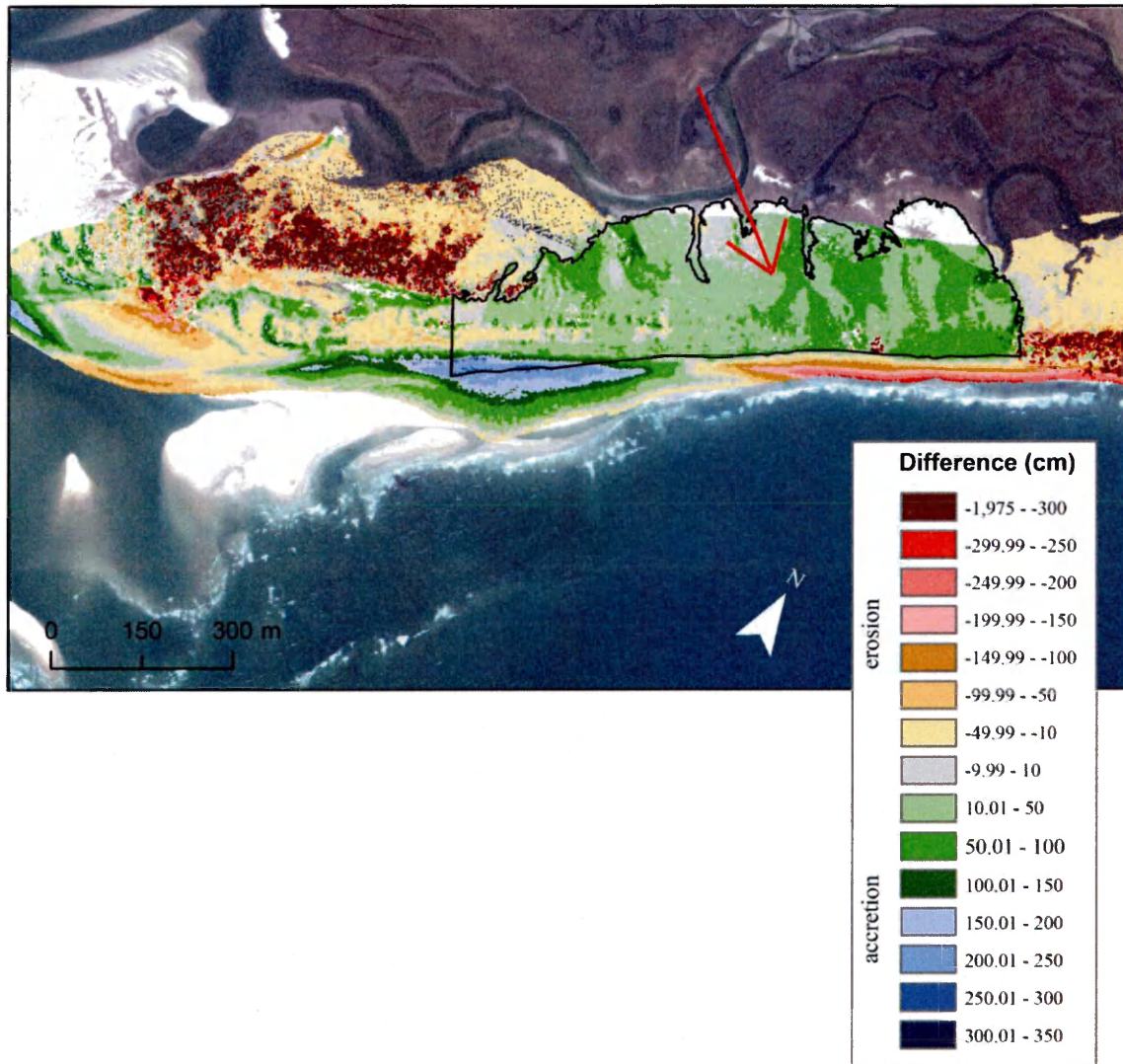
Although it was not accomplished with this study, it is possible that under proper conditions, GPR could resolve finer-scale overwash deposits. Due to the large number of properties that can result in horizontal reflection surfaces, and the very fine scale of washover deposits, it would be advised that attempts to do so be controlled by numerous sediment samples with ample control on changes in water content with depth and, ideally, collected at a time when the water table is low.

### 4.3 Major Conclusions

- The volume of the relevant-sand prism south of Riseley Pier is  $1.8 \pm 1.1 \times 10^6 \text{ m}^3$  and averages  $\sim 90$  cm in thickness.
- Sedimentologically distinct washover deposits make up approximately  $199 \pm 88 \times 10^3 \text{ m}^3$  of sediment which equals 29% of the active overwash complex or 11% of the entire study area's relevant sand-prism.
- A simple linear relationship between spatial and temporal variability in shoreline behavior and volume of the relevant-sand prism does not exist.
- A positive correlation exists between both rates of change and net movement of the shorelines and vegetation lines.
- Changes in the distance between the shoreline and the vegetation line provide a useful metric for identifying areas experiencing overwash.
- The average distance between the shoreline and the vegetation line increased from 1938 to 2008, indicating an increase in overwash area, which appears to fluctuate in accordance with storm frequency.
- The region of Onslow Beach experiencing the highest rate of erosion from 1938-2008 (3.85 m/yr) is not the region used for military amphibious training activities.
- Large overwash events are a mechanism by which sediments can accumulate on and behind the island, thereby increasing the relevant-sand prism and decreasing susceptibility to future erosion.

## 4.4 Chapter 4 Figures

Figure 4-1.

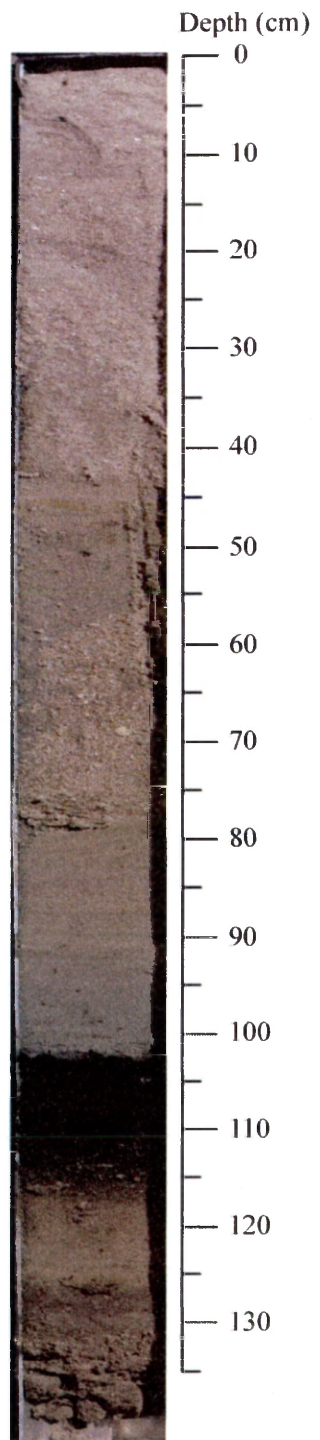


## 8 APPENDICES

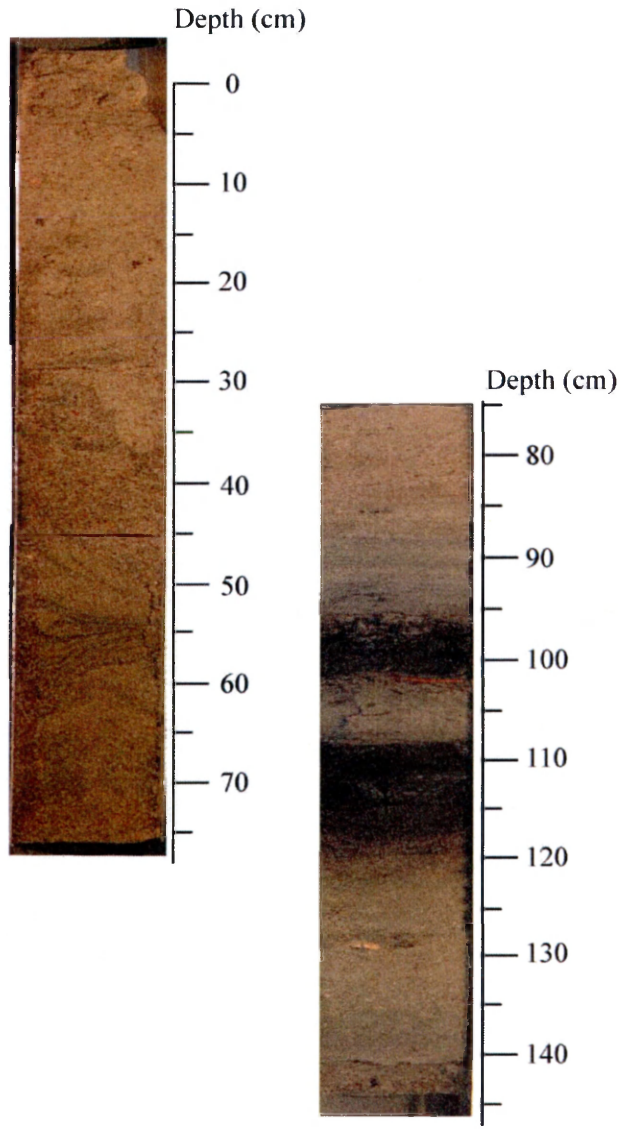


## **Appendix I**

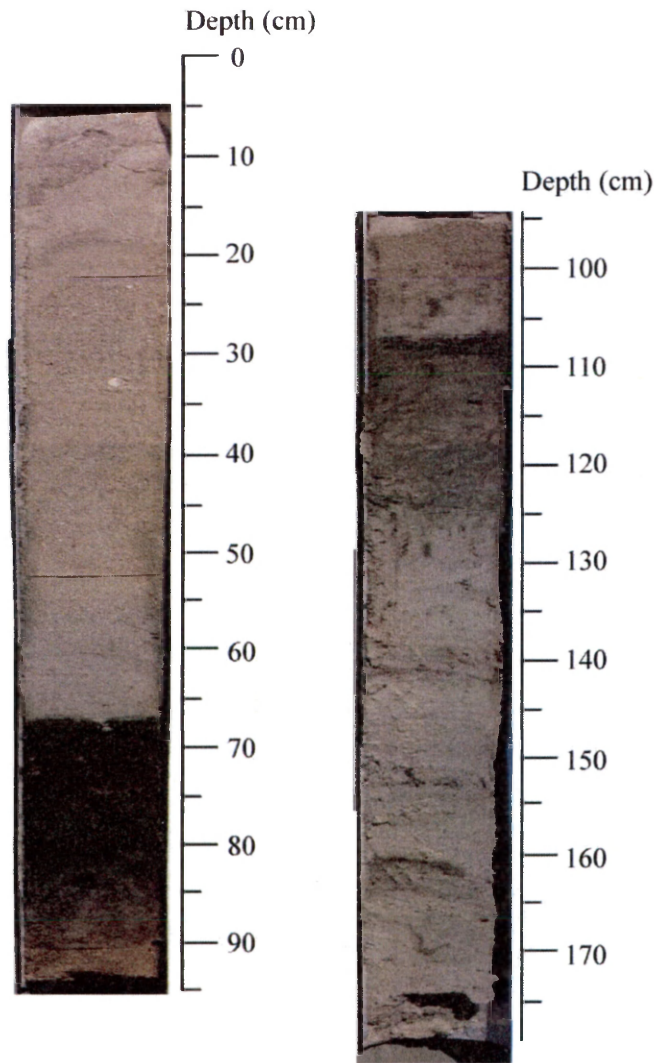
ONSVC04  
Coordinates (UTM):  
289262.43  
3825909.92



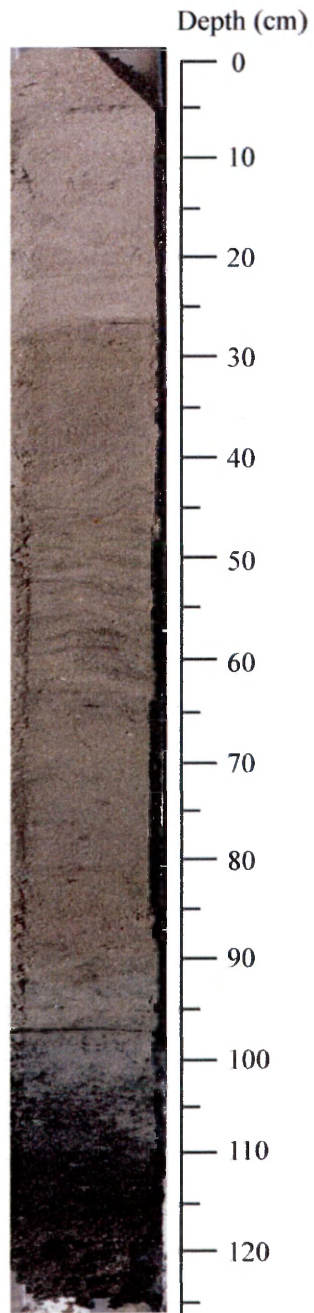
ONSVC05  
Coordinates (UTM):  
289254.60  
3825918.81



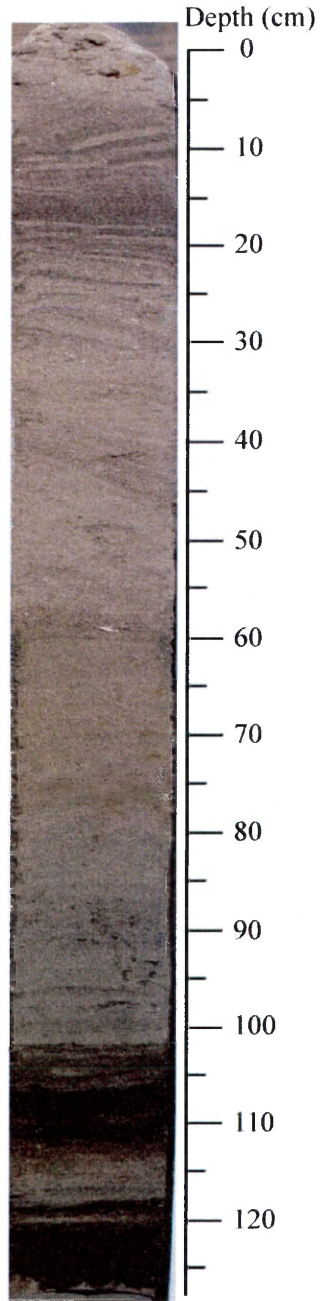
ONSVC06  
Coordinates (UTM):  
289232.73  
3825940.54



ONSVC14  
Coordinates (UTM):  
288218.97  
3825153.50

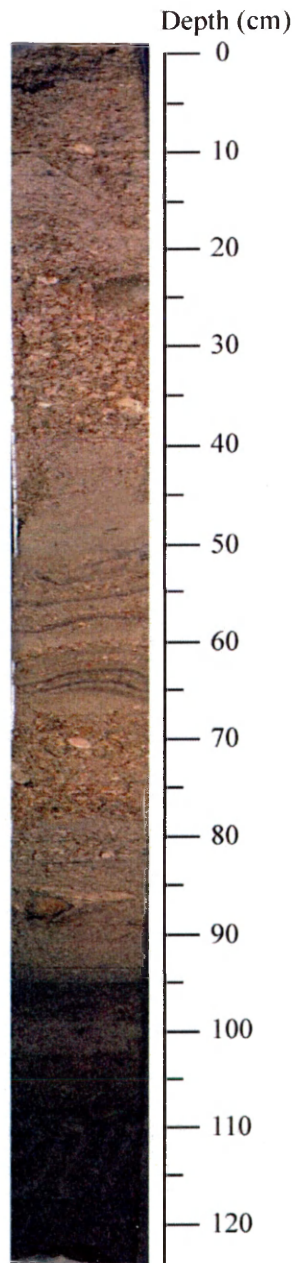


ONSVC18  
Coordinates (UTM):  
287703.03  
3824754.76

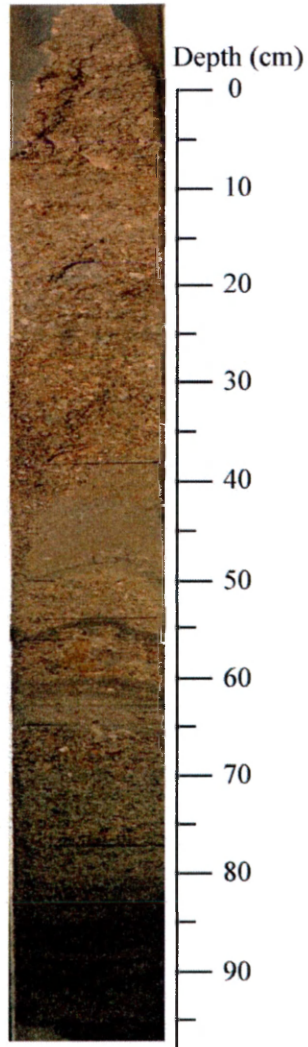




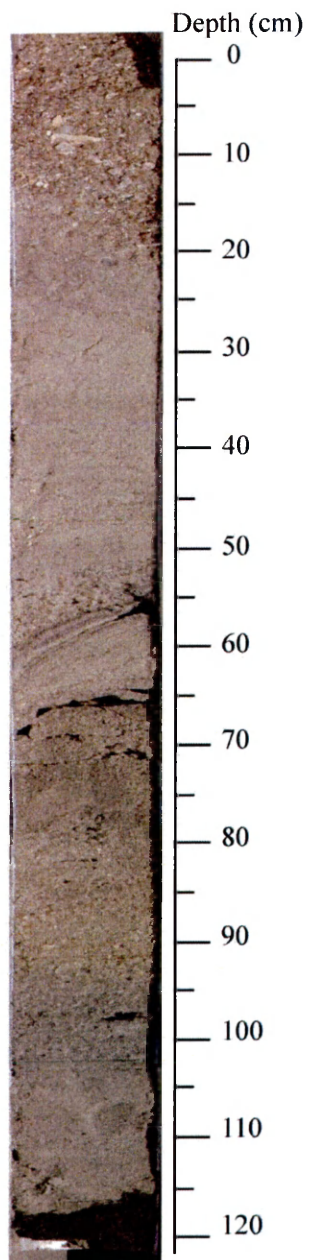
ONSVC25  
Coordinates (UTM):  
286283.38  
3824093.28



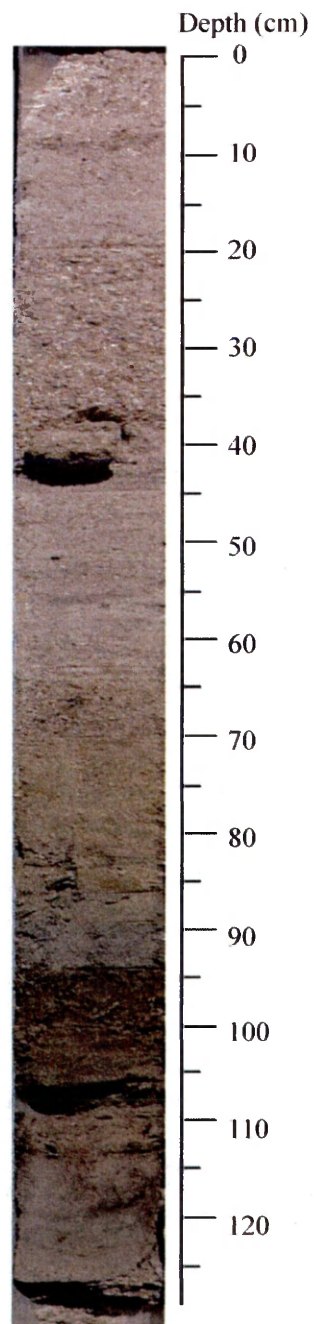
ONSVC26  
Coordinates (UTM):  
286290.51  
3824098.08



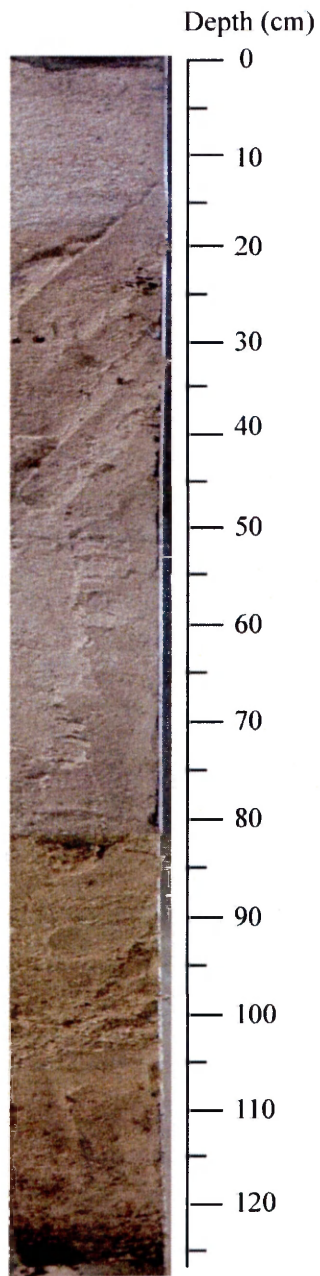
ONSVC29  
Coordinates (UTM):  
286221.72  
3824082.01



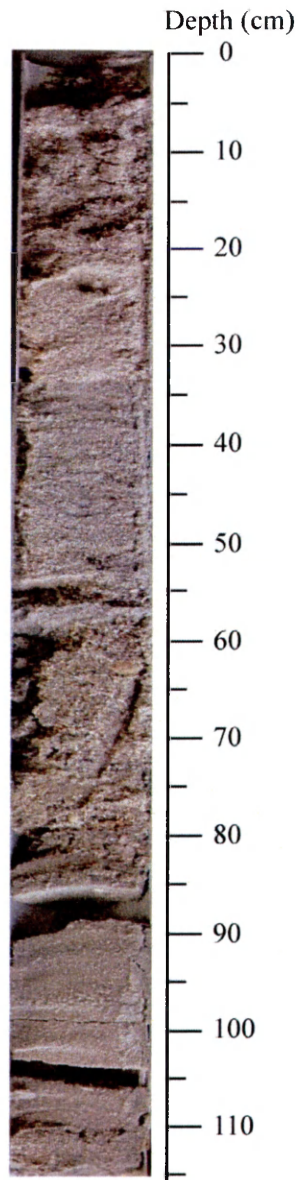
ONSVC40  
Coordinates (UTM):  
286250.46  
3824014.31



ONSPC04  
Coordinates (UTM):  
288238.60  
3825133.51

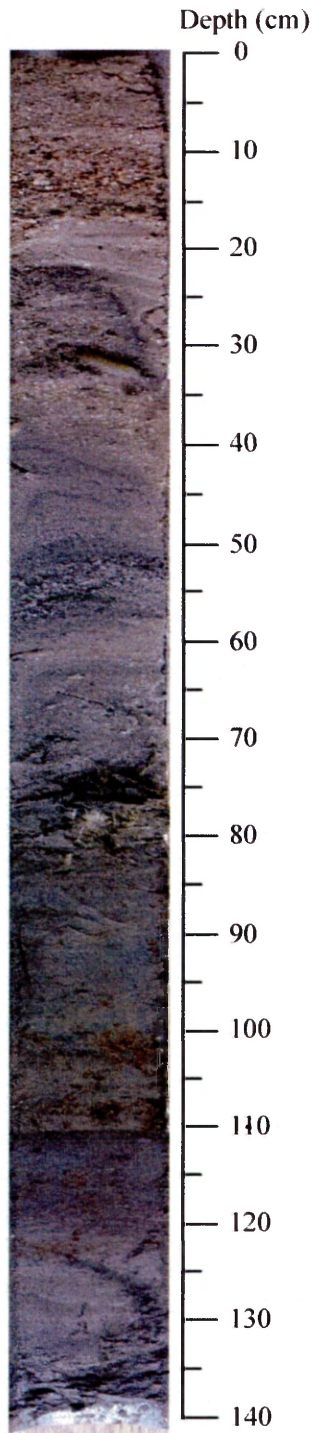


ONSPC05  
Coordinates (UTM):  
286675.96  
3824210.26





ONSPC07  
Coordinates (UTM):  
286610.79  
3824320.00



## **Appendix II**

Core ID	X (UTM, m)	Y (UTM, m)	Depth (cm)	% Fines	% Sand	% Gravel	Median (psi)	Mean (M1, psi)	STD (M2, psi)	Skewness (M3)	Kurtosis (M4)
ONVVC04	289262.43	3825909.92	0	0.41	98.38	1.21	2.10	1.87	0.71	16.056	46.99
ONVVC04	289262.43	3825909.92	10	0.37	99.30	0.33	2.10	1.93	0.61	25.3389	86.09
ONVVC04	289262.43	3825909.92	20	0.34	97.98	1.68	1.94	1.64	0.77	19.2709	57.28
ONVVC04	289262.43	3825909.92	30	0.47	98.76	0.77	1.93	1.65	0.72	23.9197	76.45
ONVVC04	289262.43	3825909.92	40	0.52	99.01	0.47	2.11	1.93	0.61	27.9161	97.19
ONVVC04	289262.43	3825909.92	50	0.51	99.49	0.00	2.36	2.30	0.38	48.517	246.06
ONVVC04	289262.43	3825909.92	60	0.75	98.36	0.89	1.47	1.36	0.75	24.8147	79.19
ONVVC04	289262.43	3825909.92	70	0.49	97.57	1.94	1.76	1.49	0.82	19.3958	57.08
ONVVC04	289262.43	3825909.92	80	0.47	99.35	0.18	2.60	2.46	0.56	10.2849	37.45
ONVVC04	289262.43	3825909.92	90	0.53	99.20	0.27	2.67	2.67	0.24	76.3071	763.96
ONVVC04	289262.43	3825909.92	100	0.83	99.17	0.00	2.63	2.64	0.22	123.2827	1227.30
ONVVC05	289254.60	3825918.81	0	0.47	98.12	1.41	2.19	1.99	0.62	20.9348	68.42
ONVVC05	289254.60	3825918.81	10	0.32	98.49	1.19	2.11	1.87	0.79	12.0969	31.98
ONVVC05	289254.60	3825918.81	20	0.45	99.55	0.00	2.37	2.30	0.39	57.6435	289.51
ONVVC05	289254.60	3825918.81	30	0.31	98.75	0.94	2.06	1.83	0.70	19.6855	60.84
ONVVC05	289254.60	3825918.81	40	0.27	99.23	0.51	2.04	1.84	0.67	21.6336	68.68
ONVVC05	289254.60	3825918.81	50	0.34	99.49	0.17	2.32	2.16	0.60	16.3892	53.04
ONVVC05	289254.60	3825918.81	60	0.34	99.66	0.00	2.35	2.30	0.37	55.9456	295.18
ONVVC05	289254.60	3825918.81	70	0.34	99.66	0.00	2.35	2.28	0.39	55.3067	272.38
ONVVC05	289254.60	3825918.81	80	0.35	99.65	0.00	2.39	2.31	0.42	40.0102	183.66
ONVVC05	289254.60	3825918.81	90	0.43	99.57	0.00	2.66	2.66	0.24	80.6735	805.95
ONVVC06	289232.73	3825940.54	0	0.57	98.32	1.11	2.35	2.25	0.48	33.3301	136.62
ONVVC06	289232.73	3825940.54	10	0.29	99.60	0.12	2.28	2.15	0.51	30.9922	119.97
ONVVC06	289232.73	3825940.54	20	0.38	99.42	0.20	2.34	2.29	0.35	68.8963	382.24
ONVVC06	289232.73	3825940.54	30	0.41	99.40	0.19	2.21	2.05	0.60	21.8858	73.49

Core ID	X (UTM, m)	Y (UTM, m)	Depth (cm)	% Fines	% Sand	% Gravel	Median (psi)	Mean (M1, psi)	STD (M2, psi)	Skewness (M3)	Kurtosis (M4)
ONSVC06	289232.73	3825940.54	40	0.45	99.55	0.00	2.31	2.23	0.47	32.1283	131.85
ONSVC06	289232.73	3825940.54	50	0.35	99.65	0.00	2.23	2.17	0.43	46.2957	208.79
ONSVC06	289232.73	3825940.54	60	0.50	99.50	0.00	2.51	2.48	0.36	42.6387	237.02
ONSVC14	288218.97	3825153.50	0	0.42	98.98	0.59	2.01	1.74	0.75	18.0265	53.07
ONSVC14	288218.97	3825153.50	10	0.41	98.96	0.63	2.12	1.91	0.67	19.4545	60.61
ONSVC14	288218.97	3825153.50	20	0.62	99.38	0.00	2.42	2.37	0.46	25.6863	108.10
ONSVC14	288218.97	3825153.50	30	1.06	98.94	0.00	2.41	2.36	0.43	32.645	146.13
ONSVC14	288218.97	3825153.50	40	0.97	99.03	0.00	2.44	2.36	0.48	23.3749	93.80
ONSVC14	288218.97	3825153.50	50	0.79	99.21	0.00	2.44	2.38	0.43	30.9247	141.24
ONSVC14	288218.97	3825153.50	60	0.79	99.21	0.00	2.38	2.28	0.50	24.5423	94.71
ONSVC14	288218.97	3825153.50	70	1.04	98.81	0.16	2.47	2.44	0.39	36.659	185.60
ONSVC14	288218.97	3825153.50	80	1.34	98.25	0.40	2.52	2.48	0.37	38.7603	208.40
ONSVC14	288218.97	3825153.50	90	0.99	98.57	0.44	2.48	2.41	0.48	22.6459	93.01
ONSVC14	288218.97	3825153.50	100	1.03	98.97	0.00	2.64	2.65	0.31	47.3601	348.13
ONSVC18	287703.03	3824754.76	0	0.41	98.89	0.70	2.32	2.28	0.39	56.2232	279.44
ONSVC18	287703.03	3824754.76	10	0.29	99.71	0.00	2.23	2.21	0.41	51.9635	245.79
ONSVC18	287703.03	3824754.76	20	0.17	99.74	0.09	2.19	2.09	0.53	31.5274	119.02
ONSVC18	287703.03	3824754.76	30	0.27	97.64	2.08	2.26	2.09	0.61	19.5305	63.74
ONSVC18	287703.03	3824754.76	40	0.36	99.44	0.20	2.21	2.13	0.48	34.7954	141.79
ONSVC18	287703.03	3824754.76	50	0.30	99.70	0.00	2.35	2.32	0.37	61.2067	322.69
ONSVC18	287703.03	3824754.76	60	0.34	99.66	0.00	2.43	2.40	0.34	50.8598	298.42
ONSVC18	287703.03	3824754.76	70	0.40	99.60	0.00	2.48	2.42	0.39	40.3051	203.11
ONSVC18	287703.03	3824754.76	80	0.38	99.62	0.00	2.46	2.43	0.33	62.9053	371.06
ONSVC18	287703.03	3824754.76	90	0.46	99.54	0.00	2.60	2.60	0.30	59.557	434.04
ONSVC18	287703.03	3824754.76	100	0.76	98.83	0.41	2.55	2.54	0.25	105.7463	865.30

Core ID	X (UTM, m)	Y (UTM, m)	Depth (cm)	Depth			% Gravel	Median (psi)	Mean (M1, psi)	STD (M2, psi)	Skewness (M3)	Kurtosis (M4)
				% Fines	% Sand	% Gravel						
ONSVC25	286283.38	3824093.28	0	0.38	82.77	16.85	1.30	1.22	0.96	16.5154	45.28	
ONSVC25	286283.38	3824093.28	10	0.31	79.93	19.76	1.80	1.45	0.92	13.7576	36.07	
ONSVC25	286283.38	3824093.28	20	0.45	85.11	14.44	1.28	1.19	0.93	18.2845	51.84	
ONSVC25	286283.38	3824093.28	30	0.54	56.50	42.96	0.87	0.94	0.95	22.7358	68.61	
ONSVC25	286283.38	3824093.28	40	0.79	77.79	21.42	1.54	1.39	0.98	14.5578	38.44	
ONSVC25	286283.38	3824093.28	50	0.49	98.36	1.15	2.53	2.49	0.45	18.9921	88.46	
ONSVC25	286283.38	3824093.28	60	0.53	93.06	6.42	2.24	1.96	0.83	8.7963	21.49	
ONSVC25	286283.38	3824093.28	70	0.53	73.32	26.15	2.18	1.93	0.71	14.9607	43.26	
ONSVC25	286283.38	3824093.28	80	0.55	83.32	16.13	1.88	1.50	0.86	15.4029	42.15	
ONSVC25	286283.38	3824093.28	90	0.44	99.17	0.39	2.33	2.21	0.50	24.6836	95.14	
ONSVC25	286283.38	3824093.28	100	0.98	98.73	0.29	2.73	2.73	0.299	27.1866	293.17	
ONSVC26	286290.51	3824098.08	0	0.40	73.46	26.14	2.05	1.67	0.90	11.0226	27.42	
ONSVC26	286290.51	3824098.08	10	0.25	76.02	23.73	1.94	1.54	0.92	11.9175	30.05	
ONSVC26	286290.51	3824098.08	20	0.34	74.51	25.15	1.20	1.18	0.94	17.9441	50.55	
ONSVC26	286290.51	3824098.08	30	0.57	75.58	23.85	1.85	1.43	0.97	13.8733	36.16	
ONSVC26	286290.51	3824098.08	40	0.58	99.16	0.26	2.51	2.45	0.42	24.6804	121.63	
ONSVC26	286290.51	3824098.08	50	0.49	91.64	7.87	2.36	2.10	0.78	8.3138	20.99	
ONSVC26	286290.51	3824098.08	60	0.33	93.94	5.73	2.19	1.89	0.79	11.4013	29.82	
ONSVC26	286290.51	3824098.08	70	0.65	88.97	10.38	1.69	1.38	0.95	13.9571	36.56	
ONSVC26	286290.51	3824098.08	80	0.38	98.83	0.79	2.27	2.21	0.51	29.3748	112.78	
ONSVC26	286290.51	3824098.08	90	2.54	97.46	0.00	2.64	2.67	0.35	22.4409	176.89	
ONSVC29	286221.72	3824082.01	0	0.16	69.04	30.80	1.12	1.11	1.01	16.368	44.52	
ONSVC29	286221.72	3824082.01	10	0.17	62.47	37.36	1.24	1.22	0.95	16.9713	46.99	
ONSVC29	286221.72	3824082.01	20	0.13	95.39	4.48	2.09	1.93	0.65	21.2224	68.22	
ONSVC29	286221.72	3824082.01	30	0.38	99.62	0.00	2.41	2.35	0.41	40.6825	193.71	

Core ID	X (UTM, m)	Y (UTM, m)	Depth (cm)	% Fines	% Sand	% Gravel	Median (psi)	Mean (M1, psi)	STD (M2, psi)	Skewness (M3)	Kurtosis (M4)
ONSVC29	286221.72	3824082.01	40	0.23	98.67	1.10	2.49	2.41	0.48	17.466	73.17
ONSVC29	286221.72	3824082.01	50	0.15	95.63	4.22	2.48	2.28	0.70	8.5684	23.43
ONSVC29	286221.72	3824082.01	60	0.34	99.16	0.50	2.25	2.22	0.44	40.4749	176.86
ONSVC29	286221.72	3824082.01	70	0.47	99.53	0.00	2.14	1.97	0.63	19.4739	62.37
ONSVC29	286221.72	3824082.01	80	0.26	98.92	0.82	2.14	2.01	0.55	27.8614	101.40
ONSVC29	286221.72	3824082.01	90	0.31	96.13	3.56	2.13	1.95	0.62	20.9892	68.68
ONSVC29	286221.72	3824082.01	100	0.36	98.07	1.57	2.04	1.80	0.73	16.3078	47.25
ONSVC40	286250.46	3824014.31	0	0.12	72.95	26.93	1.89	1.44	1.00	11.4302	28.09
ONSVC40	286250.46	3824014.31	10	0.08	96.25	3.67	2.02	1.79	0.74	17.06	49.91
ONSVC40	286250.46	3824014.31	20	0.07	75.14	24.79	1.90	1.53	0.94	12.4304	31.65
ONSVC40	286250.46	3824014.31	30	0.49	54.14	45.38	1.12	1.14	1.05	12.6404	31.67
ONSVC40	286250.46	3824014.31	40	0.59	92.40	7.01	2.08	1.80	0.80	11.5975	29.83
ONSVC40	286250.46	3824014.31	50	0.52	98.27	1.20	2.07	1.85	0.70	22.0157	70.86
ONSVC40	286250.46	3824014.31	60	0.37	97.49	2.14	1.96	1.70	0.77	17.5556	51.88
ONSVC40	286250.46	3824014.31	70	0.64	95.92	3.45	2.14	1.87	0.81	11.4095	29.61
ONSVC40	286250.46	3824014.31	80	0.68	99.32	0.00	2.44	2.36	0.43	28.7043	131.96
ONSVC40	286250.46	3824014.31	90	0.88	98.96	0.16	2.35	2.35	0.33	63.4101	373.64
ONSVC40	286250.46	3824014.31	100	1.82	98.09	0.10	2.38	2.35	0.40	37.3783	185.12
ONSVC40	286250.46	3824014.31	110	0.80	98.69	0.51	2.27	2.27	0.49	27.2549	108.32
ONSVC40	286250.46	3824014.31	120	1.14	98.51	0.35	2.72	2.71	0.31	25.9413	257.90
ONSPC04	288238.60	3825133.51	1	0.12	98.30	1.57	2.20	2.07	0.51	31.4049	121.93
ONSPC04	288238.60	3825133.51	10	0.10	96.55	3.35	2.24	2.10	0.61	17.7802	57.67
ONSPC04	288238.60	3825133.51	20	0.44	90.36	9.20	2.48	2.41	0.45	22.2605	98.09
ONSPC04	288238.60	3825133.51	30	0.42	95.54	4.03	2.40	2.35	0.43	30.1341	137.07
ONSPC04	288238.60	3825133.51	40	0.31	92.23	7.46	2.47	2.43	0.39	35.4689	181.61

Core ID	X (UTM, m)	Y (UTM, m)	Depth (cm)	% Fines	% Sand	% Gravel	Median (psi)	Mean (M1, psi)	STD (M2, psi)	Skewness (M3)	Kurtosis (M4)
ONSPC04	288238.60	3825133.51	50	0.19	99.81	0.00	2.42	2.34	0.46	28.9508	123.29
ONSPC04	288238.60	3825133.51	60	0.35	99.65	0.00	2.36	2.26	0.48	26.1193	105.91
ONSPC04	288238.60	3825133.51	70	0.34	99.54	0.11	2.45	2.40	0.35	49.5203	282.43
ONSPC04	288238.60	3825133.51	80	0.47	98.66	0.87	2.32	2.22	0.52	23.1563	86.21
ONSPC04	288238.60	3825133.51	90	0.44	99.36	0.20	2.38	2.30	0.47	25.5184	105.38
ONSPC04	288238.60	3825133.51	100	1.31	72.63	26.06	2.20	1.83	0.92	8.1915	18.95
ONSPC04	288238.60	3825133.51	110	0.78	99.22	0.00	2.51	2.48	0.32	50.2875	326.25
ONSPC04	288238.60	3825133.51	119	0.63	99.37	0.00	2.62	2.60	0.32	36.9257	280.85
ONSPC05	286675.96	3824210.26	0	0.17	94.74	5.10	1.32	1.19	0.93	18.3757	52.20
ONSPC05	286675.96	3824210.26	10	0.21	94.65	5.14	1.10	1.08	0.93	21.0028	62.04
ONSPC05	286675.96	3824210.26	20	0.00	98.46	1.54	1.74	1.50	0.78	23.2802	72.64
ONSPC05	286675.96	3824210.26	30	0.09	99.48	0.43	1.82	1.51	0.82	17.8952	51.47
ONSPC05	286675.96	3824210.26	40	0.37	98.36	1.27	2.08	1.78	0.80	13.7304	37.33
ONSPC05	286675.96	3824210.26	50	0.33	92.69	6.98	1.98	1.58	0.88	13.4221	35.30
ONSPC05	286675.96	3824210.26	60	0.36	77.74	21.90	0.76	0.82	0.93	28.3448	91.61
ONSPC05	286675.96	3824210.26	70	0.45	84.27	15.28	1.85	1.46	0.97	11.642	28.90
ONSPC05	286675.96	3824210.26	80	0.52	73.94	25.54	1.04	1.11	0.98	17.6924	49.41
ONSPC05	286675.96	3824210.26	90	0.33	98.70	0.98	2.45	2.44	0.26	109.4965	847.38
ONSPC05	286675.96	3824210.26	100	0.30	99.70	0.00	2.37	2.35	0.30	90.3122	589.19
ONSPC05	286675.96	3824210.26	108	0.15	99.85	0.00	2.55	2.57	0.24	94.3388	890.39
ONSPC05	286675.96	3824210.26	116	0.41	98.39	1.20	2.27	2.17	0.50	27.2663	105.38
ONSPC07	286610.79	3824320.00	0	0.93	92.42	6.65	2.26	1.87	0.92	7.6715	17.47
ONSPC07	286610.79	3824320.00	10	0.49	77.39	22.12	0.74	0.85	1.00	22.1669	66.07
ONSPC07	286610.79	3824320.00	20	0.19	98.10	1.72	2.18	1.92	0.80	10.702	27.62
ONSPC07	286610.79	3824320.00	30	0.16	96.08	3.76	2.16	1.82	0.82	11.421	29.47



Core ID	X (UTM, m)	Y (UTM, m)	Depth (cm)	% Fines	% Sand	% Gravel	Median (psi)	Mean (M1, psi)	STD (M2, psi)	Skewness (M3)	Kurtosis (M4)
ONSPC07	286610.79	3824320.00	40	0.17	98.87	0.96	2.32	2.17	0.62	14.5037	45.45
ONSPC07	286610.79	3824320.00	50	0.50	98.24	1.26	2.19	1.96	0.70	14.969	43.52
ONSPC07	286610.79	3824320.00	60	0.64	98.15	1.21	2.44	2.38	0.40	36.1369	179.36
ONSPC07	286610.79	3824320.00	70	0.59	99.41	0.00	2.18	2.10	0.50	30.483	118.71

## **Appendix III**

<b>Sample Depth (cm)</b>	<b>Water Content (%)</b>
<i>Core ID: OBFDW01, Coordinates: 286817.83, 3824302.77 (UTM, m)</i>	
3-5	3.0
25-27	6.4
55-57	4.7
<i>Core ID: OBFDW02, Coordinates: 286745.80, 3824396.16 (UTM, m)</i>	
10-12	8.8
24-25	17.6
40-42	20.4
60-62	16.4
70-72	17.5
<i>Core ID: OBBW01, Coordinates: 286250.46, 3824014.31 (UTM, m)</i>	
4-6	4.1
25-27	3.9
45-47	16.5
<i>Core ID: OBBW02, Coordinates: 286267.76, 3823969.75 (UTM, m)</i>	
5-7	5.5
15-17	4.5
30-32	4.5
53-56	2.9
66-68	11.4
79-81	17.2
<i>Core ID: OBEG4-01, Coordinates: 289262.43, 3825909.92 (UTM, m)</i>	
7-9	2.9
20-22	4.5
30-32	3.8
40-42	5.8
50-52	5.8
60-62	8.7
70-72	13.6
75-77	19.4
80-82	21.3

<b>Sample Depth (cm)</b>	<b>Water Content (%)</b>
<i>Core ID: OBEG4-02, Coordinates: 289254.60, 3825918.81 (UTM, m)</i>	
0-10	4.5
20-22	3.7
30-32	7.7
40-42	14.4
50-52	17.8
60-62	19.1
<i>Core ID: OBEG4-03, Coordinates: 289232.73, 3825940.54 (UTM, m)</i>	
8-10	6.3
18-20	4.0
28-30	8.9
38-40	11.9
48-50	13.3
58-60	15.8
68-70	19.4
<i>Core ID: OBEG8-01, Coordinates: 288680.55, 3825472.30 (UTM, m)</i>	
10-12	3.3
21-23	6.0
31-33	6.3
41-43	8.2
51-53	16.3
61-63	13.1
65-67	12.3
71-73	17.8
79-81	12.2
82-84	17.8

<b>Sample Depth (cm)</b>	<b>Water Content (%)</b>
<i>Core ID: OBEG-02, Coordinates: 288664.39, 3825504.43 (UTM, m)</i>	
8-10	2.8
18-20	4.3
28-30	4.1
38-40	6.0
42-44	6.1
48-50	7.5
58-60	12.0
67-69	16.3
69-71	15.1
77-79	14.4
84-87	16.5
88-90	15.9
95-97	14.2
98-100	12.5
105-107	15.5

## **Appendix IV**

Transect ID	Total Relevant-Sand Prism			Portion of Relevant-Sand Prism in Beach Area			Portion of Relevant-Sand Prism in Active Overwash Region			Washover Estimates	
	Cross-Island Transect Length (m)	Transect Prism Volume (m <sup>3</sup> )	Area-Normalized Prism Vol (m <sup>3</sup> /m <sup>2</sup> )	Beach Transect Length (m <sup>2</sup> )	Beach Prism Volume (m <sup>3</sup> )	Area-Normalized Volume (m <sup>3</sup> /m <sup>2</sup> )	Overwash Transect Length (m <sup>2</sup> )	Overwash Prism Volume (m <sup>3</sup> )	Area-Normalized Volume (m <sup>3</sup> /m <sup>2</sup> )	Washover Volume (m <sup>3</sup> )	Percentage of Relevant-Sand Prism
1	426	708.33	1.66	89	40.44	0.45	77	337.31	4.38	40.04	5.7
2	447	632.46	1.41	98	46.85	0.48	87	305.18	3.51	45.24	7.2
3	449	695.04	1.55	92	45.34	0.49	141	375.11	2.66	73.32	10.5
4	434	644.37	1.48	83	48.53	0.58	141	386.50	2.74	73.32	11.4
5	316	547.76	1.73	67	49.10	0.73	191	470.87	2.47	99.32	18.1
6	303	499.62	1.65	53	29.80	0.56	208	459.67	2.21	108.16	21.6
7	299	483.59	1.62	50	25.49	0.51	205	432.21	2.11	106.60	22.0
8	299	426.51	1.43	41	12.56	0.31	193	352.16	1.82	100.36	23.5
9	296	508.00	1.72	33	6.73	0.20	235	499.16	2.12	122.20	24.1
10	440	467.23	1.06	28	1.74	0.06	153	268.88	1.76	79.56	17.0
11	523	455.20	0.87	25	3.93	0.16	234	339.94	1.45	121.68	26.7
12	465	333.08	0.72	30	3.97	0.13	178	205.36	1.15	92.56	27.8
13	480	397.29	0.83	30	6.87	0.23	197	264.73	1.34	102.44	25.8
14	495	365.24	0.74	17	4.13	0.24	162	159.36	0.98	84.24	23.1
15	512	368.82	0.72	25	11.37	0.45	240	240.95	1.00	124.80	33.8
16	475	361.20	0.76	25	9.41	0.38	250	272.72	1.09	130.00	36.0
17	420	374.13	0.89	26	16.58	0.64	232	289.73	1.25	120.64	32.2
18	338	320.92	0.95	30	20.03	0.67	10	207.09	20.71	5.20	1.6
19	522	278.31	0.53	25	21.05	0.84	28	24.57	0.88	14.56	5.2
20	425	154.48	0.36	20	17.79	0.89	15	24.41	1.63	7.80	5.0
21	354	116.92	0.33	14	12.40	0.89	16	25.87	1.62	8.32	7.1
22	286	80.10	0.28	19	13.20	0.69	11	17.15	1.56	5.72	7.1
23	284	95.80	0.34	19	16.39	0.86	13	19.70	1.52	6.76	7.1
24	288	108.19	0.38	16	19.34	1.21	11	20.95	1.90	5.72	5.3
25	286	95.29	0.33	15	17.02	1.13	12	22.43	1.87	6.24	6.5
26	263	99.69	0.38	14	18.78	1.34	11	21.15	1.92	5.72	5.7
27	255	61.81	0.24	18	12.53	0.70	10	13.85	1.38	5.20	8.4
28	195	63.17	0.32	15	13.19	0.88	13	20.23	1.56	6.76	10.7
29	141	88.67	0.63	19	16.72	0.88	8	13.76	1.72	4.16	4.7
30	103	90.73	0.88	25	17.80	0.71	5	7.60	1.52	2.60	2.9



Transect ID	Total Relevant-Sand Prism			Portion of Relevant-Sand Prism in Beach Area			Portion of Relevant-Sand Prism in Active Overwash Region			Washover Estimates	
	Cross-Island Transect Length (m)	Transect Prism Volume (m <sup>3</sup> )	Area-Normalized Prism Vol (m <sup>3</sup> /m <sup>2</sup> )	Beach Transect Length (m <sup>2</sup> )	Beach Prism Volume (m <sup>3</sup> )	Area-Normalized Volume (m <sup>3</sup> /m <sup>2</sup> )	Overwash Transect Length (m <sup>2</sup> )	Overwash Prism Volume (m <sup>3</sup> )	Area-Normalized Volume (m <sup>3</sup> /m <sup>2</sup> )	Washover Volume (m <sup>3</sup> )	Percentage of Relevant-Sand Prism
31	127	68.67	0.54	22	17.46	0.79	4	6.46	1.62	2.08	3.0
32	161	74.86	0.46	10	7.78	0.78	9	10.88	1.21	4.68	6.3
33	172	89.27	0.52	9	6.37	0.71	13	17.76	1.37	6.76	7.6
34	278	97.00	0.35	16	9.45	0.59	7	8.26	1.18	3.64	3.8
35	388	150.69	0.39	23	10.59	0.46	99	82.22	0.83	51.48	34.2
36	414	229.57	0.55	24	7.21	0.30	20	30.34	1.52	10.40	4.5
37	436	245.03	0.56	27	7.88	0.29	17	21.40	1.26	8.84	3.6
38	450	268.99	0.60	29	11.18	0.39	85	77.02	0.91	44.20	16.4
39	463	251.35	0.54	32	9.86	0.31	35	56.56	1.62	18.20	7.2
40	471	261.13	0.55	25	3.10	0.12	2	29.37	14.69	1.04	0.4
41	484	212.83	0.44	24	14.98	0.62	29	48.30	1.67	15.08	7.1
42	493	132.63	0.27	20	14.00	0.70	20	51.47	2.57	10.40	7.8
43	507	146.98	0.29	26	20.48	0.79	11	25.82	2.35	5.72	3.9
44	528	144.55	0.27	33	16.77	0.51	15	32.48	2.17	7.80	5.4
45	533	248.09	0.47	29	29.49	1.02	35	46.60	1.33	18.20	7.3
46	545	416.81	0.76	26	30.34	1.17	24	47.84	1.99	12.48	3.0
47	566	464.33	0.82	28	27.11	0.97	24	34.74	1.45	12.48	2.7
48	574	444.16	0.77	28	17.60	0.63	57	56.89	1.00	29.64	6.7
49	576	407.56	0.71	25	16.97	0.68	97	155.62	1.60	50.44	12.4
50	591	377.05	0.64	26	25.65	0.99	64	110.70	1.73	33.28	8.8
51	594	433.03	0.73	28	25.73	0.92	41	92.03	2.24	21.32	4.9
52	598	556.09	0.93	29	22.45	0.77	32	88.19	2.76	16.64	3.0
53	591	392.48	0.66	22	21.49	0.98	36	79.61	2.21	18.72	4.8
54	590	506.05	0.86	24	25.20	1.05	27	68.72	2.55	14.04	2.8
55	570	432.64	0.76	29	27.88	0.96	56	103.92	1.86	29.12	6.7
56	565	468.30	0.83	24	19.02	0.79	114	168.76	1.48	59.28	12.7
57	563	414.43	0.74	27	23.54	0.87	28	56.79	2.03	14.56	3.5
58	559	465.35	0.83	25	27.74	1.11	35	71.83	2.05	18.20	3.9
59	550	447.45	0.81	29	31.96	1.10	83	129.55	1.56	43.16	9.6
60	527	334.87	0.64	25	30.88	1.24	114	176.99	1.55	59.28	17.7
61	522	291.11	0.56	26	33.22	1.28	94	149.74	1.59	48.88	16.8

Transect ID	Total Relevant-Sand Prism			Portion of Relevant-Sand Prism in Beach Area			Portion of Relevant-Sand Prism in Active Overwash Region			Washover Estimates	
	Cross-Island Transect Length (m)	Transect Prism Volume (m <sup>3</sup> )	Area-Normalized Prism Vol (m <sup>3</sup> /m <sup>2</sup> )	Beach Transect Length (m <sup>2</sup> )	Beach Prism Volume (m <sup>3</sup> )	Area-Normalized Volume (m <sup>3</sup> /m <sup>2</sup> )	Overwash Transect Length (m <sup>2</sup> )	Overwash Prism Volume (m <sup>3</sup> )	Area-Normalized Volume (m <sup>3</sup> /m <sup>2</sup> )	Washover Volume (m <sup>3</sup> )	Percentage of Relevant-Sand Prism
62	484	325.46	0.67	25	32.72	1.31	92	198.38	2.16	47.84	14.7
63	511	314.89	0.62	22	29.31	1.33	65	156.44	2.41	33.80	10.7
64	514	271.42	0.53	27	35.46	1.31	45	94.35	2.10	23.40	8.6
65	501	384.00	0.77	21	33.02	1.57	49	124.36	2.54	25.48	6.6
66	487	354.71	0.73	17	24.12	1.42	34	75.96	2.23	17.68	5.0
67	486	327.82	0.67	18	24.76	1.38	65	136.91	2.11	33.80	10.3
68	493	368.98	0.75	18	27.89	1.55	108	177.99	1.65	56.16	15.2
69	474	378.58	0.80	25	38.15	1.53	40	97.81	2.45	20.80	5.5
70	456	405.23	0.89	19	33.10	1.74	54	117.73	2.18	28.08	6.9
71	447	458.30	1.03	22	40.20	1.83	184	275.22	1.50	95.68	20.9
72	437	533.28	1.22	22	34.98	1.59	81	207.23	2.56	42.12	7.9
73	418	364.49	0.87	21	29.61	1.41	34	78.92	2.32	17.68	4.9
74	414	324.47	0.78	19	19.97	1.05	77	101.79	1.32	40.04	12.3
75	418	344.97	0.83	14	13.62	0.97	37	67.20	1.82	19.24	5.6
76	389	295.82	0.76	9	11.70	1.30	20	42.37	2.12	10.40	3.5
77	390	406.61	1.04	12	20.64	1.72	21	41.45	1.97	10.92	2.7
78	408	520.07	1.27	20	31.72	1.59	16	38.06	2.38	8.32	1.6
79	393	584.18	1.49	17	32.39	1.91	33	79.64	2.41	17.16	2.9
80	376	498.54	1.33	18	37.96	2.11	91	204.10	2.24	47.32	9.5
81	381	589.87	1.55	16	31.56	1.97	106	214.18	2.02	55.12	9.3
82	373	607.83	1.63	14	26.70	1.91	76	237.84	3.13	39.52	6.5
83	378	590.91	1.56	15	29.83	1.99	52	141.33	2.72	27.04	4.6
84	375	731.62	1.95	13	23.71	1.82	69	166.60	2.41	35.88	4.9
85	369	538.43	1.46	11	17.69	1.61	94	213.50	2.27	48.88	9.1
86	352	540.28	1.53	13	21.84	1.68	86	264.05	3.07	44.72	8.3
87	327	374.77	1.15	11	18.72	1.70	41	121.93	2.97	21.32	5.7
88	353	478.99	1.36	10	16.66	1.67	65	148.42	2.28	33.80	7.1
89	339	523.70	1.54	13	20.38	1.57	47	112.54	2.39	24.44	4.7
90	334	426.79	1.28	9	12.92	1.44	107	201.17	1.88	55.64	13.0
91	333	480.36	1.44	8	12.83	1.60	93	200.13	2.15	48.36	10.1
92	320	525.66	1.64	6	8.12	1.35	56	141.90	2.53	29.12	5.5

Transect ID	Total Relevant-Sand Prism			Portion of Relevant-Sand Prism in Beach Area			Portion of Relevant-Sand Prism in Active Overwash Region			Washover Estimates	
	Cross-Island Transect Length (m)	Transect Prism Volume (m <sup>3</sup> )	Area-Normalized Prism Vol (m <sup>3</sup> /m <sup>2</sup> )	Beach Transect Length (m <sup>2</sup> )	Beach Prism Volume (m <sup>3</sup> )	Area-Normalized Volume (m <sup>3</sup> /m <sup>2</sup> )	Overwash Transect Length (m <sup>2</sup> )	Overwash Prism Volume (m <sup>3</sup> )	Area-Normalized Volume (m <sup>3</sup> /m <sup>2</sup> )	Washover Volume (m <sup>3</sup> )	Percentage of Relevant-Sand Prism
93	313	574.36	1.84	5	6.66	1.33	49	118.08	2.41	25.48	4.4
94	311	534.00	1.72	5	4.88	0.98	65	94.48	1.45	33.80	6.3
95	301	380.24	1.26	7	5.11	0.73	73	73.48	1.01	37.96	10.0
96	293	367.34	1.25	4	3.64	0.91	126	137.26	1.09	65.52	17.8

## **9 VITA**

AMY C. FOXGROVER

Born in Lancaster, California January 2<sup>nd</sup> 1978. Earned a B.A. in Environmental Studies from the University of California, Santa Barbara in 2000. Worked as a geographer for the Coastal and Marine Geology division of the US Geological Survey in Santa Cruz, CA until entering the MS program at the College of William and Mary, School of Marine Science in 2007.

## 10 REFERENCES

- Barnes, J. (2001), *North Carolina's Hurricane History*, 3rd ed., The University of North Carolina Press, Chapel Hill, 319 pp.
- Bristow, C.S., and Jol, H. M. (2003), An introduction to ground penetrating radar (GPR) in sediments, in *Ground penetrating radar in sediments* edited by C.S. Bristow and H.M. Jol, The Geological Society of London, London, pp. 1-9.
- Buynevich, I.V., FitzGerald, D. M., and Van Heteren, S. (2004), Sedimentary records of intense storms in Holocene barrier sequences, Maine, USA; Storms and their significance in coastal morpho-sedimentary dynamics, *Marine Geology*, 210(1-4), 135-148.
- Christiansen, T.A., Batholdy, J., Christiansen, M., Nielsen, J., Nielsen, N., Pedersen, J., and Vinther, N. (2004), Total sediment budget of a transgressive barrier-spit, Skallingen, SW Denmark: A Review, *Geografisk Tidsskrift, Danish Journal of Geography* 104(1), 107-126.
- Cleary, W.J., and Hosier, P.E. (1979), Geomorphology, washover history, and inlet zonation; Cape Lookout, North Carolina to Bird Island, North Carolina, in *Barrier islands from the Gulf of St. Lawrence to the Gulf of Mexico* edited by S.P. Leatherman, Academic Press, Inc. New York, New York, pp. 237-272.
- Cleary, W.J., McLeod, M.A, Rauscher, M.A., Johnston, M.J., and Riggs, S.R. (2001), Beach nourishment on hurricane impacted barriers in southeastern North Carolina, USA: Targeting Shoreline and Tidal Inlet Sand Resources, *Journal of Coastal Research Special Issue 34*, 232-255.
- Cleary, W.J., and Pilkey, O.H. (1968), Sedimentation in Onslow Bay, *Southeastern Geology, Special Publication*, (1), 1-17.
- Cleary, W.J., and Pilkey, O.H. (1996), Environmental coastal geology: Cape Lookout to Cape Fear, North Carolina regional overview in *Carolina Geological Society Guidebook for 1996 Annual Meeting* edited by W.J. Cleary, pp. 73-107.
- Cleary, W.J. and Riggs, S.R. (1999), Beach erosion and hurricane protection plan for Onslow Beach, Camp Lejeune; Comprehensive geologic characteristics report, North Carolina, US Marine Corps, Camp Lejeune, NC Report, United States (USA).
- Cloutier, M., and Hequette, A. (1998), Aeolian and overwash sediment transport across a low barrier spit, southeastern Canadian Beaufort Sea, *Zeitschrift fur Geomorphologie* 42(3) 349-365.
- Crowell, M., Leatherman, S.P., and Buckley, M.K. (1991), Historical shoreline change: Error analysis and mapping accuracy, *Journal of Coastal Research*, 7(3), 839-852.
- Davies, J.L. (1964), A morphogenic approach to world shorelines, *Zeitschrift fur Geomorphologie* (8) 27-42.

- Davis, J.L., and Annan, A.P. (1989), Ground-penetrating radar for high-resolution mapping of soil and rock stratigraphy, *Geophysical Prospecting*, 37(5), 531-551.
- Davis, R.A., Jr. (1994), Barrier island systems - a geologic overview, in *Geology of Holocene barrier island systems* edited by R.A. Davis Jr., Springer-Verlag, Berlin, Federal Republic of Germany (DEU), pp. 1-46.
- Davis, R.A., Batholdy, J., Pejrup, M., and Nielsen, N. (1997), Stratigraphy of Skallingen- A Holocene Barrier in the Danish Wadden Sea, *Aarhus Geoscience* (7) 9-19.
- De Beaumont, L.A. (1845), Lecons de geologie pratique, in *Barrier islands, Benchmark Papers in Geology*, edited by R.K. Schwartz, Dowden, Hutchinson & Ross, Stroudsburg, PA, pp.5-43.
- Dolan, R., Hayden, B.P., May, P., and May, S. (1980), The reliability of shoreline change measurements from aerial photographs, *Shore Beach*, 48(4), 22-29.
- Dolan, R., Hayden, B., Rea, C., and Heywood, J. (1979), Shoreline erosion rates along the middle Atlantic coast of the United States, *Geology* (Boulder), 7(12), 602-606.
- Donnelly, J.P., Butler, J., Roll, S., Wengren, M., and Webb, T. III (2004), A backbarrier overwash record of intense storms from Brigantine, New Jersey; Storms and their significance in coastal morpho-sedimentary dynamics, *Marine Geology*, 210(1-4), 107-121.
- Donnelly, C., Kraus, N., and Larson, M. (2006), State of knowledge on measurement and modeling of coastal overwash, *Journal of Coastal Research*, 22(4), 965-991.
- Federal Geographic Data Committee (1998), Geospatial Positioning Accuracy Standards Part 3: National Standard for Spatial Data Accuracy FGDC-STD-007.3-1998.
- Fisher, J.J., and Simpson, E.J. (1979), Washover and tidal sedimentation rates as environmental factors in development of a transgressive barrier shoreline, in *Barrier islands from the Gulf of St. Lawrence to the Gulf of Mexico* edited by S.P. Leatherman, Academic Press, Inc. New York, New York, pp. 127-148.
- Fisher, J.S. and Stauble, D.K. (1977), Impact of Hurricane Belle on Assateague Island washover, *Geology*, 5, 765-768.
- Gilbert, G.K. (1885), The topographic features of lake shores, in *Barrier Islands, Benchmark Papers in Geology*, edited by R.K. Schwartz, Dowden, Hutchinson & Ross, Stroudsburg, PA, pp. 45-46.
- Godfrey, P.J. (1970), Oceanic overwash and its ecological implications on the outer banks of North Carolina, in *Overwash Processes, Benchmark Papers in Geology*, edited by S.P. Leatherman, Hutchinson Ross Publishing Company, Stroudsburg, PA, pp. 321-333.
- Hayes, M.O. (1979), Barrier island morphology as a function of tidal and wave regime, in *Barrier islands from the Gulf of St. Lawrence to the Gulf of Mexico*, edited by S.P. Leatherman, Academic Press, Inc. New York, New York, pp. 1-28.

Heron, S.D., Jr., Moslow, T.F., Berelson, W.M., Herbert, J.R., Steele G.A. III, and Susman, K.R. (1984), Holocene sedimentation of a wave-dominated barrier island shoreline: Cape Lookout, North Carolina, *Marine Geology*, 60(1-4), 413-434.

Hippensteel, S.P., and Martin, R.E. (1999), Foraminifera as an indicator of overwash deposits, barrier island sediment supply, and barrier island evolution; Folly Island, South Carolina; Taphonomy as a tool in paleoenvironmental reconstruction and environmental assessment, *Palaeogeography, Palaeoclimatology, Palaeoecology*, 149(1-4), 115-125.

Hoeke, R.K., and Zarillo, G.A., Synder, M. (2001), A GIS based tool for extracting shoreline positions from aerial imagery (BeachTools), ERDC/CHL CHETN-IV-37 [<http://chl.erd.usace.army.mil/library/publications/chetn/pdf/chetn-iv-37.pdf>].

Horton B.P., Peltier, W.R., Culver, S.J., Drummond, R., Engelhart, S.E., Kempa, A.C., Mallinson D., Thieler, E.R., Riggs, S.R., Ames, D.V., Thomson, K.H. (2009), Holocene sea-level changes along the North Carolina Coastline and their implications for glacial isostatic adjustment models, *Quaternary Science Reviews*, (28) 1725-1736.

Inman, D.L., and Dolan, R. (1989), The Outer Banks of North Carolina: Budget of sediment and inlet dynamics along a migrating barrier system, *Journal of Coastal Research*, 5(2), 193-237.

Jol, H.M. (1995), Ground penetrating radar antennae frequencies and transmitter powers compared for penetration depth, resolution and reflection continuity, *Geophysical Prospecting*, 43(5), 693-709.

Jol, H.M., Smith, D. G., and Meyers, R.A. (1996), Digital ground penetrating radar (GPR): a new geophysical tool for coastal barrier research (examples from the Atlantic, Gulf and Pacific Coasts, U.S.A.), *Journal of Coastal Research*, 12(4), 960-968.

Kochel, R.C., and Dolan, R. (1986), The role of overwash on a Mid-Atlantic coast barrier island, *Journal of Geology*, 94(6), 902-906.

Kochel, R.C., and Wampfler, L.A. (1989), Relative role of overwash and aeolian processes on washover fans, Assateague Island, Virginia-Maryland, *Journal of Coastal Research*, 5(3), 453-475.

Leatherman, S.P. (1976), Barrier island dynamics: overwash processes and aeolian transport. *Proceedings 15<sup>th</sup> International Coastal Engineering Conference*, Honolulu, Hawaii, pp. 1958-1974.

Leatherman, S.P. (1979), *Barrier island handbook*, National Park Service Cooperative Research Unit, The Environmental Institute, University of Massachusetts at Amherst, Amherst, MA, United States (USA), 101 pp.

Leatherman, S.P. (1983), Barrier dynamics and landward migration with Holocene sea-level rise, *Nature* (London), 301(5899), 415-417.

Mason, C.C., and Folk, R.L. (1958), Differentiation of beach, dune, and aeolian flat environments by size analysis, Mustang Island, Texas, *Journal of Sedimentary Petrology*, 28(2), 211-226.



- McCubbin, D.G. (1982), Barrier-island and strand-plain facies; Sandstone depositional environments, *Memoir - American Association of Petroleum Geologists*, 31, 247-279.
- McGee, W.J. (1890), Encroachments of the sea, in *Barrier islands. Benchmark Papers in Geology*, edited by R.K. Schwartz, Dowden, Hutchinson & Ross, Stroudsburg, PA, pp. 49-61.
- McNinch, J.E., and Wells, J.T. (1999), Sedimentary processes and depositional history of a cape-associated shoal, Cape Lookout, North Carolina, *Marine Geology*, 158(1-4), 233-252.
- Middleton, G.V. (1967), Experiments on density and turbidity currents, 3. The deposition of sediment, *Canadian Journal of Earth Science*, (4), 475-505.
- Miller, T.L., Morton, R.A., Sallenger, A.H. (2005), National assessment of shoreline change: a GIS compilation of vector shorelines and associated shoreline change data for the U.S. southeastern Atlantic coast. US Geological Survey Open-File Report 2005-1326 [ <http://pubs.usgs.gov/of/2005/1326>].
- Miselis, J.L., and McNinch, J.E. (2006), Calculating shoreline erosion potential using nearshore stratigraphy and sediment volume; Outer Banks, North Carolina, *Journal of Geophysical Research*, 111(F2), 15.
- Moller, I., and Anthony, D. (2003), A GPR study of sedimentary structures within a transgressive coastal barrier along the Danish North Sea coast, in *Ground penetrating radar in sediments, Geological Society Special Publication No. 211*, edited by C.S. Bristow and H.M. Jol, the Geological Society of London, London, pp. 55-65.
- Moore, L.J. (2000), Shoreline mapping techniques, *Journal of Coastal Research*, 16(1), 111-124.
- Moore, L.J., Jol, H. M., Kruse, S., Vanderburgh, S., and Kaminsky, G.M. (2004), Annual layers revealed by GPR in the subsurface of a prograding coastal barrier, southwest Washington, U.S.A, *Journal of Sedimentary Research*, 74(5), 690-696.
- Morton, R.A. (1994), Texas Barriers, in *Geology of Holocene barrier island systems* edited by R.A. Davis Jr., Springer-Verlag, Berlin, Federal Republic of Germany (DEU), Federal Republic of Germany (DEU), pp. 75-114.
- Morton, R.A., Gonzalez, J.L., Lopez, G.I., and Correa. I.D. (2000), Frequent non-storm washover of barrier islands, Pacific Coast of Colombia, *Journal of Coastal Research*, 16(1), 82-87.
- Morton, R.A., and Miller, T.L. (2005), National assessment of shoreline change: Part 2: Historical shoreline changes and associated coastal land loss along the U.S. Southeast Atlantic Coast: U.S. Geological Survey Open-file Report 2005-1401 [ <http://pubs.usgs.gov/of/2005/1401>].
- Moslow, T.F., and Heron, S.D., Jr. (1994), The Outer Banks of North Carolina, in *Geology of Holocene barrier island systems* edited by R.A. Davis Jr., Springer-Verlag, Berlin, Federal Republic of Germany (DEU), Federal Republic of Germany (DEU), pp. 47-74.
- Neal, A. (2004), Ground-penetrating radar and its use in sedimentology: principles, problems and progress, *Earth-Science Review*, 66(3-4), 261-330.

NOAA Coastal Services Center Digital Coast website (Feb. 2009), U.S. Dept. of Commerce, [<http://www.csc.noaa.gov/digitalcoast>].

NOAA Coastal Services Center website, Historical Hurricane Tracks (Sept. 2009), U.S. Dept. of Commerce [<http://www.csc.noaa.gov/digitalcoast/tools/hurricanes>].

North Carolina Division of Coastal Management website (Feb. 2009), North Carolina Department of Environment and Natural Resources [<http://dcm2.enr.state.nc.us/Maps/chdownload.htm>].

Pierce, J.W. (1970), Tidal inlets and washover fans, *Journal of Geology*, 78(2), 230-234.

Reed, W.E., Fever, R.L., and Moir, G.J. (1975), Depositional environment interpretation from settling-velocity ( $\Psi$ ) distributions, *Geological Society of America Bulletin* 86(50917), 1321-1328.

Reimer, B.A. (2004), Influences of major storm events on backbarrier salt marsh change: Masonboro Island, southeastern North Carolina, University of North Carolina at Wilmington, M.S. Thesis, 93 pp.

Rosen, P.S. (1979), Eolian dynamics of a barrier island system, in *Barrier Islands- from the Gulf of St. Lawrence to the Gulf of Mexico* edited by S.P. Leatherman, Academic Press, New York. pp. 81-98.

Sallenger, A.H., Jr. (2000), Storm impact scale for barrier islands, *Journal of Coastal Research*, 16(3), 890-895.

Scavia, D., Field, J.C., Boesch, D.F., Buddemeier, R.W., Burkett, V., Cayan, D.R., Fogarty, M., Harwell, M.A., Howarth, R.W., Mason, C., Reed, D.J., Royer, T.C., Sallenger, A.H., Titus, J.G. (2002), Climate Change Impacts on U.S. Coastal and Marine Ecosystems, *Estuaries*, 25(2), 149-164.

Schwartz, R.K. (1975), *Nature and genesis of some storm washover deposits*, Technical Memorandum 61, US Army Corps of Engineers, Coastal Engineering Research Center, Fort Belvoir, VA, 69 pp.

Schwartz, R.K. (1982), Bedform and stratification characteristics of some modern small-scale washover sand bodies, *Sedimentology*, 29(6), 835-849.

Sensors & Software Inc. (2003), EKKO Update, January 2003 Newsletter, Sensors & Software Inc., Mississauga, ON Canada [[www.sensoft.ca](http://www.sensoft.ca)].

Smith, G.L., and Zarillo, G.A. (1990), Calculating long-term shoreline recession rates using aerial photographic and beach profiling techniques, *Journal of Coastal Research*, 6(1), 111-120.

Sproat, A.M. (1999), Origin and evolutionary history of back-barrier estuarine system, Onslow Beach, NC, East Carolina University, M.S. Thesis, 160 pp.

Stockdon, H.F., Sallenger, A.H., Jr., Holman, R.A., and Howd, P.A. (2007), A simple model for the spatially-variable coastal response to hurricanes, *Marine Geology*, 238(1-4), 1-20.

- Stutz, M.L., and Pilkey, O.H. (2001), A review of global barrier island distribution, *Journal of Coastal Research Special Issue 34*, 15-22.
- Syvitski, J.P.M., Asprey, K.W., and Clattenburg, D.A. (1991), Principles, design, and calibration of settling tubes in *Principles, methods and application of particle size analysis* edited by J.P.M. Syvitski, Cambridge University Press, Cambridge, UK, pp. 45-63.
- Thieler, E.R. (1996), Shoreface processes in Onslow Bay, in *Environmental Coastal Geology: Cape Lookout to Cape Fear, NC* edited by W.J. Cleary, Durham, NC, 23 pp.
- Thieler, E.R., and Danforth, W.W. (1994), Historical shoreline mapping; (I), Improving techniques and reducing positioning errors, *Journal of Coastal Research*, 10(3), 549-563.
- Thieler, E.R., Himmelstoss, E.A., Zichichi, J.L., and Miller, T.L. (2005), Digital Shoreline Analysis System (DSAS) version 3.0: An ArcGIS extension for calculating shoreline change: U.S. Geological Survey Open-File Report 2005-1304 [<http://woodshole.er.usgs.gov/project-pages/dsas>].
- Van Heteren, S., FitzGerald, D.M., Barber, D.C., Kelley, J.T., and Belknap, D.F. (1996), Volumetric analysis of a New England barrier system using ground-penetrating-radar and coring techniques, *Journal of Geology*, 104(4), 471-483.
- Van Heteren, S., Fitzgerald, D.M., McKinlay, P.A., and Buynevich, I.V. (1998), Radar facies of paraglacial barrier systems; coastal New England, USA, *Sedimentology*, 45(1), 181-200.
- Wadman, H. M., McNinch, J.E., Foxgrover, A.C., and Rodriguez, A.B. (2008), Spatial variation of shoreline change along an important marine corps amphibious training ground, Onslow Beach, NC; Part 1: nearshore geology and morphology. (abs.) Fall 2008 Geological Society of America Meeting, Houston, TX.
- Woodward, J., Ashworth, P.J., Best, J.L., Sambrook Smith, G.H., and Simpson, C.J. (2003), The use and application of GPR in sandy fluvial environments: methodological considerations, in *Ground penetrating radar in sediments* edited by C.S. Bristow and H.M. Jol, The Geological Society of London, London, pp. 127-142.